

**The essential function of neuroplastins for fertility and associative
memories in mice**

for the degree of

doctor rerum naturalium (Dr. rer. nat.)

approved by the Faculty of Natural Sciences of Otto von Guericke University Magdeburg

by M.Eng. Ella Juanjuan Chen

born on 18th September 1985 in Hunan (China)

Examiner: PD Dr. Dirk Montag

Prof. Dr. Hans-Jürgen Kreienkamp

submitted on 19th December 2023

defended on 22nd July 2024

SUMMARY

Neuroplastins are glycoproteins belonging to the immunoglobulin superfamily of cell adhesion molecules (CAMs). They play a crucial role in learning, memory, and mouse fertility. Neuroplastins are closely associated with the expression of the calcium pump in the cell membrane (Plasma Membrane Calcium ATPase; PMCA), which regulate calcium homeostasis within cells, and any disruption in this balance can result in various neurobiological consequences.

Our research is based on various mutant mouse models with altered neuroplastin expression. In the first part of this study, we examined neuroplastin-deficient male mice. These mice exhibited lower testosterone levels in their blood from 3 months to adult age as compared to wild-type male mice, however, intratesticular testosterone levels were similar in mutants and wildtypes. Immunohistochemical and immunoblotting studies revealed decreased expression of PMCA1, particularly in the testes and Leydig cells of mutant mice. In the second part of this thesis, inducible conditional neuroplastin-deficient mice were employed to study neuroplastin functions in GABAergic interneurons. The findings indicated that reduced PMCA2 expression in parvalbumin-positive (PV+) interneurons is associated with impaired learning and memory. In PV+ interneurons, decreased PMCA2 expression could impair synaptic transmission and plasticity, ultimately resulting in deficits in learning and memory.

In conclusion, my study postulates that the reduction of PMCA1 due to the loss of neuroplastin affects the fertility of male mice. Additionally, decreased PMCA2 levels resulting from the ablation of neuroplastins in GABAergic neurons, especially in PV+ interneurons, may lead to retrograde amnesia.

Zusammenfassung

Die Neuroplastine sind Isoformen eines Glykoproteins, das zur Immunoglobulin-Superfamilie der Zelladhäsionsmoleküle (CAMs) gehört. Es spielt eine entscheidende Rolle beim Lernen, der Gedächtnisbildung und der Fruchtbarkeit von Mäusen. Neuroplastine stehen in enger Verbindung mit der Expression der membranständigen Calcium-Pumpe (Plasma Membrane Calcium ATPase; PMCA), die die Calcium-Homöostase in Zellen reguliert. Neuroplastin spielt eine entscheidende Rolle bei der Regulierung der PMCA-Expression und dementsprechend bei der zellulären Calcium-Homöostase. Jegliche Störung dieses Gleichgewichts kann zu verschiedenen neurobiologischen Konsequenzen führen.

Unsere Forschung basiert auf verschiedenen Mutanten-Mausmodellen mit veränderter Neuroplastin-Expression. Im ersten Teil dieser Studie sind neuroplastindefiziente männliche Mäuse untersucht worden. Diese Mäuse zeigten im Vergleich zu Wildtyp-Mäusen ab dem Alter von 3 Monaten bis zum Erwachsenenalter niedrigere Testosteronspiegel im Blut, jedoch ähnliche intratestikuläre Testosteronspiegel. Immunohistochemische und Immunoblotting-Studien ergaben eine verminderte Expression von PMCA1, insbesondere in den Hoden und Leydig-Zellen der Mausmutanten. Im zweiten Teil dieser Arbeit wurden induzierbar konditional-Np-defiziente Mäuse verwendet, um Neuroplastinfunktionen in GABAergen Interneurone zu untersuchen. Die Ergebnisse deuteten darauf hin, dass eine verringerte Expression von PMCA2 in Parvalbumin-positiven (PV+) Interneuronen mit Beeinträchtigungen von Lernen und Gedächtnis assoziiert war. In PV+ Interneuronen könnte die verringerte PMCA2-Expression die synaptische Übertragung und Plastizität beeinträchtigen und letztendlich zu Defiziten beim Lernen und Gedächtnis führen.

Zusammenfassend postuliert unsere Studie, dass die Verringerung von PMCA1 aufgrund des Verlusts von Neuroplastin die Fruchtbarkeit männlicher Mäuse beeinflusst. Darüber hinaus deuten meine Befunde darauf hin, dass die verringerte PMCA2-Expression nach Ablation von Neuroplastin in GABAergen Neuronen, insbesondere in PV+ Interneuronen, zu retrograder Amnesie führt.

Table of Contents

SUMMARY	I
Zusammenfassung	II
1 General Introduction	1
1.1 General properties of Neuroplastins and their functions	1
1.1.1 Neuroplastins are a regulator of neuronal plasticity and synaptic function.....	1
1.1.2 Neuroplastin structure, expression, isoforms, and glycosylation	3
1.2 Plasma membrane Calcium ATPases (PMCA)	7
1.2.1 Properties of PMCA.....	7
1.2.2 Regulation of intracellular Calcium level by PMCA	9
1.3 Neuroplastin interaction with PMCA	12
1.3.1 Complex formation of neuroplastin and PMCA	12
1.3.2 Regulation of intracellular Calcium levels by neuroplastin and PMCA	13
1.4 Hormone regulation in male mice fertility	14
1.4.1 Spermatogenesis.....	14
1.4.2 Hormonal regulation of Spermatogenesis	17
1.4.3 The role of Ca ²⁺ in the testosterone signaling pathway.....	21
1.5 Neuroplastin and its role in learning and memory	24
1.5.1 Associative learning and associative memory	24
1.5.2 Anterograde and retrograde amnesia	24
1.5.3 Ablation of neuroplastin induces retrograde amnesia	25
1.6 Hypothesis and aims of the study	25
1.6.1 State of the art evidence underlying the hypothesis.....	25
1.6.2 Hypotheses	26
1.6.3 Aims	26
2 Materials and methods	27
2.1 Materials	27
2.1.1 Antibodies	27
2.1.2 Chemicals.....	28
2.1.3 Buffers and solutions	29
2.1.4 Kits and equipment.....	31
2.1.5 Gene expression assays	31

2.2 Mice32

2.3 Methods.....33

2.3.1 DNA isolation from mouse tails/ears33

2.3.2 Genotyping for detection of the *Nptn* alleles.....34

2.3.3 Protein Extraction35

2.3.4 Protein determination, SDS-PAGE, Western Blotting36

2.3.5 Enzyme-linked Immunosorbent assay of hormones.....38

2.3.6 Histological techniques and immunohistochemistry38

2.3.7 Mouse sperm count40

2.3.8 Behavioral experiments41

2.3.9 Statistical analysis42

3 Results43

3.1 Testis and sperm in *Nptn*^{-/-} male mice show no anatomical differences.....43

3.2 Neuroplastin expression in testis and sperm.....44

3.3 The testosterone level in the testis of adult neuroplastin-deficient (*Nptn*^{-/-}) male mice is not different from that in wild-type (*Nptn*^{+/+}) male mice50

3.4 PMCA1 is reduced in Leydig cells of neuroplastin- deficient (*Nptn*^{-/-}) mice52

3.5 Inducible Cre recombinase with promoter GAD2 mediated inactivation of the neuroplastin gene results in retrograde amnesia with significantly reduced memory54

3.6 Ablation of neuroplastins expression in Parvalbumin positive interneurons63

**3.7 PMCA2 is reduced in GABAergic neuron-specific inducible Neuroplastin - deficient mice
66**

3.8 PMCA2 is reduced in PV+ GABAergic interneurons69

4 Discussion70

4.1 Neuroplastin-deficient (*Nptn*^{-/-}) male mice do not reproduce nor display normal mating behavior70

4.2 The ability of male mice to produce offspring was not affected by the ablation of Neuroplastins expression in spermatogonia, Sertoli cells or central nervous system70

4.3 Testosterone plays a crucial role in the development and maintenance of the male reproductive system72

4.4 The reduced PMCA1 level in Leydig cells of *Nptn*^{-/-} male mice may result in an elevated intracellular Ca²⁺ level preventing a correct response to LH signals triggering testosterone production.....74

4.5 Ablation of neuroplastin in GABAergic interneurons after associative learning is sufficient to induce retrograde amnesia of associative memories75

4.6 Parvalbumin positive interneurons play an important role in associative learning and memories79

4.7 Reduced PMCA2 levels may affect GABA release from PV+ interneurons, leading to retrograde amnesia of associative memories80

4.8 Conclusion.....84

5 *References*.....85

6 *Appendix*..... 103

6.1 Abbreviations103

6.2 List of figures105

6.3 List of tables107

6.4 Ehrenerklärung.....108

1 General Introduction

1.1 General properties of Neuroplastins and their functions

1.1.1 Neuroplastins are a regulator of neuronal plasticity and synaptic function

Neuroplastins were first discovered as glycoprotein components of the synaptic membrane and postsynaptic density (PSD) fractions of rat brain (Hill et al., 1988). Twenty-five years ago, synaptic membrane glycoproteins gp65 and gp55 were identified as new members of the Ig superfamily (Langnaese et al., 1997). In 2000, they were named neuroplastin due to their significant role in the regulation of synaptic plasticity (Smalla et al., 2000).

More than a century has passed since the term "plasticity" was coined to suggest that the brain is naturally malleable (Berlucchi and Buchtel, 2009). Plasticity contradicts localizationism, which holds that the human brain acts as a collection of discrete pieces, each serving a single function. Plasticity endows the brain with a very specific and distinguishing feature: the ability to develop or adapt itself to variable or persistent demands (Latash et al., 2000; Duffau, 2017).

Synaptic efficacy is commonly defined as the ability to elicit postsynaptic actions in response to neurotransmitter release by the presynaptic terminal. Synaptic plasticity refers to the ability of synapses to change their efficacy as a result of previous activation. Synaptic effectiveness fluctuates as the synapse continues to function (Bernhardi and Nicholls, 1999). Short-term synaptic plasticity (STSP) refers to changes in synaptic efficacy that occur within milliseconds to minutes (Zucker and Regehr, 2002). Changes in effectiveness that occur over tens of minutes to hours, or even longer, are referred to as long-term synaptic plasticity (LTSP) and tend to be long-lasting (Abraham, 2003). Long-term synaptic plasticity is described as a long-lasting, activity-dependent change in synaptic efficacy. Long-term plasticity can

change synaptic strength in both directions, either increasing long-term potentiation (LTP) or decreasing long-term depression (LTD) (Yang and Calakos, 2013). Previous experiments have shown an enhanced association of neuroplastin, especially the longer isoform neuroplastin-65 (Np65), with synaptic structures, which may reflect the involvement of this molecule in the reorganization process induced by LTP plasticity (Smalla et al., 2000).

The analysis showed that neuroplastin-55(Np55) is expressed more widely (Langnaese et al., 1997) while Np65 is primarily expressed in the brain as a cell adhesion molecule regulating synaptic function and neuronal plasticity. Neuronal plasticity refers to the brain's ability to change and adapt to experiences and environmental stimuli, crucial for learning and memory, as well as recovery from brain injury or disease, which is critical for information processing in the brain. Np65 and Np55 promote neurite outgrowth by trans-homophilic binding and FGFR activation (Beesley et al., 2014a).

Neuroplastins are transmembrane protein Ig superfamily and are most closely related to Basigin/CD147 (Langnaese et al., 1997; Beesley et al., 2014). The small basigin gene family in mammals consists of the three paralogs, neuroplastins, basigin (also known as CD147, EMMPRIN), and embigin (Yates et al., 2020). Neuroplastin or basigin - control Ca^{2+} ion homeostasis by acting as an essential subunit of plasma membrane calcium ATPase (PMCA) (Herrera-Molina et al., 2017; Korthals et al., 2017; Schmidt et al., 2017). Polymorphisms in the regulatory region of the human *NPTN* gene are linked to cortical thickness and IQ in adolescents (Desrivieres et al., 2015). Vemula et al. (2020) report the interaction of neuroplastins with TRAF6 and the induction of neuritogenesis by neuroplastins via TRAF6. Research summarized by Lin et al. (2021a) indicates that neuroplastins play a role in pathways affected by neuropsychiatric and neurodegenerative diseases. Loss of neuroplastins or disruption of molecular pathways involving neuroplastins in neuronal processes are associated with various neurological disorders, such as dementia, schizophrenia, and Alzheimer's disease (AD). Additionally, neuroplastins have significant functions in the immune system (Korthals et al., 2017) and are also essential for hearing (Lin et al., 2021b).

1.1.2 Neuroplastin structure, expression, isoforms, and glycosylation

Neuroplastins belong to the immunoglobulin superfamily of cell adhesion molecules (CAMs), which play a crucial role in cell adhesion, enabling cells to bind to the extracellular matrix (ECM) or other cells (Chothia and Jones, 1997) (see Table 1). Neuroplastins consist of two isoforms, neuroplastin-65 (Np65) and neuroplastin-55 (Np55) were named referring to their molecular weights (Hill et al., 1988; Smalla et al., 2000; Owczarek and Berezin, 2012).

Several CAMs, including neural cell adhesion molecule (NCAM), L1, and cadherins, bind to and activate the fibroblast growth factor receptor (FGFR) tyrosine kinase for communication (Walsh and Doherty, 1997; Hansen et al., 2008). FGFRs comprise up to three Ig domains, D1-D3, with the D2 (Ig2) and D3 (Ig3) domains being sufficient for fibroblast growth factor (FGF) binding. Np55 and Np65 have two and three extracellular Ig domains, respectively, a transmembrane domain, and a small intracellular C-terminal tail region. The isoforms are distinguished by the presence of the Ig1 module specific to Np65 and lacking in Np55 (see Figure 1) (Owczarek et al., 2012). A short cytoplasmic domain may contain 34 or 38 amino acids, depending on the insertion of the four amino acids DDEP resulting from alternative splicing, and a single pass transmembrane domain are found by all isoforms (Langnaese et al., 1997).

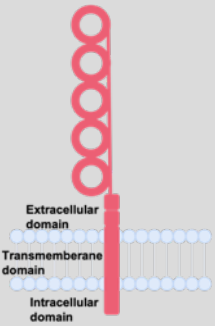
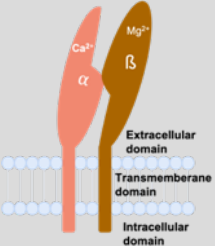
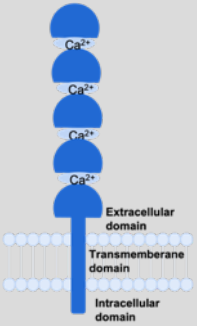
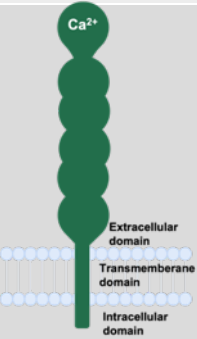
Family	Immunoglobulin superfamily(Ig-SF)	Integrin	Cadherin	Selectin
Ca ²⁺ dependent	independent	dependent	dependent	dependent
Members	VCAM NCAM ICAM PECAM	VLA4(α 4/ β 1) VLA5(α 5/ β 1) LFA(α L/ β 2) ...	E-cadherin P-cadherin N-cadherin	E-selectin P-selectin L-selectin
Interaction	homophilic/heterophilic	heterophilic	homophilic/heterophilic	heterophilic
Function	cell signalling leucocyte extravasation immune system function	attachment of cells to ECM signal transduction leucocyte extravasation cell migration role in cell cycle neuroregeneration in PNS	cell adhesion embryonic development tumor metastasis morphogenesis	lymphocyte homing inflammation process leucocyte migration
Type				

Table 1: Summary of cell adhesion molecules

Np65 is predominantly expressed in the forebrain of rodents, including the cortex, striatum, and hippocampus. Although Np65 is detected in the CA1 area and dentate gyrus, its expression is moderate in the CA3 region of the hippocampus (Herrera-Molina et al. 2014).

The human neuroplastin (*NPTN*) gene, as listed in Gene ID 27020 from NCBI, is located on chromosome 15q22 and contains nine exons. There are four splice variants of Np65 and Np55, each with or without a 4 amino acid acidic 340-Asp-Asp-Glu-Pro-(DDEP)-343 insert in the intracellular domain, referred to as Np+ DDEP and Np-DDEP. Np65 and Np55 both have a glutamate at the same position in the transmembrane domain, which may be important for molecular interactions within the membrane region. The amino acid numbering is for Np65, as reported by Langnaese et al. (1997), Kreutz et al. (2001), and Beesley et al. (2014b). In both the rat and human brain, there are six potential N-glycosylation sites, but nine in the mouse, all of which are located on the common Ig2 and Ig3 domains (Figure 1). Although Np65 and Np55 can be fully deglycosylated, resulting in a reduction in apparent molecular weight from 65 and 55 kDa to 40 and 28 kDa respectively, most of the potential glycosylation sites are utilized (Willmott et al., 1992). Moreover, X-ray crystallography of recombinant protein containing the ecto Np55, i.e., Np55 Ig2 and Ig3 domains, reveals the presence of N-acetylglucosamine at four of the six possible N-glycosylation sites in the rat (Owczarek et al., 2010). Furthermore, studies by Sarto-Jackson et al. (2012) and Herrera-Molina et al. (2014) reported that the localization of GABA_A receptors at inhibitory synapses is regulated by neuroplastin.

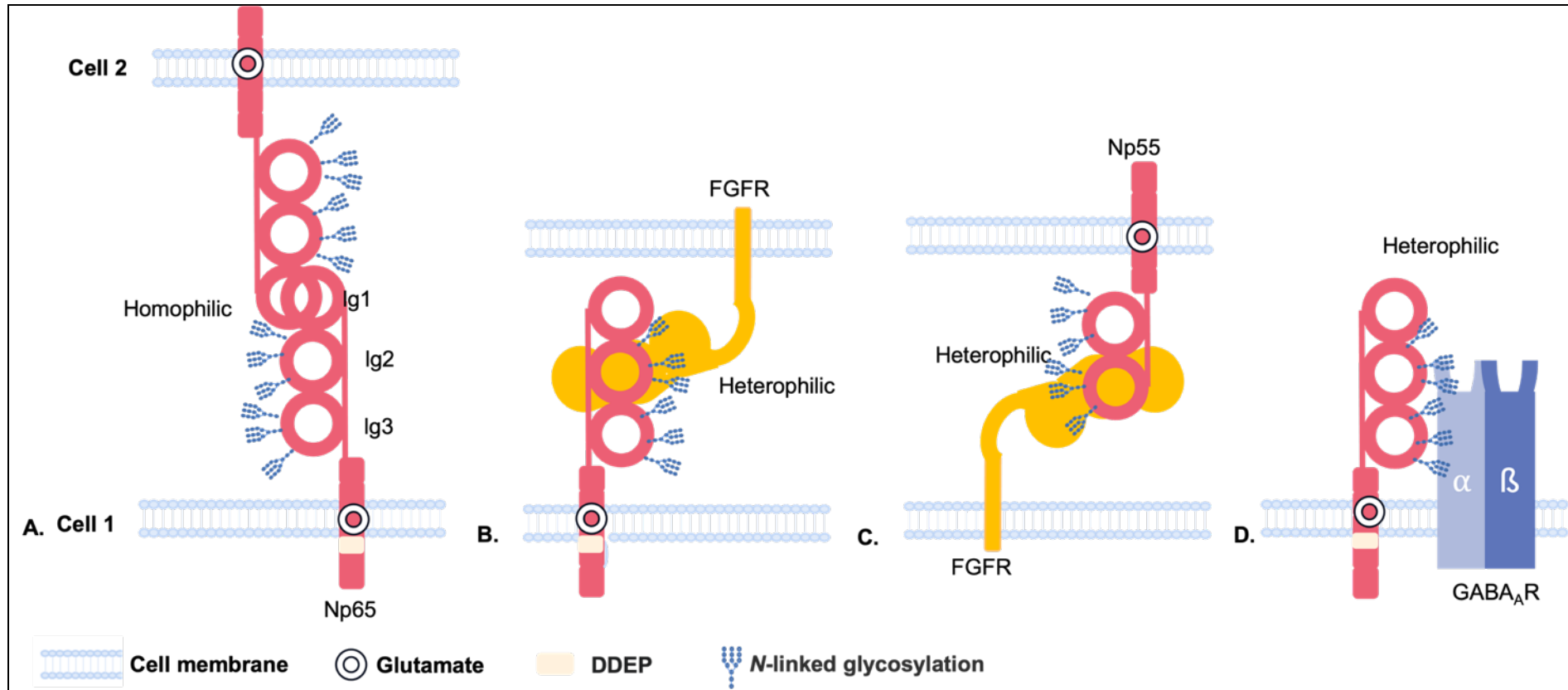


Figure 1: Neuroplastin binding interactions

A. Homophilic binding occurs in trans only between Np65 with the binding site located in the N-terminal Ig domain. **B.** Heterophilic binding occurs between Np65 and fibroblast growth factor receptors (FGFR), with the interaction occurring between the two middle Ig domains. **C.** Similar to Np65, Np55 also interacts with FGFR through its Ig2 domain. **D.** Heterophilic binding occurs between Np65 and GABA_A receptor α1, α2, and β2 subunits.

1.2 Plasma membrane Calcium ATPases (PMCA)

1.2.1 Properties of PMCA

Plasma Membrane Calcium ATPases (PMCA) are important proteins located in the plasma membrane of cells, which play a key role in regulating the concentration of calcium ions within cells. PMCA are ion pumps by which cells extrude Ca^{2+} ions (Carafoli, 1991) and are members of the P-type main ion transport ATPase family that forms aspartyl phosphate intermediates. Jensen et al. (2004) reported that PMCA utilize ATP (adenosine triphosphate) as an energy source to export calcium ions out of cells, thereby contributing to the maintenance of low cytoplasmic calcium concentrations. This is crucial for various cellular functions such as muscle contraction, neurotransmitter release, and cell communication.

PMCA are transmembrane proteins, consisting of 10 transmembrane domains and a large cytoplasmic domain containing the ATP-binding site (refer to Figure 2). There are four different genes that code for PMCA (PMCA1-4) isoforms and differ in their tissue distribution and regulatory properties (e.g. Jensen et al., 2007; Brini and Carafoli, 2009).

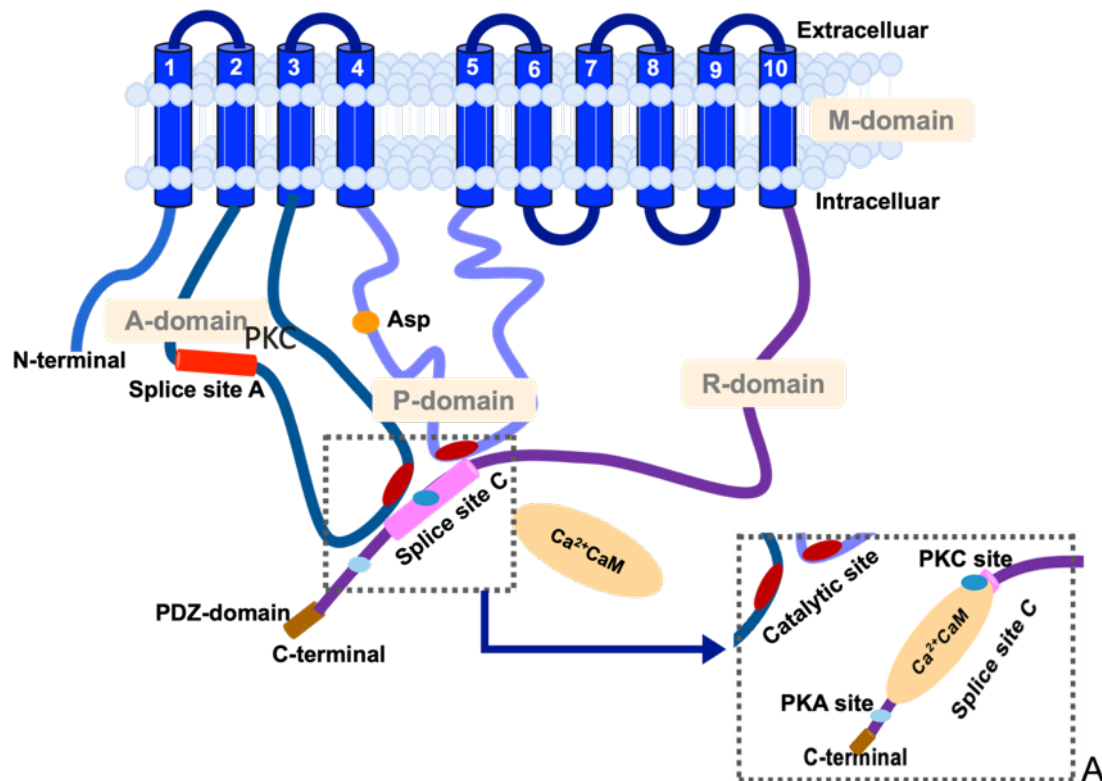


Figure 2: Schematic overview of the PMCA structure

This figure is modified from (Carafoli and Lim, 2009) and (Jason, 2018). The major domain, called the M-domain, is comprised of ten transmembrane segments. The amino- (N-terminal) and carboxy-terminal (C-terminal) ends are indicated. The ATP binding region is formed by the conserved aspartate (Asp), which creates the phosphorylated intermediate during the enzyme reaction cycle. There are four major cytosolic protein domains: A (actuator), P (phosphorylation), N (nucleotide-binding), and R (regulatory). Alternative splicing at splice site A and the C-terminal tail (splice site C) generates isoform diversity in the first cytosolic loop and the calmodulin-binding domain, respectively. The PMCA's C-terminal tail contains essential regulatory domains, which bind to the catalytic domain at rest and inhibit the PMCA (indicated by the dashed box in Figure 2). When Ca^{2+} influx is elevated, Ca^{2+} -CaM binds to this autoinhibitory domain, it undergoes a conformational shift that decreases its affinity for the catalytic site (indicated by the dashed box A in Figure 2), thereby enhancing the PMCA's ability to transport Ca^{2+} (Carafoli, 1994).

In Figure 3, the impact of alternative splicing at sites A and C is illustrated for each of the four PMCA genes. Although PMCA1 and PMCA4 are present in most tissues, PMCA2 and PMCA3 are expressed in a limited number of tissues, including the brain, striated muscle, and mammary gland. PMCA2 is highly concentrated in specialized cells and tissues such as cerebellar Purkinje neurons, cochlear hair cells, and the

uterus and lactating mammary glands. It is also present in high levels in the liver and kidney. PMCA3 has a relatively restricted distribution, with high expression levels in the choroid plexus (Brini and Carafoli, 2009).

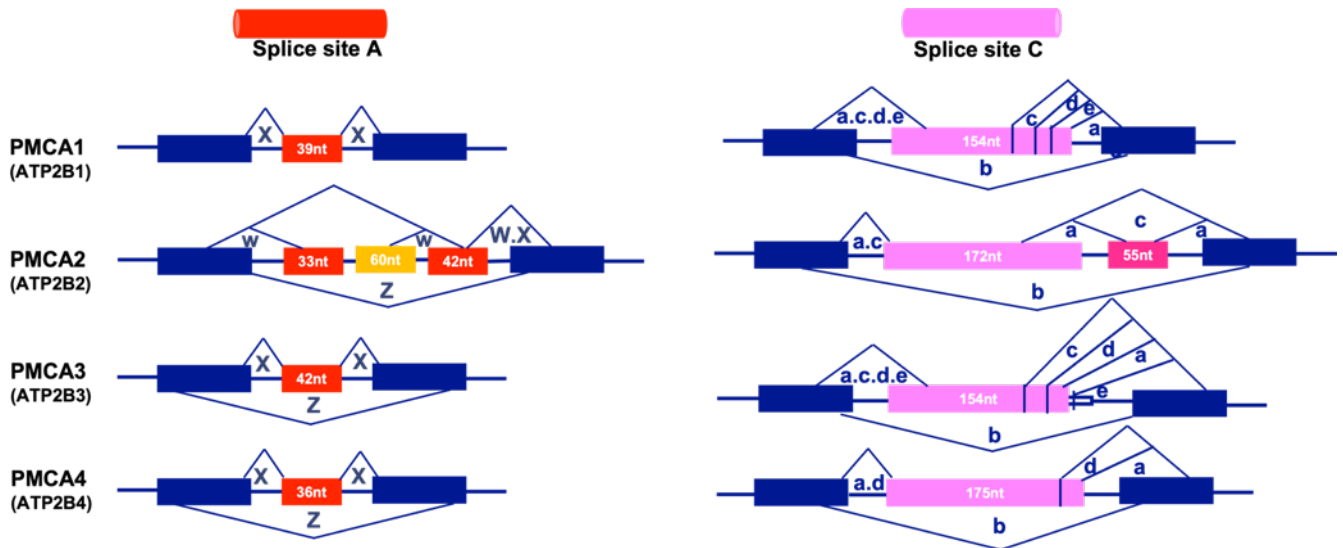


Figure 3: Exon structure of the regions in alternative splicing from the four mammalian PMCA genes

The figure illustrates the exon structure of the PMCA genes and the regions impacted by alternative splicing at sites A and C. The PMCA genes are represented by horizontal bars, and the constitutively spliced exons are depicted as dark blue boxes. The areas impacted by alternative splicing at sites A and C are highlighted in different colors and their sizes are given in nucleotides. The alternative splicing possibilities are represented by connecting lines, and the resultant splice products are designated by lowercase symbols. Splicing at site C leads to two primary RNAs "a" and "b," which differ in the encoded protein.

1.2.2 Regulation of intracellular Calcium level by PMCA

Ca^{2+} is an important second messenger involved in the transduction of numerous signaling pathways and plays a variety of roles in the development and physiology of the central nervous system. Increases in cytosolic Ca^{2+} concentration occur via a variety of mechanisms, including voltage-gated Ca^{2+} channels (VGCCs) upon

depolarization and ligand-gated Ca^{2+} channels, such as the N-Methyl-d-Aspartate (NMDA) ionotropic glutamate receptor (NMDAR), which allows Ca^{2+} influx upon glutamate binding (Flavell and Greenberg, 2008).

PMCA uses ATP as an energy source to transport calcium ions out of the cell, against their concentration gradient. This process aids in the maintenance of low intracellular calcium levels, thereby regulating the concentration of calcium ions within and outside the cellular environment. This regulation is crucial for diverse cellular functions, including muscle contraction, neurotransmitter release, and gene expression (Carafoli, 1991; Strehler and Zacharias, 2001). The plasma membrane contains multiple Ca^{2+} entry channels from the extracellular environment, as well as two systems for Ca^{2+} extrusion: a low affinity, high-capacity $\text{Na}^+ / \text{Ca}^{2+}$ exchanger (NCX) and a high-affinity, low-capacity Ca^{2+} -ATPase (PMCA). PMCA has a high affinity for calcium ions, with a dissociation constant (K_d) in the nanomolar range. This allows PMCA to effectively remove calcium from the cytoplasm even at low calcium concentrations (Di Leva et al., 2008). PMCA activity can be regulated by several mechanisms, such as phosphorylation, calmodulin binding, and interaction with other proteins and other Ca^{2+} -ATPases. For instance, binding of calmodulin to PMCA enhances its activity, while phosphorylation can either enhance or inhibit its activity, depending on the site and the kinase involved. The type of channel and the relative amounts of NCX and PMCA differ depending on the cell type, with NCX being especially prevalent in excitable tissues such as the heart and brain. The controlled opening of Ca^{2+} channels by voltage gating, ligand interaction, or the emptying of intracellular storage enables a restricted amount of Ca^{2+} to enter the cell and relay signals to their assigned targets (Brini and Carafoli, 2011). PMCA is involved in regulating cellular Ca^{2+} homeostasis. In addition to PMCA, the sarco/endoplasmic reticulum Ca^{2+} ATPase (SERCA) and the secretory pathway Ca^{2+} ATPase (SPCA) also play roles in Ca^{2+} regulation (see Figure 4).

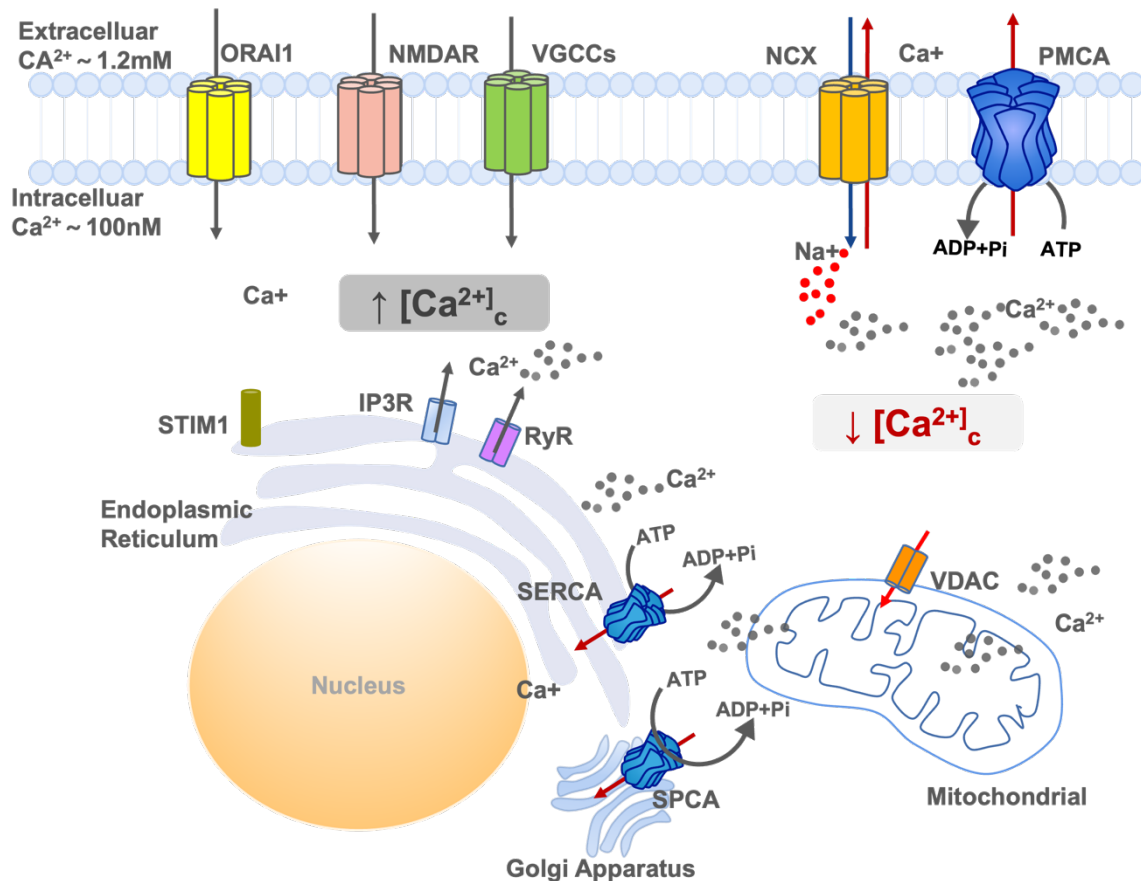


Figure 4: PMCA involved in regulating cellular Ca^{2+} homeostasis

This diagram illustrates the structures involved in regulating cellular Ca^{2+} homeostasis. The diagram includes Ca^{2+} -ATPases, such as plasma membrane Ca^{2+} ATPase (PMCA), sarco/endoplasmic reticulum Ca^{2+} ATPase (SERCA), and secretory pathway Ca^{2+} ATPase (SPCA), as well as plasma membrane Ca^{2+} channels, Na^+/Ca^{2+} exchangers (NCX), 1,4,5-triphosphate receptor (IP3R), ryanodine receptor (RyR), and the mitochondrial Ca^{2+} uniporter (U) (Brini and Carafoli, 2011; Bagur and Hajnoczky, 2017). These various Ca^{2+} -transporting mechanisms work together to maintain the Ca^{2+} concentration gradient between the extracellular and intracellular environments, ensuring that Ca^{2+} is available for the appropriate physiological processes.

The tight regulation of intracellular calcium levels is essential for normal cellular function, and PMCA activity, coordination with other calcium transporters, and role in calcium signaling all contribute to achieve this regulation.

1.3 Neuroplastin interaction with PMCA

1.3.1 Complex formation of neuroplastin and PMCA

Plasma Membrane Ca^{2+} ATPase (PMCA) expression requires the support of Neuroplastin as an auxiliary subunit. Bhattacharya et al. (2017) first reported that the expression of PMCA is reduced in mice lacking neuroplastin. Korthals et al. (2017) conducted experiments that showed a reduction of over 70% in PMCA levels in *Nptn*^{-/-} T cells. This reduction provides a potential explanation for the altered handling of Ca^{2+} and identifies plasma membrane Ca^{2+} ATPases (PMCA) as the primary molecular-level interaction partners of neuroplastins.

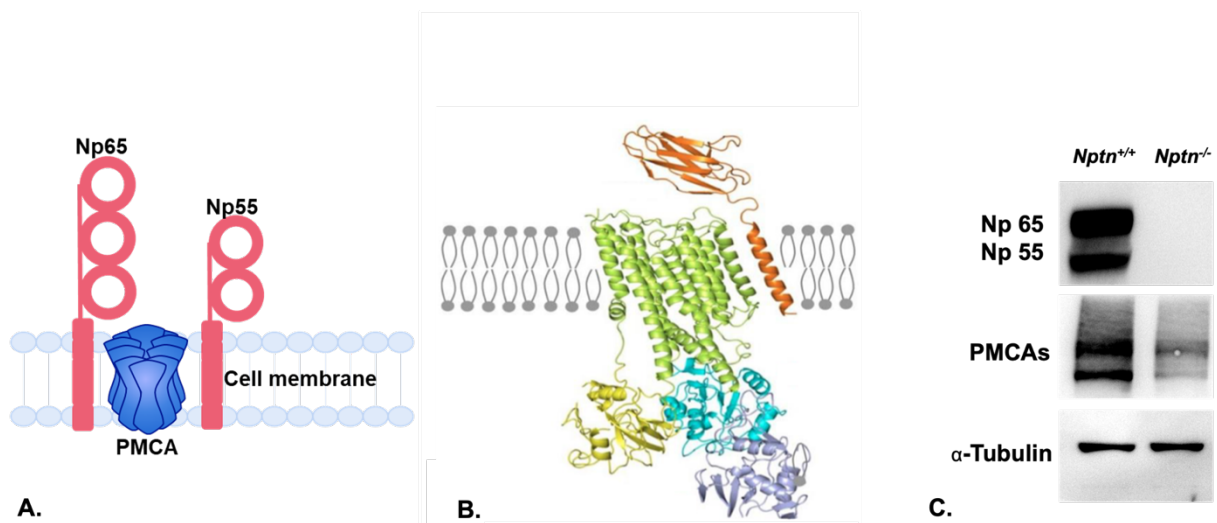


Figure 5: Complex formation of neuroplastin and PMCA

A. Neuroplastin forms a complex with PMCA. **B.** Cited from (Gong et al., 2018), this is a model of the interaction between PMCA and neuroplastin based on cryo-electron microscopy. The transmembrane domain of neuroplastin (in orange) interact with the transmembrane domains of PMCA in the cell membrane (in green). The intracellular portion of PMCA consists of an actuator (in yellow), nucleotide-binding sites (in purple), and phosphorylation sites (in blue). **C.** PMCA expression levels are severely reduced in neuroplastin-deficient mice.

1.3.2 Regulation of intracellular Calcium levels by neuroplastin and PMCA

Recent studies have identified that PMCA and neuroplastin can form heterotetramers consisting of two neuroplastins and two PMCA subunits (Schmidt et al., 2017; Gong et al., 2018). Basigin, a CAM closely related to neuroplastin, can also form heterotetramers with PMCA, although to a lesser extent than neuroplastin. When neuroplastin is deleted, the level of Basigin can be partially increased and association for PMCAs. However, the ability of cells to extrude calcium is impaired when neuroplastin is knocked out, leading to an increase in basal calcium levels. This effect can be further amplified by also eliminating Basigin (Schmidt et al., 2017).

HEK cells, known for their reliable and rapid growth as well as their propensity for transfection, were used to investigate the interaction between neuroplastin and PMCA. The HEK cells experiments from Herrera-Molina et al. (2017) revealed that neuroplastins in rat and human can promote PMCA protein levels. A neuroplastin mutation that is retained in the endoplasmic reticulum (ER) was used in further experiments by Schmidt et al. in 2017, which showed that the interaction between the proteins probably occurs during the early stages of protein biosynthesis. PMCAs do not reach the plasma membrane in these conditions and are most likely degraded in *Nptn*^{-/-} CHO cells. The fact that PMCAs are uniformly reduced in all membrane compartments in neuroplastin knockout (*Nptn*^{-/-}) cells and that PMCA mRNA levels are unaffected by neuroplastin deletion supports the idea that the interaction occurs during protein biosynthesis (Herrera-Molina et al., 2017).

The precise location of the interaction between neuroplastins and PMCAs is critical for understanding the interaction between these proteins. Studies involving the transmembrane segment along with the adjacent N- and C-terminal domains of the neuroplastin protein show that these regions interact with PMCA and influence calcium levels, suggesting that the Ig domains of neuroplastin are not involved. (Schmidt et al., 2017). The presence of a glutamate residue within the transmembrane domain may be crucial for this interaction, as it is at an uncommon place for a hydrophilic amino acid and is also present in another PMCA binding partner, Basigin.

1.4 Hormone regulation in male mice fertility

1.4.1 Spermatogenesis

Spermatogenesis is a complex process that occurs in the seminiferous tubules of the testis, leading to the formation of mature spermatozoa from germ cells. The process begins with the mitotic division of spermatogonial stem cells located near the basement membrane of the tubules (de Kretser et al., 1998). Spermatogonial stem cells undergo mitosis to produce two types of cells, type A and type B. Type A cells give rise to more stem cells, while type B cells differentiate into primary spermatocytes.

Primary spermatocytes then undergo meiosis I to form two haploid secondary spermatocytes, which undergo meiosis II to form four haploid spermatids. These spermatids further mature and differentiate into spermatozoa or sperm cells. Therefore, each primary spermatocyte produces four haploid sperm cells, which contain half the number of chromosomes as the parent cell (Table 2 and Figure 6). This process is critical for male fertility and is regulated by various factors, including hormones, growth factors, and other signaling molecules.

Stage of cycle	Cell type	Ploidy/chromosomes
Spermatocytogenesis	Spermatocytogonia Type A Spermatocytogonia Intermediate type Spermatocytogonia Type B	Diploid (2N) / 40
Spermatidogenesis I	Primary spermatocytes	Diploid (2N) / 40
Spermatidogenesis II	Secondary spermatocytes	Haploid (N) / 20
Spermiogenesis	Spermatids	Haploid (N) / 20

Table 2: Summary of spermatogenesis

Indeed, spermatogenesis is crucial for successful sexual reproduction, and its progression is highly reliant on favorable environmental conditions. The process initiates in the basal compartment of the seminiferous tubules and continues through different maturation stages until mature spermatozoa reach the lumen, where they are eventually ejaculated. Notably, spermatogenesis occurs in an asynchronous manner, resulting in the production of cells at different maturation phases. When a cross-section of the tubule is taken, distinct phases of maturation can be observed. These observations suggest that spermatogenesis occurs in waves, with groups of cells at various maturation stages being produced at the same time (Schulze, 1982).

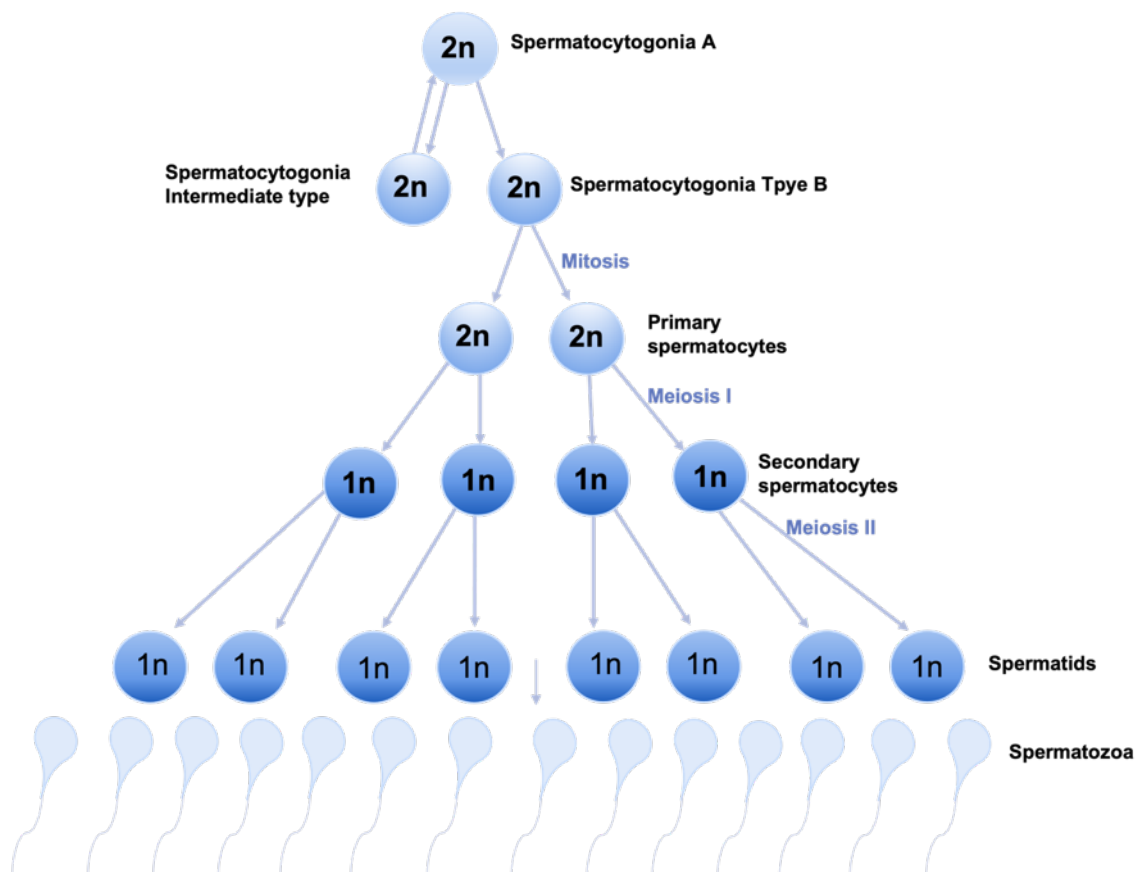


Figure 6: Progress of spermatogenesis

The process of spermatogenesis in mice can be classified into several distinct stages, each corresponding to a specific type of cell. It takes approximately 35 days or four cycles for spermatogonial stem cells to undergo multiple differentiation steps to become spermatozoa. As the process progresses, germ cells migrate gradually from the basement membrane towards the lumen, where they are eventually released (Oakberg, 1956).

Seminiferous tubules, located in the testicles, are the specific sites where spermatogenesis occurs. They contain Sertoli or sustentacular cells, which are tall and columnar in shape, and line the tubules. Spermatogenic cells, which differentiate through meiosis to become sperm cells, are located between the Sertoli cells (refer to Figure 7).

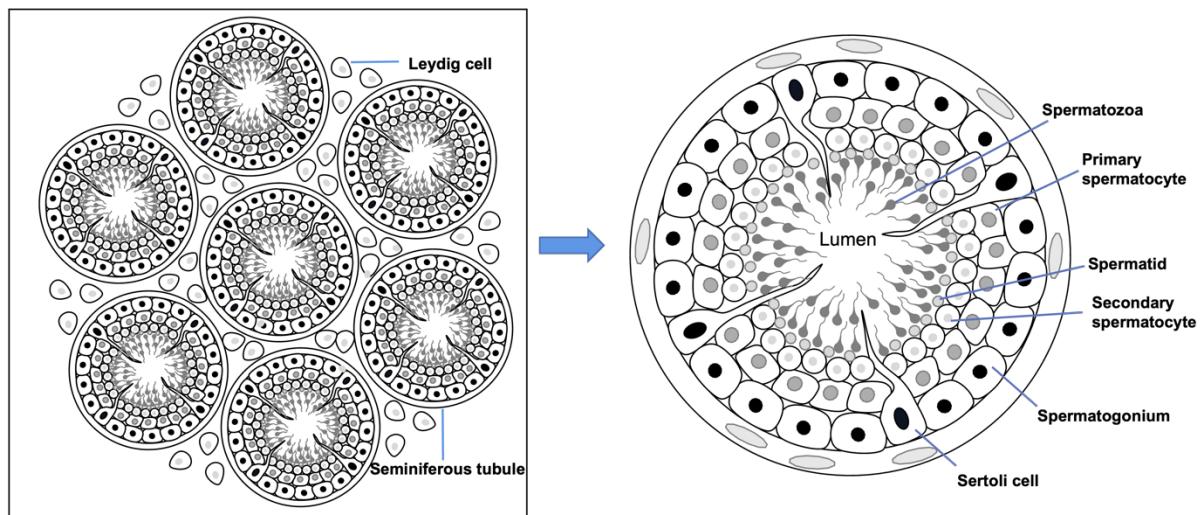


Figure 7: Structure of seminiferous tubule

A cross section of the seminiferous tubule reveals that the tubule is divided into two compartments by the Sertoli cell. Spermatogenic cells locate in the space between the Sertoli cells and undergo meiosis to develop into sperm cells. Mature spermatozoa are discharged into the tubule lumen (de Kretser et al., 1998).

Testosterone is an essential hormone required for spermatogenesis and male fertility. Without testosterone or activation of the androgen receptor (AR), spermatogenesis does not progress beyond the meiosis stage (Walker, 2009). When testosterone is withdrawn, germ cells that have advanced beyond meiosis detach from the supporting Sertoli cells and perish, resulting in sterility. In addition, mature sperm cannot be

released from Sertoli cells in the absence of testosterone, leading to further infertility (Walker, 2010).

AR is expressed in the testis in peritubular myoid cells that surround the seminiferous tubules and in Leydig cells located between the seminiferous tubules. However, only Sertoli cells have testosterone receptors within the seminiferous tubules, germ cells do not express AR. Therefore, Sertoli cells are the primary transmitters of testosterone signals that are essential for germ cell survival and growth (Sar et al., 1990; Walker, 2010).

1.4.2 Hormonal regulation of Spermatogenesis

Hormonal modulation of spermatogenesis varies between animal species. The interaction of the hypothalamus, pituitary gland, and Leydig cells triggers the onset of spermatogenesis during puberty. Leydig cells, also called interstitial cells of the testes, are situated in the testicles near the seminiferous tubules and synthesize testosterone in the presence of luteinizing hormone (LH) (Shima et al., 2013). In rats, fetal Leydig cells begin producing testosterone at 15.5 days into pregnancy and reach peak levels before birth. In contrast to rats, in mice, the initial development of fetal interstitial cells or testosterone production does not require LH. Instead, it involves the production of androstenedione, which is then converted into testosterone by fetal Sertoli cells. Subsequently, fetal Leydig cells express Luteinizing Hormone Receptor (LHR) and respond to LH stimulation (Zirkin et al., 2018).

LH, a hormone generated by the anterior pituitary gland's gonadotropic cells, is regulated by the hypothalamic gonadotropin-releasing hormone (GnRH) (Stamatiades and Kaiser, 2018). LH works in conjunction with follicle-stimulating hormone (FSH). When blood testosterone levels are low, the pituitary gland releases LH. As testosterone levels rise, it acts on the pituitary in a negative feedback loop, inhibiting the release of GnRH and LH. Androgens such as testosterone and dihydrotestosterone inhibit monoamine oxidase (MAO) in the pineal gland, resulting in

increased melatonin and decreased LH and FSH via melatonin-induced increases in gonadotropin-inhibitory hormone (GnIH) synthesis and secretion (Stamatiades and Kaiser, 2018).

FSH stimulates both Sertoli cell synthesis of androgen-binding protein (ABP) and the development of the blood-testis barrier. ABP is necessary to maintain testosterone concentrations high enough to initiate and sustain spermatogenesis. Sertoli cells, which are in close contact with spermatogenic cells at all stages of differentiation, offer structural and metabolic support to developing sperm cells (Griswold, 1998). They have several roles during spermatogenesis, including facilitating the maturation of germ cells into spermatozoa through direct contact and by regulating the environment within the seminiferous tubules (Griswold, 1998). They secrete supportive testicular fluid and ABP, which concentrates testosterone near developing gametes. They also secrete pituitary gland-controlled hormones that regulate spermatogenesis, particularly the polypeptide hormone inhibin. Sertoli cells also phagocytose remaining spermiogenesis cytoplasm and establish and maintain the spermatogonial stem cell niche, ensuring stem cell renewal and the differentiation of spermatogonia into mature germ cells that progress through the long process of spermatogenesis, culminating in the release of spermatozoa in a process known as spermiation. However, the primary function of Sertoli cells is to nourish growing sperm cells during the phases of spermatogenesis, making them known as the "mother" or "nurse" cells (Rato et al., 2012).

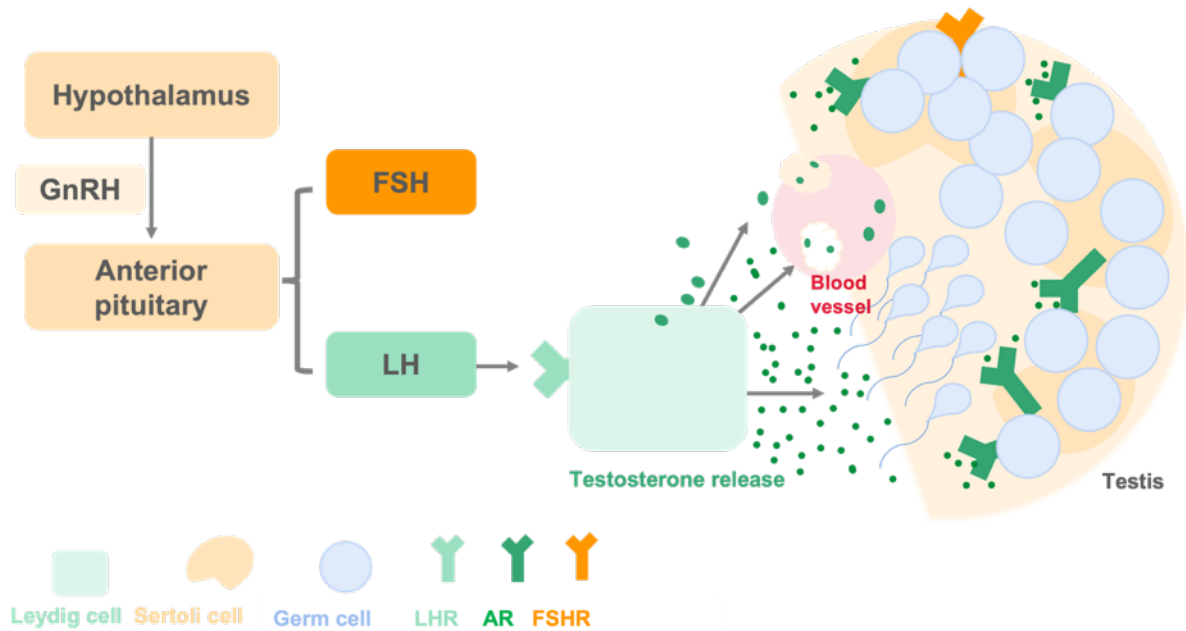


Figure 8: Testosterone release in male mice fertility

The hypothalamus secretes gonadotropin-releasing hormone (GnRH), which stimulates the pituitary gland to release luteinizing hormone (LH) and follicle-stimulating hormone (FSH). LH then travels to the gonads and activates the Leydig cells to produce and release testosterone, which is essential for spermatogenesis. Sertoli cells, on the other hand, require FSH to support spermatogenesis (Rato et al., 2012).

The hypothalamus initiates the release of FSH and LH into the blood for the first time at the commencement of puberty. As seen in Figure 9, FSH enters the testis and induces the Sertoli cells to begin facilitating spermatogenesis via negative feedback. LH also reaches the testis and stimulates the Leydig interstitial cells to produce and release testosterone into the testis and blood for virilizing effect and spermatogenesis. Rising testosterone levels could act on the hypothalamus and anterior pituitary to inhibit the release of GnRH, FSH, and LH, resulting in a negative feedback mechanism. When the sperm count is excessively high, the Sertoli cells create the hormone inhibin, which is released into the bloodstream. It would also reduce the release of GnRH and FSH, then cause the spermatogenesis to slow down (Sternbach, 1998).

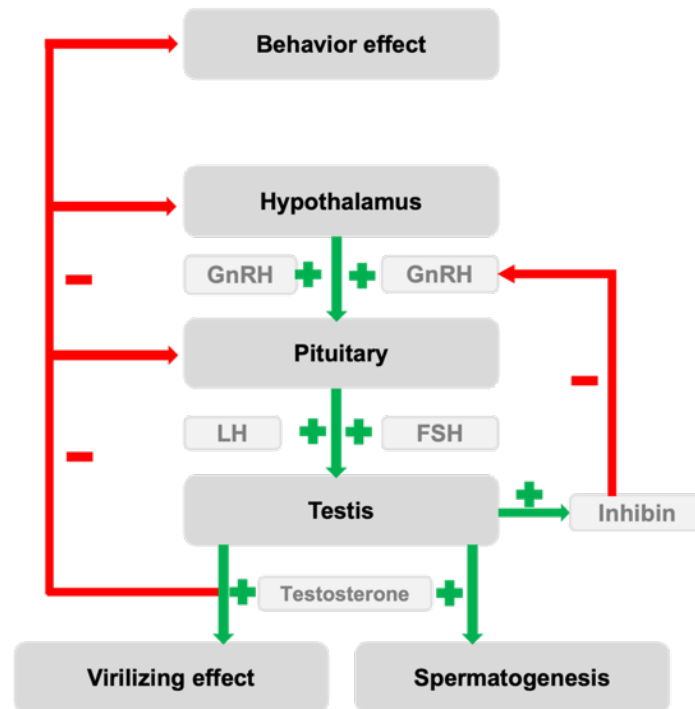


Figure 9: The regulation of male sexual functions by hormones

The diagram depicts several phases, including the hypothalamus, which secretes gonadotropin-releasing hormone (GnRH), the anterior pituitary, which releases follicle-stimulating hormone (FSH) and luteinizing hormone (LH), negative feedback, testosterone secretion, inhibin secretion, and spermatogenesis. When the testes produce excess of testosterone, the brain sends signals to the pituitary gland to reduce LH secretion, which, in turn, instructs the testes to decrease testosterone levels, thereby establishing a negative feedback mechanism. Furthermore, Sertoli cells produce inhibin, which controls FSH secretion through a negative feedback mechanism. This process helps regulate spermatogenesis and maintain a balance of hormones in the male reproductive system

1.4.3 The role of Ca^{2+} in the testosterone signaling pathway

Testosterone is the primary hormone produced by the testes, with Leydig cells responsible for the vast majority of its synthesis (approximately 95%). However, smaller amounts of testosterone are also synthesized by the adrenal cortex (Luu-The and Labrie, 2010). The production and secretion of testosterone are regulated by the stimulation of luteinizing hormone (LH). LH-receptor stimulation leads to an increase in intracellular Ca^{2+} levels in Leydig cells, which triggers testosterone production (Figure 10) (Costa et al., 2010).

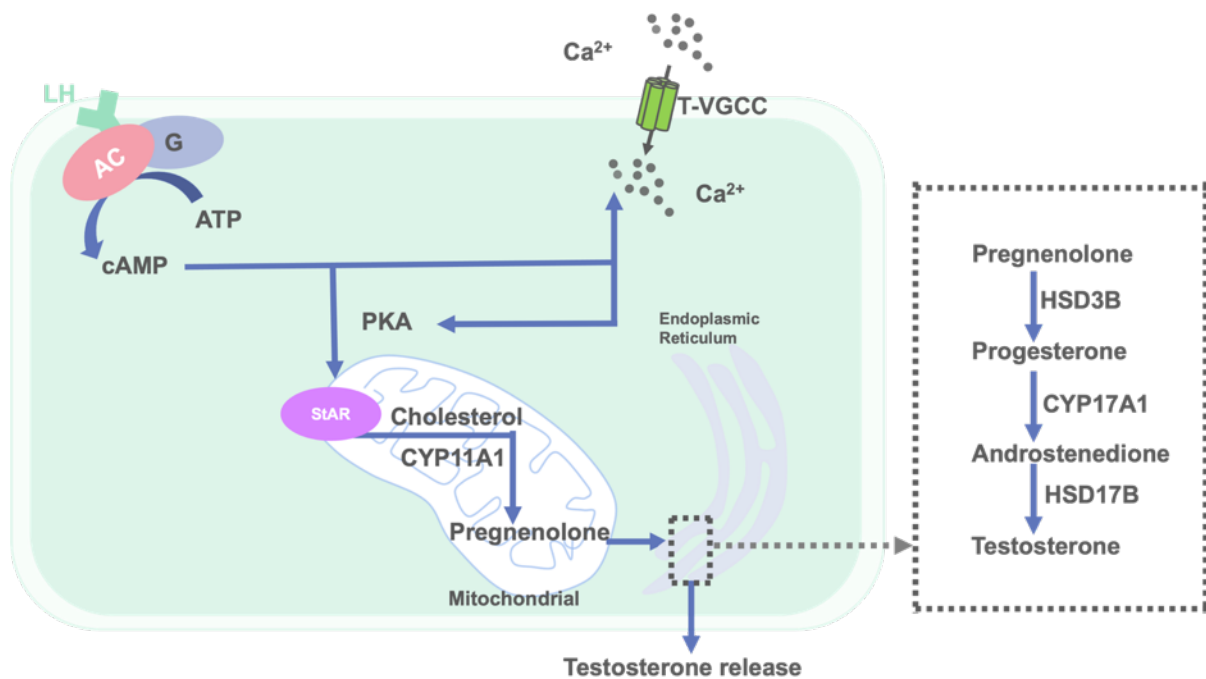


Figure 10: Steroidogenesis in Leydig Cell and testosterone release

When luteinizing hormone (LH) binds to its receptors on the plasma membrane of Leydig cells, a sequence of events is initiated. First, there is an increase in intracellular cyclic adenosine monophosphate (cAMP) formation. Then, cholesterol is translocated into the mitochondria and associates with CYP11A1. Pregnenolone is produced from cholesterol in the mitochondria, and it is translocated from the mitochondria to the smooth endoplasmic reticulum. In the smooth endoplasmic reticulum, pregnenolone is converted to testosterone via a series of reactions. Finally, testosterone is released into the testis and bloodstream (Costa et al., 2010).

After LH binds to the plasma membrane receptor in Leydig cells, a signal cascade reaction is initiated, resulting in the entry of extracellular calcium into Leydig cells through T-type voltage-gated calcium channels (T-VGCC) on the cell membrane (Costa et al., 2010). Concurrently, the activation of adenylyl cyclase (AC) and the subsequent increase in cAMP production results in cholesterol transport to mitochondria facilitated by steroidogenic acute regulatory (StAR) protein and peripheral benzodiazepine receptors (PBR). In the mitochondria, cholesterol is converted to pregnenolone by the action of side-chain cleavage of cytochrome P450 family 11 subfamily A member 1 (CY11A1) (Costa et al., 2010). Pregnenolone then diffuses into the smooth endoplasmic reticulum, where the calcium channels RyRs and IP3Rs of the ER are activated by the influx of calcium ions. Ca^{2+} is then released from the ER into the cytoplasm to facilitate the next step of testosterone release. Pregnenolone is further metabolized to progesterone by the action of 3 β -hydroxysteroid dehydrogenase Δ 5- Δ 4-isomerase (HSD3 β) in the endoplasmic reticulum. Progesterone is then converted to androstenedione by a two-step process involving 17 α -hydrogenase (17 α -OH-enzyme) and C17-20 lyase (CY17A1). Finally, androstenedione is converted by 17 β -hydroxysteroid dehydrogenase III type (HSD17 β) to testosterone. Following biosynthesis, testosterone can be converted to dihydrotestosterone (DHT) by 5 α -reductase or to estradiol by CYP19A1 (aromatase). Testosterone or DHT exert their physiological function through the androgen receptor (Amaral et al., 2013).

Testosterone has been shown to function via two pathways: classical and non-classical (Walker, 2009; Walker, 2010). In the classical testosterone signaling pathway (see figure 11), testosterone diffuses across the plasma membrane and binds to the AR. There are two non-classical testosterone signaling pathways. The first is the kinase activation pathway, in which testosterone interacts with AR, which subsequently recruits and activates Src tyrosine kinase, resulting in intracellular activation of the epidermal growth factor receptor (EGFR). The second is the Ca^{2+} influx pathway (see figure 11) with an influx of Ca^{2+} induced by testosterone via L-type voltage-gated calcium channels (L-VGCC) into Sertoli cells (Gorczyńska and Handelsman, 1995; Lyng et al., 2000). Testosterone is also thought to activate an Gq type G protein-coupled receptor and phospholipase C (PLC), which hydrolyzes PIP2

in the plasma membrane to create IP3 and diacylglycerol (DAG). A decrease in PIP2, induced by an inhibitor of ATP-mediated activation of K^+_{ATP} channels, promotes channel closure, increasing membrane resistance and depolarization of the cell. As a result, voltage-dependent L-type calcium channels open and allow Ca^{2+} to enter the cell, potentially altering several physiological processes (Figure 11) (Von Ledebur et al., 2002; Walker, 2011).

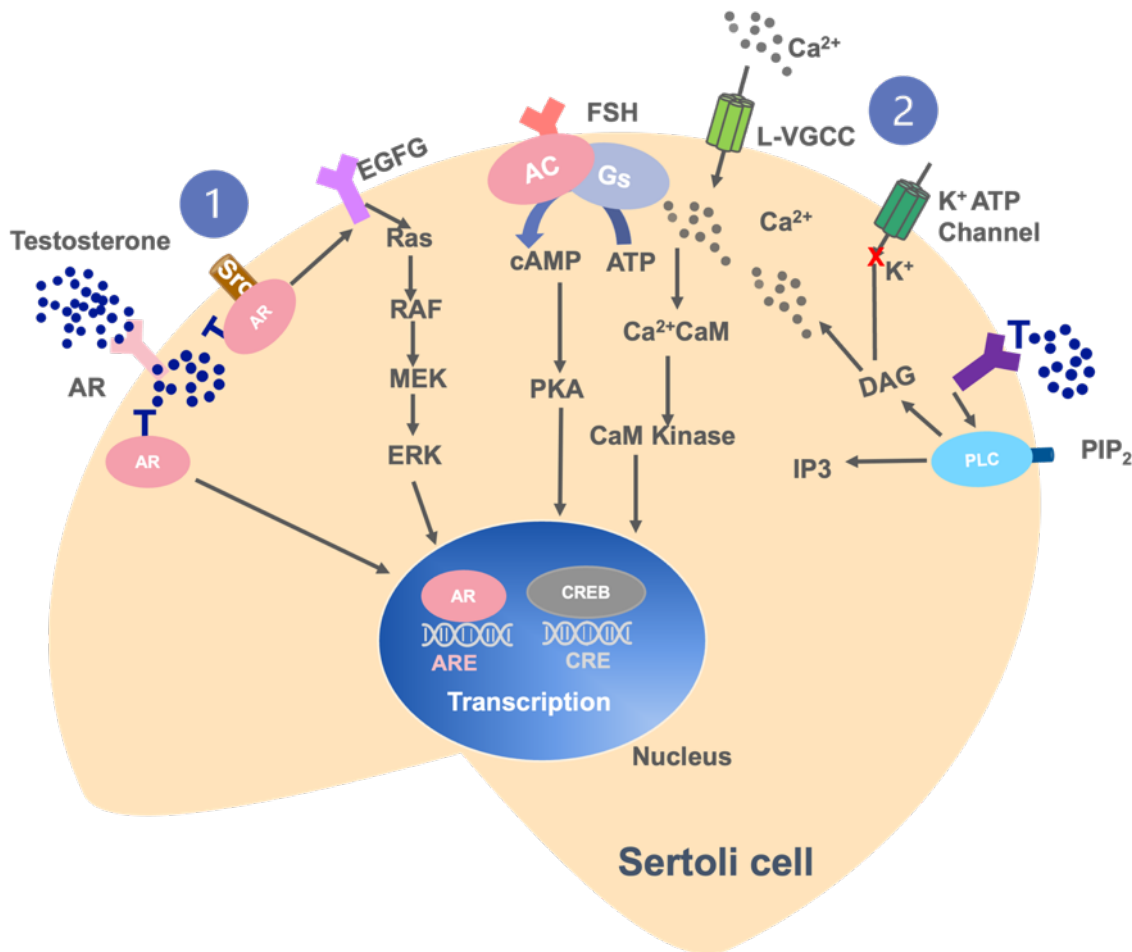


Figure 11: Testosterone signaling pathways in Sertoli cell

The figure is modified from (Walker, 2011). Testosterone signaling pathways in Sertoli cells can be classified into two pathways: 1. classical and 2. non-classical. The Ca^{2+} influx pathway belongs to the non-classical category.

1.5 Neuroplasticity and its role in learning and memory

1.5.1 Associative learning and associative memory

Associative learning and associative memory are related psychological concepts that involve the formation of connections between different stimuli or events. Associative learning is the process by which an organism learns to associate two or more stimuli or events. For example, in classical or Pavlovian training, a dog may learn to identify the sound of a bell with the arrival of food and begin to salivate at the mere sound of the bell (Suzuki and Brown, 2005).

Associative memory, on the other hand, involves the ability to learn and recall the relationship between unrelated information. This could involve recalling someone's name or the scent of a particular perfume (Suzuki and Brown, 2005). This type of memory involves the formation of connections between different pieces of information, allowing them to be retrieved together. For example, if someone is trying to remember the name of a person they met at a party, they may recall other details about the party, such as the location or the food that was served, to help them retrieve the name.

Both associative learning and associative memory are thought to be based on the same underlying neural mechanisms. In particular, they involve the formation of connections, or synapses, between neurons in the brain. These connections are thought to be strengthened through a process known as long-term potentiation (LTP) (Gruart et al., 2017), which is a key mechanism of learning and memory.

1.5.2 Anterograde and retrograde amnesia

Anterograde amnesia refers to the inability to form new memories after an event that caused amnesia, leading to difficulty recalling recent events while long-term memories from before the event remain intact (Markowitsch, 2008). In contrast, retrograde amnesia involves the loss of memories created before an injury or disease occurred but the ability to form new memories remains intact task (Hunkin et al., 1995). Both types of amnesia can occur concurrently in the same patient. The exact mechanism of memory storage in the brain is not fully understood, but it is known that specific areas in the temporal cortex, particularly the hippocampus and surrounding subcortical regions, are involved in the process.

1.5.3 Ablation of neuroplastin induces retrograde amnesia

Neuroplastins play a crucial role in learning and memory. Ablation of the neuroplastin gene can cause retrograde amnesia after an associative learning task (Bhattacharya et al., 2017).

1.6 Hypothesis and aims of the study

1.6.1 State of the art evidence underlying the hypothesis

Neuronal cell recognition molecules have been implicated in synaptic plasticity (Smalla et al., 2000; Maness and Schachner, 2007; Dityatev et al., 2008). Constitutive *Nptn*^{-/-} mice demonstrate neuroplastin actions that are related with pleiotropic consequences for the animal. *Nptn*^{-/-} mice have a shorter life span, higher corticosterone levels, dysregulation of the HPA axis, male infertility, less anxious behavior, motivational deficits, altered social interaction, increased despair-like behavior, and learning deficits (Bhattacharya et al., 2017), which may be linked to psychopathologic conditions such as depression, autism, and affective disorders (Lin et al., 2021a). Neuroplastin deficiency, both constitutive and induced, affects primarily associative learning and memory, such as the acquisition, retention, and retrieval of learned associations, but does not impair all forms of memory. Retrograde amnesia following neuroplastin ablation was consistently detected in the active avoidance and fear

conditioning paradigms but spared other memories. (Bhattacharya et al., 2017). Neuroplastins are binding partners of fibroblast growth factor receptors (Owczarek et al., 2010) and gamma-aminobutyric acid type A (GABA_A) receptors (Herrera-Molina et al., 2014). Recent studies employing hippocampus neurons produced from mice with altered *Nptn* gene expression demonstrate that Np65 regulates both the construction and function of glutamatergic and GABAergic synapses in the hippocampal CA1 and DG regions (Herrera-Molina et al., 2014). PMCA is important for the extrusion of cytoplasmic calcium (Strehler and Thayer, 2018). Bhattacharya et al. (2017) showed a knockdown of neuroplastin affects the PMCA isoforms differently in mouse neurons and *Nptn*^{lox/loxEmx1Cre} mice learned the associative fear conditioning task in the two-way active avoidance (shuttle-box) paradigm and showed that expression of neuroplastins in glutamatergic neurons is not essential for the acquisition (Herrera-Molina et al., 2017).

1.6.2 Hypotheses

- Loss of neuroplastin expression leads to fertility issues of male mice
- The expression of neuroplastins in GABAergic interneurons is crucial for associative memories.

1.6.3 Aims

- To determine the importance of neuroplastin expression in the testes.
- To examine the expression of neuroplastin in the testis and its correlation with PMCA isoforms.
- To deduce the factors preventing reproduction in neuroplastin-deficient male mice
- To clarify the effect of Np expression in GABAergic neurons on retrograde amnesia.
- To determine the primary GABAergic neurons expressing neuroplastins responsible for retrograde amnesia.
- To investigate the variations in PMCA2 expression among different neuroplastins mutant mice.

2 Materials and methods

2.1 Materials

2.1.1 Antibodies

Antibodies	Class/Clone	Host/ Isotype	Supplier	Catalog No.	Dilution
Anti-Sox9	Polyclonal	Rabbit	EMD Millipore	AB5535- 25UG	1:500(IHF)
Anti-PMCA ATPase	Monoclonal	Mouse/ IgG2	Thermofisher	MA3-914	1:500(IHF)
Anti-Neuroplastin 55/65	Polyclonal	Sheep/ IgG	R&D Systems	AF7818	1:300(IHF) 1:1000(WB)
Anti-Neuroplastin 65	Polyclonal	Goat/ IgG	R&D Systems	AF5360	1:1000(WB)
Anti- α -SMA	Polyclonal	Rabbit/ IgG	Abcam	ab5694	1:500(IHF)
Anti-Cytochrome P450 17A1	Monoclonal	Rabbit	Abcam	ab12502 2	1:500(IHF)
Anti-Stra8	Polyclonal	Rabbit	Abcam	ab49602	1:500(IHF)
Anti- α -Tubulin	Monoclonal	Rabbit/ IgG	Cell Signaling	2125	1:1000(WB)
Anti-HSD3B1	Polyclonal	Rabbit/ IgG	Sigma Aldrich	HPA0432 64	1:500(IHF)
Anti-Actin	Monoclonal	Sheep/ IgG1	Thermofisher	AM4302	1:500(IHF)
Anti-GAPDH	Monoclonal	Mouse/ IgG1	Santa Cruz	sc-47724	1:5000(WB)
Anti-PMCA1	Polyclonal	Rabbit/ IgG	Thermofisher	PA1-914	1:500(IHF) 1:1000(WB)
Anti-PMCA2	Polyclonal	Rabbit	Abcam	ab3529	1:500(IHF) 1:1000(WB)
Anti-Parvalbumin	Monoclonal	Mouse	Sigma Aldrich	MAB1572	1:500(IHF)
Anti-Parvalbumin	Polyclonal	Rabbit/ IgG	Thermofisher	PA1-933	1:500(IHF)
Anti-Calbindin	Monoclonal	Mouse/ IgG1	Swant	300	1:500(IHF)
Anti-LH-receptor	Polyclonal	Rabbit/ IgG	Thermofisher	PA5- 115508	1:500(IHF) 1:1000(WB)
Anti- anti-PKARIIa	Monoclonal	Mouse/ IgG1	BD Biosciences	612242	1:500(IHF) 1:1000(WB)

Table 3:Primary Antibodies

Secondary Antibodies	Host/ Isotype	Supplier	Catalog No.	Dilution
Cy3-Anti-Sheep IgG(H+L)	Donkey	Jackson Immuno Research	713-165-147	1:1000
Cy5-Anti-Mouse IgG(H+L)	Donkey	Jackson Immuno Research	715-175-151	1:1000
Cy5-Anti-Rabbit IgG(H+L)	Donkey	Jackson Immuno Research	711-175-152	1:1000
Alexa Fluor 488-Anti-Mouse IgG(H+L)	Goat	Jackson Immuno Research	115-545-003	1:1000
Alexa Fluor 488 Phalloidin -iFluor	-	Abcam	ab176753	1:1000
Anti-Goat IgG(H+L)	Donkey	Jackson Immuno Research	705-035-003	1:5000
Anti-Sheep IgG(H+L)	Donkey	Jackson Immuno Research	713-035-147	1:5000
Anti-Rabbit IgG(H+L)	Donkey	Jackson Immuno Research	711-035-152	1:5000

Table 4: Secondary Antibodies

2.1.2 Chemicals

Chemicals	Supplier	Product/Order number
DAPI Fluoromout-G	Southern Biotech	0100-20
Tamoxifen	Sigma Aldrich	T5648
Protease inhibitor cocktail	Roche	4693116001
Acetone	Roth	9372.5
Ethanol	Roth	9065.4
Methanol	Roth	8388.2

Table 5: Chemicals

2.1.3 Buffers and solutions

Solution	Composition/ Catalog number	Application
PCR-Tail solution	102-T	Isolation of DNA from tail cuts
DNA sample loading buffer	30% glycerol, 0.25% Bromopheol Blue, 0.25% Xylenecyanol, 50mM EDTA, pH8.0	Loading dye for agarose gel electrophoresis
Protein extraction buffer A	8ml (2M Sucrose) 0.5ml (0.5M HEPES) 41.5ml H ₂ O 1 Tablet Omplete ULTRA phosphatase inhibitor cocktail (Total 50ml)	Extraction of proteins
500 mM HEPES	5.958 g HEPES, pH 7.4, 50 ml ddH ₂ O	For Buffer A
2 M Sucrose	410,76 g Sucrose, 600 ml ddH ₂ O	For Buffer A
Cell lysis extraction buffer recipe	0.5 m EDTA 100µl 0.5m EGTA 100µl 1M Tris 7.5 pH 5ml 1M NaCl 7.5 ml 1% Triton X-100 0.5ml 0.5% SD 0.25g (for 50ml) D.H ₂ O ca 37ml 50ml/1 phosphatase inhibitor cocktail	Extraction of proteins from membrane and cytoplasmic fractions
Phosphate Buffer Saline(10XPBS)	1.37 M NaCl, 2.7 M KCl, 14 mM KH ₂ PO ₄ , 43 mM Na ₂ HPO ₄ add pH 7.3-7.4 with 1N NaOH	Washing, Perfusion, Storage
Tris Buffer Saline (10x TBS)	200 mM Tris-HCl, 1.5 M NaCl, pH 7.4	Antibody incubation and washing
Wash solution	Methanol: acetic acid (9:1) 450 ml methanol, 50ml acetic acid	Purification of proteins for determination
Amido Black solution	14.4 g Amido Black, 1L wash solution	Staining solution
Eosin	Sigma 10132	Staining solution
Ponceau stain	Sigma 78376	Staining solution
Trypan blue	Sigma T8154	Staining solution

BSA standard	Stock solution of 1mg BSA in 1ml H ₂ O(1µg/µl)	Standard curve for protein determination
Precision Plus Protein Standards	Bio-Rad 161-0374	Western blot
Mild stripping buffer	15 g glycine 1 g SDS 10 ml Tween 20 Dissolve in 800 ml distilled water Adjust pH to 2.2 Bring volume up to 1L with distilled water	Reprobing a western blot
Harsh stripping buffer	20 ml SDS 10% 12.5 ml Tris HCl, pH 6.8, 0.5 M 67.5 ml distilled water Add 0.8 ml β-mercaptoethanol under the fume hood	Reprobing a western blot
LDS-Sample Buffer 4X	Thermofisher B0007	Denaturing sample buffer for SDS-PAGE
SDS Loading buffer 2x	125 mM Tris-HCl, pH 6.8, 4% SDS, 20% glycerin, 0.2% bromophenol blue, 10% β- mercaptoethanol.	Denaturing sample buffer for SDS-PAGE
Electrophoresis buffer 10x	1610772	For protein electrophoresis
Blotting buffer 10x	0.25 M Tris-base, 1.92 M glycine, 0.2% SDS	Transfer buffer with 15% methanol and antioxidant for reduced samples
Cryoprotection solution	150 ml ethylene, 150 ml glycerine, 50 ml 1xPBS for 500ml	Protect certain material from freezing damage
Poly-D-Lysin solution	100 mg/ml in 0.15 M boric acid, pH 8.4	Facilitate cell adhesion to tissue culture-treated plastic and glass surfaces.
HEPES saline (HS) medium	135 mM NaCl, 5 mM KCl, 2 mM CaCl ₂ , 1 mM MgCl ₂ , 30 mM Hepes, 10 mM glucose, 10 mM lactic acid, and 1mM sodium pyruvate (pH 7.4)	Sperm isolated medium

Table 6: Buffers and solution

2.1.4 Kits and equipment

Kits /Devices	Supplier	Catalog number
PCR core kit	QIAGEN	201225
Rneasy	QIAGEN	74104
Testosterone ELISA Kit	TECAN IBL International	RE52151
Follicle Stimulating Hormone ELISA Kit	TECAN IBL International	RE52121
Luteinizing Hormone ELISA Kit	USCN life sciences	E90441Mu

Table 7: Kits

Equipment	type	Supplier
Confocal Microscope	SP5	Leica
Microscope	Axioplan2	Zeiss
Centrifuge		Eppendorf AG
ECL-Imaging		Intas
Flowcytometer	PAS III	Sysmex Deutschland
QIAxcel Advanced		QIAGEN
PCR Cycler		Eppendorf

Table 8: Equipment

2.1.5 Gene expression assays

Tagman gene expression assay	Assay ID
Neuroplastin	Mm00485993_m1 Mm00485990_m1
Corticotropin Releasing Hormone	Mm04206019_m1
Glucocorticoid receptor	Mm00433832_m1

Table 9: Gene expression assays

2.2 Mice

Mouse lines	Detail
<i>Nptn</i> ^{lox/lox}	Floxed <i>neuroplastin</i> allele(lox) mice
<i>Nptn</i> ^{-/-}	Neuroplastin-deficient(ko) mice
<i>Nptn</i> ^{lox/loxAmhCre}	Lacking neuroplastin conditionally in Sertoli cells
<i>Nptn</i> ^{lox/loxStra8Cre}	Lacking neuroplastin conditionally in spermatogonia cells
<i>Nptn</i> ^{lox/loxAmhCre+Stra8Cre}	Lacking neuroplastin conditionally in Sertoli cells and spermatogonia cells
<i>Nptn</i> ^{lox/loxEmx1Cre}	Glutamatergic neuron-specific Neuroplation-deficient mice
<i>Nptn</i> ^{lox/loxPrCreERT}	Inducible neuron-specific neuroplastin-deficient mice
<i>Nptn</i> ^{lox/loxGAD2CreERT}	GABAergic neuron-specific inducible-Np-deficient mice
<i>Nptn</i> ^{lox/loxEmx1CreGAD2CreERT}	Glutamatergic neuron-specific and GABAergic neuron-specific inducible-Np-deficient mice

Table 10: List of mouse lines

Neuroplastin-deficient mice *Nptn*^{-/-} (*Nptn*^{tm1.2Mtg}) and floxed *Nptn*^{lox/lox} mice with neuronspecific inducible PrCreERT (*Nptn*^{lox/loxPrCreERT}) or with conditional lack of neuroplastin in Emx1-expressing cells (*Nptn*^{lox/loxEmx1Cre}) were described and used in previous studies by Bhattacharya et al. (2017) and Herrera-Molina et al. (2017). Mice lacking neuroplastin conditionally in Sertoli cells (*Nptn*^{lox/loxAmhCre}) or spermatogonia cells (*Nptn*^{lox/loxStra8Cre}) were obtained by crossing floxed *Nptn*^{lox/lox} mice with 129S.FVB-Tg (Amh-cre)8815Reb/J (The Jackson Laboratory) or B6.FVB-Tg(Stra8-cre)1Reb/LguJ (The Jackson Laboratory), respectively, and further backcrossing to *Nptn*^{lox/lox} mice. Double Cre-mutants (*Nptn*^{lox/loxAmhCre+Stra8Cre}) lacking neuroplastin in Sertoli cells and in spermatogonia were obtained by intercrossing the single mutants.

To obtain *Nptn*^{lox/loxEmx1Cre} mice, B6.129S2-Emx1tm1(Cre) (The Jackson Laboratory) were crossed with *Nptn*^{lox/lox} mice and maintained on a *Nptn*^{lox/lox} background. Similarly, Gad2-CreERT2- mice (The Jackson Laboratory) were crossed with *Nptn*^{lox/lox} mice and maintained on a *Nptn*^{lox/lox} background. *Nptn*^{lox/loxGAD2CreERT} mice allowed inactivation of

the neuroplastin gene in GABAergic interneurons by tamoxifen activation of the GAD2 promoter driven Cre recombinase. *Gad2-CreERT2* drivers provide robust and flexible genetic tools to manipulate GABAergic neurons throughout the mouse CNS (Taniguchi, He et al. 2011). For double Cre mutants (*Nptn^{lox/loxEmx1CreGAD2CreERT}*), the glutamatergic neuron-specific and GABAergic neuron-specific inducible-Np-deficient mice were obtained by intercrossing the mutants *Nptn^{lox/loxEmx1Cre}* and *Nptn^{lox/loxGAD2CreERT}*.

Mice were housed under a 12-hour light/dark cycle with ad libitum access to food and water. Animal husbandry and tissue collection were conducted in accordance with German (Tierschutzgesetz TierSchG) and European legislation (European Communities Council Directive (2010/63/EU) for the care of laboratory animals) and with the respective legal approval by the legal authorities (Landesverwaltungsamt Halle, Sachsen-Anhalt, Germany).

2.3 Methods

2.3.1 DNA isolation from mouse tails/ears

DNA isolation is the process of extracting DNA from cells or tissues in order to obtain pure DNA for downstream applications such as PCR, sequencing, or cloning. Here we did the DNA isolation from the tails. Tissue lysis: The tail was cut about 0.5 cm long and first lysed with 200µl PCR-Tail solution containing 4µl Proteinase K in 1.5ml Eppendorf Tubes to release the DNA. The DNA-lysis solution was left to shake overnight at 55°C, then allowed to settle at 85°C for 1 hour.

Removal of protein and other contaminants was done after cooling down the DNA-lysis solution to room temperature. This step was proceeded by centrifugation at 4°C with 8000 rpm in 10 minutes. The DNA suspension was collected as the resulting DNA solution could then be quantified and used for downstream applications.

2.3.2 Genotyping for detection of the *Nptn* alleles

The PCR procedure used for genotyping involves the following steps:

Step	Temperature	Time	
Initial Denaturation	94°C	3 minutes	
Denaturation	94°C	30 seconds	45 Cycles
Annealing	57°C	45 seconds	
Extension	72°C	1 minute	
Final Extension	72°C	7 minutes	
Hold	4°C	—	

Table 11:PCR procedure

Sample preparation: PCR was carried out using Qiagen Taq PCR core kit.

Denaturation: The reaction mixture was heated to a high temperature of 94°C for 3 minutes, to denature the double-stranded DNA into single-stranded DNA.

Annealing: The temperature was lowered to 57°C for 45 seconds, which allows the primers to bind to the single-stranded DNA at the target site. The primers define the boundaries of the DNA segment to be amplified.

Extension: The temperature was raised to 72°C for 1 minute, which is the optimal temperature for the Taq-DNA polymerase to attach to the primers and synthesize a complementary strand of DNA.

Repeat: Steps of 94°C for 30 seconds, 57°C for 45 seconds and 72°C for 1 minute were repeated for 45 cycles. Each cycle doubles the amount of DNA present in the reaction mixture. After the final cycle, the reaction mixture was cooled to room temperature. The amplified DNA product was then used immediately for detection of *Nptn* alleles by QIAxcel Advabced System (Ex=600bp, WT=180bp, Lox=270bp).

Reagent	3 Primer	2Primer
DNA sample solution	4 μ l	4 μ l
H ₂ O	11.75 μ l	12.25 μ l
10X PCR master mix	2.5 μ l	2.5 μ l
5Q-solution	5.0 μ l	5.0 μ l
dNTPS	0.5 μ l	0.5 μ l
1 Primer NP1	0.5 μ l	0.5 μ l
2 Primer NP2	0.5 μ l	0.5 μ l
3 Primer NP5	0.5 μ l	
Taq	0.25 μ l	0.25 μ l

Table 12: PCR reaction

NP1	(AGCAGGGTTTTGATAAGGGGTA)
NP2	(CATCCTCTGCTCATTTTCCTCT)
NP5	(GGCGGAGTACAGTTCTCACTTC)

Table 13: Primer

2.3.3 Protein Extraction

The tissue (brain, testis, sperm) was dissected with clean tools, preferably on ice, and as quickly as possible to prevent degradation by proteases.

The different tissues were placed in round bottom microfuge tubes and immersed in liquid nitrogen to 'snap freeze'. Samples were stored at -80°C for later use or kept on ice for immediate homogenization. For every 1mg of tissue, 10 μ l Buffer A was added to the tube and the mixture was homogenized with an electric homogenizer. The constant agitation was maintained for 2 hours at 4°C by placing it on an orbital shaker in the cold room. The solution was then centrifuged for 20 min at 13,000rpm at 4°C. The prepared aliquot supernatant (the soluble protein extract) placed on ice was poured into a fresh, chilled tube and the sample was stored at -80°C. Freeze/thaw cycles were minimized from this step on.

A second option was occasionally pursued. For a ~5mg piece of tissue, ~300 μ l complete extraction buffer was added into the tube and the mixture was homogenized with an electric homogenizer. The blade was rinsed twice using 300 μ l complete extraction buffer for each rinse, then constant agitation was maintained for 2 hours at 4°C; and again, placed on an orbital shaker in the cold room. The solution was centrifuged for 20 min at 13,000rpm at 4°C. The aliquot supernatant (the soluble protein extract) placed on ice was poured into a fresh, chilled tube and stored sample at -80°C. Freeze/thaw cycles were minimized from this step on.

2.3.4 Protein determination, SDS-PAGE, Western Blotting

Protein determination:

Protein concentration was determined by Amido Black assay using 1mg/ml BSA solution as a standard. For every estimation, double 2ml Eppendorf cups (EP) were prepared for each value. Standards curves were prepared for the samples: 1 μ g, 2 μ g, 4 μ g, 8 μ g, 16 μ g (10 cups). BSA and water were added to make up a total volume of 100 μ l, which equates to 2 μ l per sample (the remaining 98 μ l was supplemented with water). The added 200 μ l Amido black solution for each EP was incubated with the mixture of each sample for at least 20 minutes at room temperature or placed on an orbital shaker at 4°C. After incubation, all samples were centrifuged for 5 minutes with 14000rpm at room temperature. All sample protein were removed from the centrifuge and 1 ml of wash solution was added to each. Centrifugation was repeated for 5 minutes with 14000rpm at room temperature and the supernatant was discarded. The washing procedure was repeated 3x until the supernatant remained colorless. Lastly, the pellet was dried for around 10 minutes until no solution remained in the Eps. The pellet was dissolved in 300 μ l 0.1N NaOH and shaken briefly. The absorbance of the supernatant is measured in a spectrophotometer, using a short path-length flow-through cuvette at a fixed wavelength, the protein estimation was measured at OD620 against 0.1N NaOH.

per Gel	Seperation Gel 8%	Seperation Gel 10%	Seperation Gel 15%	Stacking Gel 5%
Water	3.32ml	2.91ml	2.16ml	1.83ml
Tris pH6.8(0.5M)	-	-	-	0.75ml
Tris pH8(1.5M)	1.5ml	1.5ml	1.5ml	-
20% SDS	30µl	30µl	30µl	15µl
40% Pac	1.2ml	1.5ml	2.25ml	375µl
10%APS	60µl	60µl	60µl	30µl
TEMED	2.4µl	2.4µl	2.4µl	3µl

Table 14: SDS-PAGE Gels

Western blot progress:

The protein samples were denatured using either 2X SDS loading buffer at 95°C for 5 minutes or 4X LDS loading buffer at 70°C for 10 minutes. The electrophoretic gel was prepared according to Table 14. The running buffer was poured into the electrophoresis chamber, the gel was placed inside, and the system was connected to a power supply. Care was taken to ensure that the gel was completely covered with buffer and the comb was carefully removed once the gel had solidified. Each well was loaded with a 5µl Dual-Color prestained Protein Marker followed by 15µl of the protein samples. The gel was run at a low voltage of 60V for approximately 30 minutes for the separating gel, followed by a higher voltage of 110V for the stacking gel, which took about 1.5 hours until the dye migrated from the front to the bottom of the gel. For the electrotransfer step, filter sheets were cut to fit the gel dimensions accurately, and a nitrocellulose (NC) membrane was cut to the same size. The sponge, filter paper, and NC membrane were wetted with methanol in the transfer buffer. The glass plates were separated, and the gel was retrieved. A transfer sandwich was assembled as follows: sponge-filter paper-gel-NC membrane-filter papers. To eliminate any air bubbles between the gel and NC membrane, excess liquid was gently squeezed out. The transfer sandwich was placed in the transfer apparatus, which was kept on ice at 4°C. Transfer buffer was added to the apparatus, ensuring that the sandwich was fully submerged. The electrode was positioned on top of the sandwich, with the NC membrane between the gel and the positive electrode. The transfer was conducted

for 90 minutes at a constant current of 200mA. Following the transfer, the membrane was subjected to blocking and antibody incubation. The membrane was blocked with 5% skimmed milk (5mg milk powder in 100ml of 5%TBST) for 1 hour. Primary antibodies at a dilution of 1:1000 (based on specific antibody requirements) in a blocking buffer of 5% skimmed milk and 5%TBST (1:1) were added and incubated overnight at 4°C. The membrane was then washed four times for 10 minutes each with 5%TBST. A secondary antibody at a dilution of 1:5000 in the blocking buffer was added, and the membrane was incubated for 1 hour at room temperature. Finally, an ECL mix was prepared, and the results were visualized.

2.3.5 Enzyme-linked Immunosorbent assay of hormones

ELISAs were performed exactly according to the instructions provided by the manufacturer. Pipetted volumes of 25µl of each standard, control and sample (5µl sample with 20µl standard A) into the respective wells of a microtiter plate, followed by pipetted volumes of 200µl of Enzyme Conjugate into each well. the plate was covered with adhesive foil, then thoroughly mixed for 10 seconds. The plate was incubated for 60 minutes at room temperature(18-25°C) on an orbital shaker. The adhesive foil was removed, and the incubation solution was discarded. The plate was washed 3 times with 300µl of diluted wash buffer, and excess buffer solution was removed by tapping the inverted plate onto a paper towel. Pipetted volumes of 100µl of TMB substrate were placed into each well and left to incubate for 15 minutes at room temperature. The reaction was stopped by adding 100µl of TMB stop solution into each well. The contents were briefly mixed by gently shaking the plate. Colours would change from blue to yellow if the reaction was successfully stopped. The optical density was measured with a photometer at 450nm within 10 minutes of pipetting the stop solution.

2.3.6 Histological techniques and immunohistochemistry

The experiment performed according to (Bhattacharya et al., 2017):

Testis Immunofluorescence staining:

Adult mice were anesthetized using isoflurane and transcardially perfused with PBS, followed by freshly prepared 4% paraformaldehyde (PFA). The testis was dissected and post-fixed in the same fixative at 4 °C overnight, sequentially infiltrated with 15% and 30% sucrose for 24-48 hours each until it sank to the bottom. Coronal sections, 6 µm thick, were obtained on glass coverslips at -19°C. Subsequently, soaking the glass coverslips with testis for 5-minute in a container filled with cold acetone, the sections were placed in a fume hood for drying.

The testis sections were blocked with 20% horse serum in DPBS for one hour at room temperature and then incubated with primary antibodies in DPBS containing 0.3% Triton X-100 and 20% horse serum overnight at 4°C. Primary antibodies included sheep polyclonal anti-neuroplastin detecting Np65 and Np55 (pan-Np55/65; 1:500, R&D Systems), rabbit polyclonal anti-PMCA1 (1:500, ThermoFisher, Germany), rabbit polyclonal anti-Stra8 (Stimulated By Retinoic Acid 8, used as a marker for spermatogonia and spermatocytes, 1:500, Abcam, Berlin, Germany), anti-CPY11A1 (Cytochrome P450 Family 11 Subfamily A Member 1, marker for Leydig cells, 1:500, Abcam), anti-alpha smooth muscle actin (marker for myoid cells, 1:500, Abcam), and anti-Sox9 (SRY-Box Transcription Factor 9, marker for Sertoli cells, 1:500, EMD Millipore, Darmstadt, Germany). Secondary antibodies were Alexa Fluor 488-conjugated anti-mouse (1:1000, Jackson ImmunoResearch), Cy3-conjugated anti-sheep, and Cy5-conjugated anti-rabbit (1:1000, Jackson ImmunoResearch). After washing with PBS and briefly with water, the sections were mounted on glass slides using fluoromount-G with DAPI (Southern Biotech, Birmingham, AL).

Sperm Immunofluorescence staining:

Two *cauda epididymus* were collected in a petri dish which was previously prepared with DMEM and prewarmed to 37°C. A sharp scalpel blade was used to open the epididymal duct and the sperm was released by shaking the testes softly. The tissue was incubated at 37°C for 10-15 min to allow sperm to swim out. The sperm suspension was thoroughly mixed several times with a pipet. The diluted sperm solution was placed in centrifuge tube and centrifuged at 300 rpm for 5 min, and the supernatant was carefully aspirated with a 200 µL pipette and discarded. Then, 4% paraformaldehyde solution was added to the centrifuge tube, fixed for 3 h, and centrifuged at 300 rpm for 5 min. After removing the supernatant, 0.1 M sucrose

solution was added at room temperature for 3 h, and a pipette was used to smear it on the poly-L-lysine-coated glass coverslips in 12-well plate, predropped with 1% paraformaldehyde and 0.15% TritonX-100. After air-drying, the slides were washed three times in PBS for 5 minutes each to eliminate any residual paraformaldehyde, sucrose, and TritonX-100. Then the sperm were permeabilized in ice-cold acetone (-20 °C) for 5 min and washed in PBS. After washing in PBS, the samples were blocked in 20% horse serum in PBS for 1 hour at room temperature (RT). Sperm were stained using sheep polyclonal antibodies against neuroplastin detecting Np65 and Np55 (pan-Np55/65 1:500, R&D systems). Counterstaining used phalloidin-iFluor 488 green (1:1000, Abcam, Berlin, Germany) and fluoromount-G DAPI (Southern Biotech). Immunofluorescence was visualized using a Leica SP5 confocal microscope.

Brain immunofluorescence Staining:

Adult mice were anesthetized with isoflurane and transcardially perfused with PBS followed by freshly prepared 4% PFA. The brain was dissected and post fixed in the same fixative at 4 °C overnight, serially infiltrated with 15% and 30% sucrose for 24-48 hours each. Coronal sections 30 µm thick were obtained on glass coverslips by using cryostat at -19°C. The Brain sections were blocked (20% horse serum in PBS, one hour, room temperature) and incubated with primary antibodies in DPBS containing 0.3% Triton X-100 and 20% horse serum (overnight, 4°C). Primary antibodies used were sheep polyclonal anti-neuroplastin detecting Np65 and Np55 (pan-Np55/65; 1:300, R&D systems), and rabbit polyclonal anti-PMCA1(1:500, Thermofisher,Germany), rabbit polyclonal anti-PMCA2 (1:500, Abcam,Berlin, Germany), and rabbit polyclonal anti-Parvalbumin, mouse monoclonal anti-Calbindin (1:500, Swant, Switzerland). Secondary antibodies were Alexa Fluor 488-conjugated anti-mouse (1:1000, Jackson Immunoresearch), Cy3-conjugated anti-sheep and Cy5-conjugated anti-rabbit (1:1000, Jackson Immunoresearch). After washing with PBS and briefly with water, the sections were mounted on glass slides with fluoromount-G DAPI (Southern Biotech, Birmingham, AL).

2.3.7 Mouse sperm count

Euthanasia was performed using isoflurane, followed by decapitation of the mouse. The testes were removed from the mouse via a small lateral abdominal incision, creating a cavity using small surgical scissors. The cauda, located at the end of the epididymis and beneath the testes, was identified. Excess fat was trimmed away by making a cut from the junction area. The weight of the cauda was measured and recorded. Next, the cauda was placed in a prewarmed petri dish containing DMEM (Dulbecco's Modified Eagle Medium) at 37°C. Using a sharp scalpel blade, the epididymal duct was opened, and the sperm were released by gently shaking the testes. The tissue was incubated for 15 minutes at 37°C, and the sperm suspension was thoroughly mixed several times using a pipette. Then, 0.5ml of the sperm suspension was transferred from the petri dish into a pre-prepared 1.5ml DMEM tube, being careful to avoid including the epididymal tissue. The contents were gently mixed. The tube was submerged in a water bath set at 60°C for 10-15 minutes. Afterward, the diluted sperm suspension was mixed again, and 20µl of the solution was measured with a pipette and loaded onto one side of a hemocytometer. To assess sperm viability, 5µl of trypan blue was added to the solution and mixed. The loaded hemocytometer chamber was covered with a moistened coverslip. The hemocytometer was then placed on the microscope stage, and the lens was focused on the secondary square before proceeding to count the sperm.

2.3.8 Behavioral experiments

In this section, I provide an introduction to the behavioral experiments that were conducted as part of this study. It is important to note that these experiments were not personally conducted by the author, but they will be discussed in the thesis. Sex- and age-matched littermate wild-type mice were used as control animals for comparison. During the light phase of a 12-hour light-dark cycle, mice underwent a series of behavioral tests. The experimenter conducting the tests was blinded to the genotype of the mice to minimize bias. Initially, general parameters related to health and neurological function were assessed, following the neurobehavioral examination described in previous studies (Montag-Sallaz & Montag, 2003). Subsequently, several behavioral paradigms were employed to evaluate different aspects of mouse behavior. These paradigms included:

Two-way active avoidance test: A standard two-chambered shuttlebox (TSE) was used for conditioning. During the conditioning stimulus (CS, 10 seconds of light), the animals had to move to the dark side of the shuttlebox to avoid an electrical footshock (US, 5 seconds, 0.3 mA pulsed) delivered after the light. The mice were injected with tamoxifen for 10 days and were tested 8 weeks later (80 trials per day). Compartment transitions during the CS were counted as correct or conditioned avoidance reactions, while transitions during the US were counted as unconditioned avoidance reactions.

Mating analysis: Adult socially naive male mice were exposed to socially naive wild-type females for a 30-minute period, and their behavior was recorded using an overhead camera. The latency to mount, number of mounts with thrusts, and duration of sniffing behavior were scored.

Fear conditioning: Mice were trained and tested over two consecutive days. Training involved placing the subject in an operant chamber (San Diego Instruments) and allowing exploration for 2 minutes. An auditory cue was then presented for 15 seconds, followed by a footshock for 2 seconds (1.5 mA unpulsed). This procedure was repeated, and the mice were returned to their home cage 30 seconds after the last trial. After a 24-hour interval, the mice were placed back in the same chamber (context) for a 5-minute test, and freezing behavior was recorded. Following the context test, the mice were placed in a novel environment, and freezing behavior was recorded for 3 minutes. The auditory cue (CS) was then presented for 3 minutes, and freezing behavior was recorded. Freezing scores were expressed as a percentage for each portion of the test.

2.3.9 Statistical analysis

Statview 5.0.1 (SAS Institute, Inc., Cary, NC) was used for analysis of variance, post hoc analysis (Scheffé or Fisher's protected least significant difference), repeated-measures analysis of variance, and t-tests. GraphPad Prism 9.4.1 (San Diego, CA) was used for t-tests and graph design. A p-value less than 0.05 was considered statistically significant.

3 Results

This chapter comprises two parts: the expression of neuroplastins in relation to fertility (Chapter 3.1 to 3.3) and the expression of neuroplastins concerning associative learning and memory (Chapter 3.4 to 3.8). In the first part (Chapter 3.1 to 3.3), built upon prior experimental findings from Bhattacharya et al. 2017 observing that *Nptn*^{-/-} male mice exhibited no mating behavior, leading to a lack of offspring. Additionally, testosterone levels in the blood of *Nptn*^{-/-} male mice were consistently lower than those in wild-type male mice from the age of 3 months to 11 months. Notably, collaborative efforts with our partners Wennemuth & Wiesehofer (University Hospital Duisburg-Essen) revealed that the quantity and concentration of sperm isolated from the cauda of the epididymis in adult *Nptn*^{-/-} mice were comparable to those of their wild-type littermate males. In the second part (Chapter 3.4 to 3.8), drawing on results from Bhattacharya et al. findings in 2017 demonstrated that mice *Nptn*^{-/-} and those induced with *Nptn*^{lox/loxPrCreERT} exhibited impaired learning capacity. The work of Herrera-Molina et al. (2017) also reported that the expression of neuroplastins is not critical in glutamatergic neurons for associative learning.

3.1 Testis and sperm in *Nptn*^{-/-} male mice show no anatomical differences

To investigate potential anatomical differences in the testes and sperm between *Nptn*^{+/+} and *Nptn*^{-/-} male mice, I conducted an assessment of the testicular weight and morphology in adult *Nptn*^{-/-} males, comparing them to *Nptn*^{+/+} males at 6 months of age. The results of the examination revealed that the overall testicular morphology in *Nptn*^{-/-} males was comparable to that of their wild-type littermates (Figure 12A). Moreover, the testicular weights in *Nptn*^{-/-} males during adulthood were similar to those in their wild-type littermates (Figure 12B). Quantitative analysis and comparison of the circumference of seminiferous tubules per cross-section, obtained from the testis of different genotypes, did not show any statistically significant differences (Figure 12C). Additionally, there were no statistically significant differences observed in the sperm count per cauda (Figure 12D).

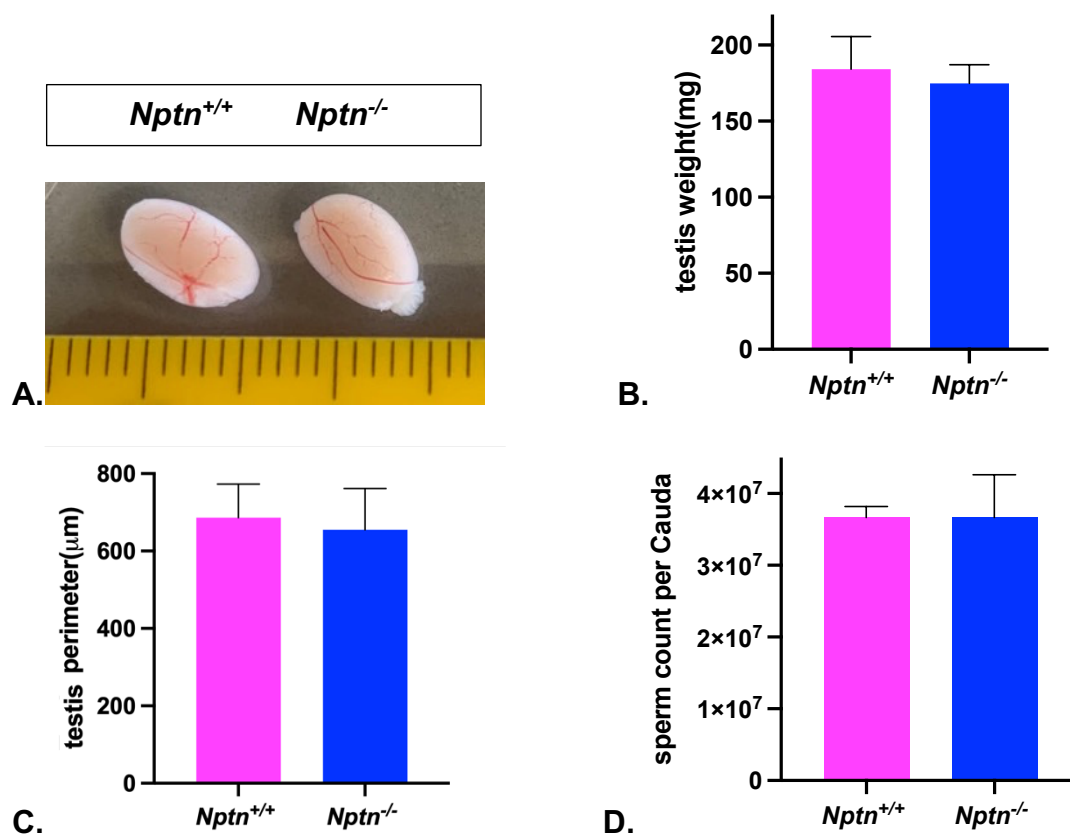
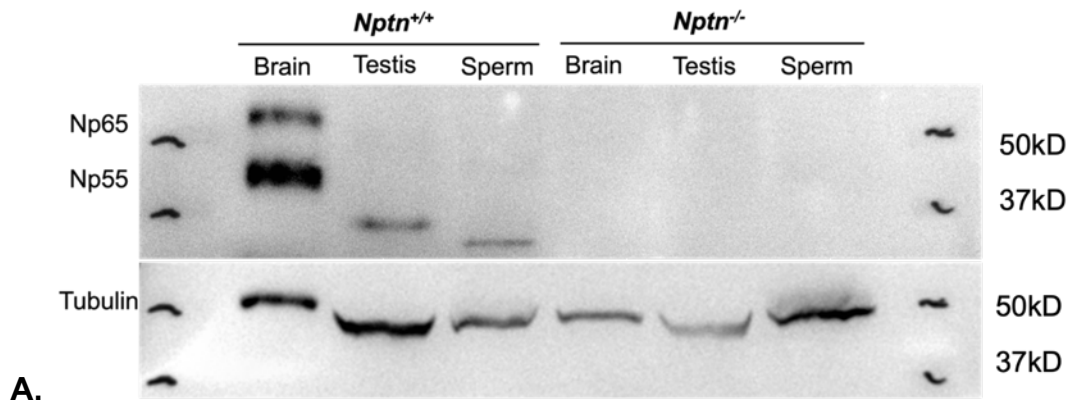


Figure 12: Normal appearance of testis of *Nptn*^{-/-} male mice

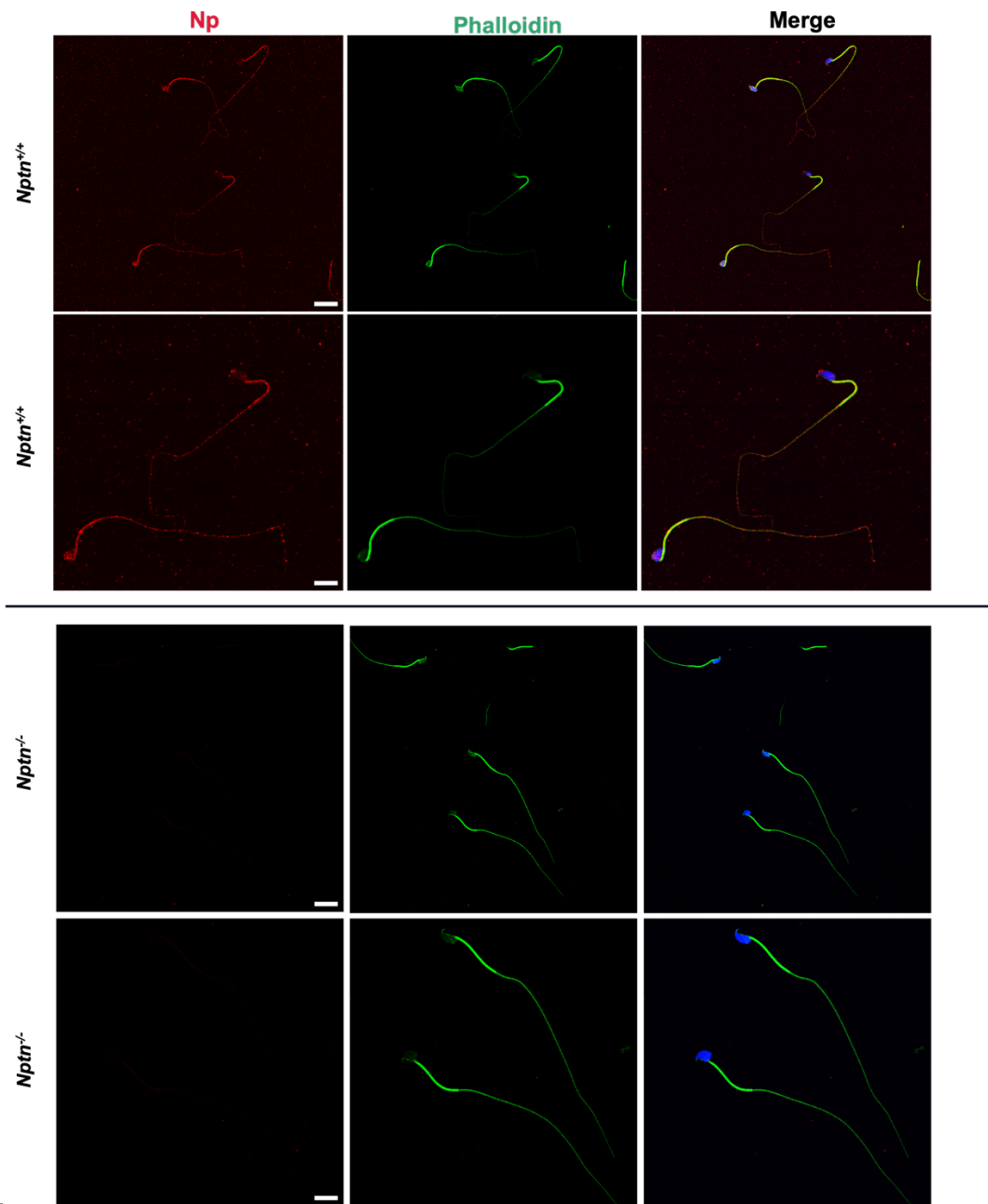
A. Testicular morphology and size appear normal in *Nptn*^{-/-} male mice (scale: mm). **B.** The average testicular weight of *Nptn*^{-/-} and *Nptn*^{+/+} male littermates is not significantly different. **C.** The average circumference of seminiferous tubules is similar in *Nptn*^{-/-} and *Nptn*^{+/+} male mice. **D.** The number of sperm in the cauda epididymidis of *Nptn*^{-/-} and *Nptn*^{+/+} male mice is similar.

3.2 Neuroplastin expression in testis and sperm

At the protein level, polyclonal antibodies against neuroplastin revealed two bands at 55 kDa and 65 kDa in the brain from *Nptn*^{+/+} male mice, and a single band at 50 kDa in the testis and a band at 45 kDa in sperm (Figure 13A). The Np65 isoform was detected specifically in the brain and was not detectable in testicular tissue or sperm. Neuroplastin was found with punctate surface staining in isolated wild-type sperm in both the head and tail regions (Figure 13B), but was undetectable in sperm from *Nptn*^{-/-} male mice.

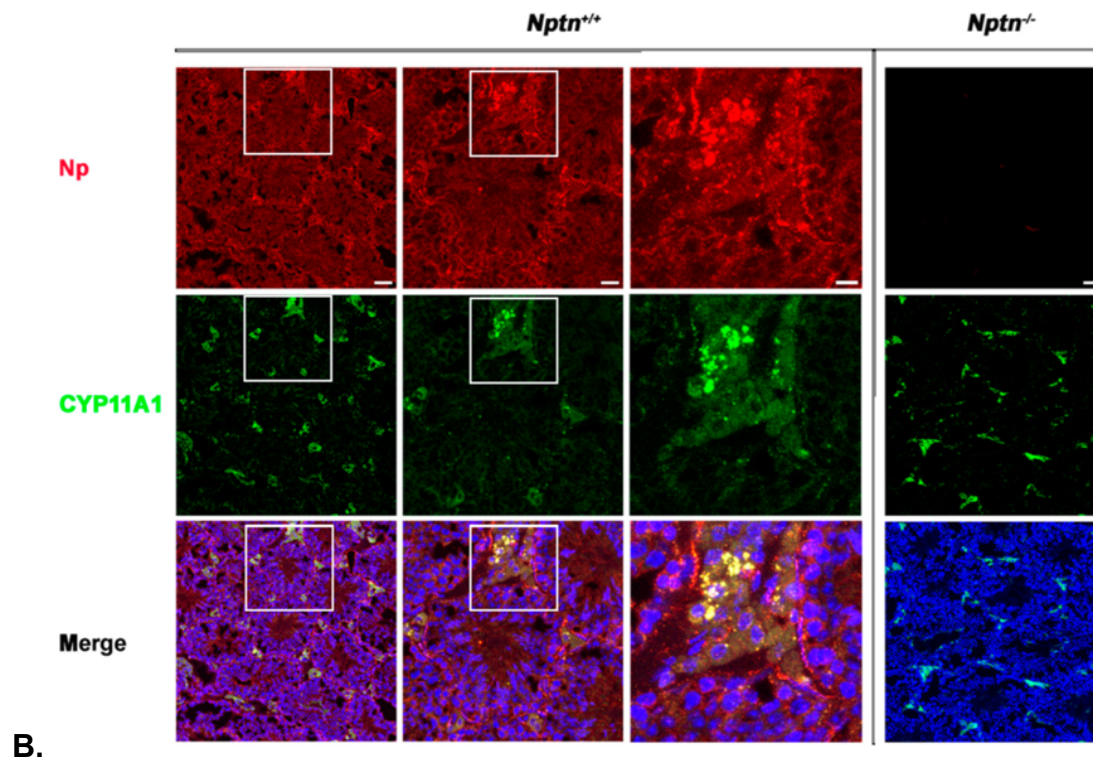


A.



B.

Figure 13: Neuroplastin expression in testis and sperm



B.

Figure 14: Neuroplastin expression by Leydig and peritubular myoid cells

Antibodies targeting the two neuroplastin isoforms (shown in red) clearly revealed the expression of neuroplastin in the testes. Neuroplastin was undetectable in the testes of *Nptn*^{-/-} mice. **A.** Antibodies against alpha-smooth muscle actin (α -SMA, in green) identified peritubular myoid cells, confirming the expression of neuroplastin by myoid cells in *Nptn*^{+/+} mice but not in *Nptn*^{-/-} mice (scale bar left = 50 μ m; middle = 20 μ m; right = 10 μ m; for *Nptn*^{-/-}, scale bar = 50 μ m). The expression of α -smooth muscle actin remained unchanged in *Nptn*^{-/-} mice. **B.** Antibodies targeting CYP11A (in green) identified Leydig cells, confirming the expression of neuroplastin in Leydig cells of *Nptn*^{+/+} mice but not in *Nptn*^{-/-} mice (scale bar left = 50 μ m; middle = 20 μ m; right = 10 μ m; for *Nptn*^{-/-}, scale bar = 50 μ m). It is important to note that the expression of CYP11A was unaltered in *Nptn*^{-/-} mice.

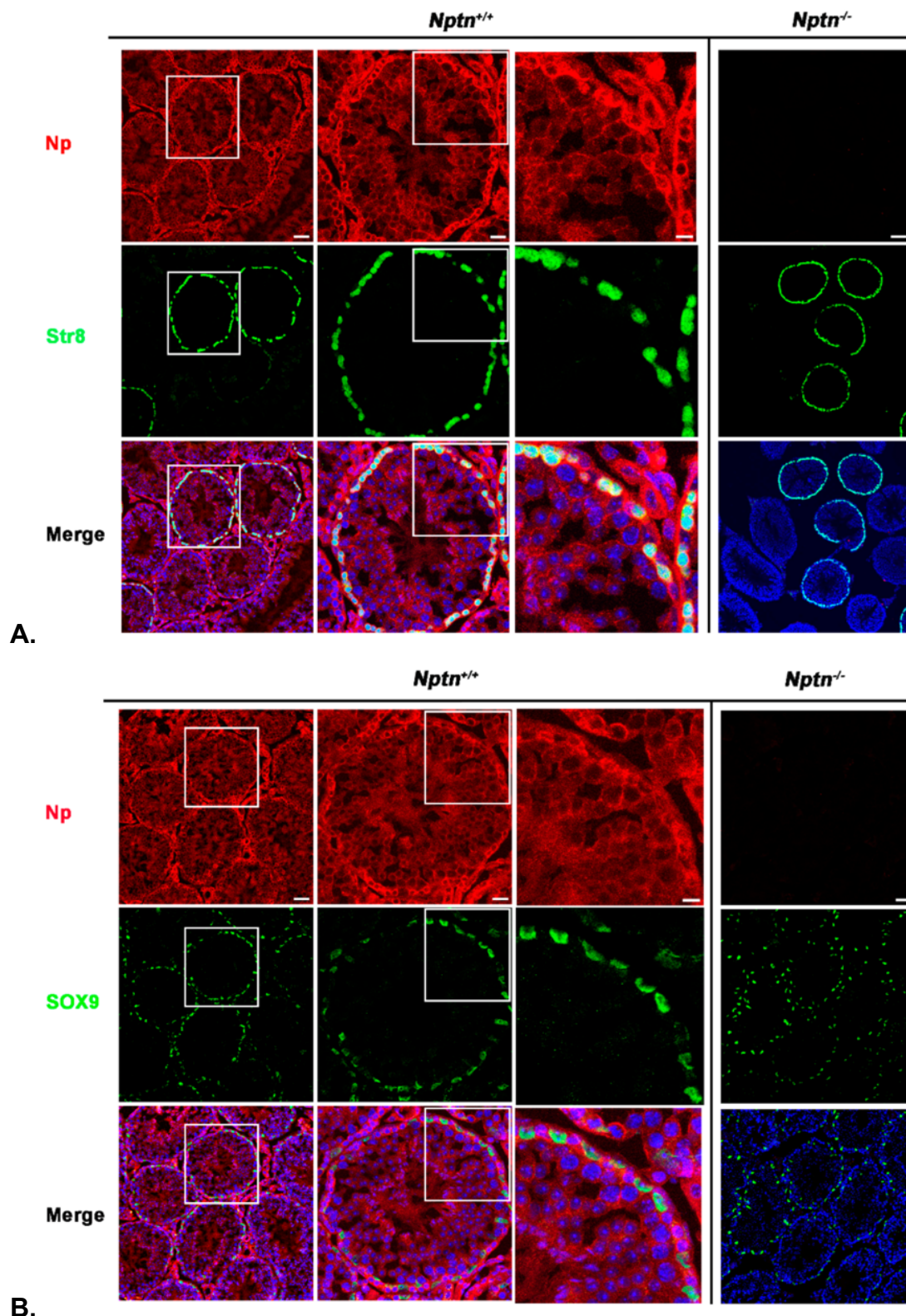


Figure 15: Neuroplastin expression by spermatogonia, spermatocytes, and Sertoli cells

A. Spermatogonia and spermatocytes were identified by antibodies against Stra8, confirming the expression of neuroplastin in spermatogonia and spermatocytes in *Nptn^{+/+}* mice but not in *Nptn^{-/-}* mice

(scale bar left = 50 μm ; middle = 20 μm ; right = 10 μm ; for *Nptn*^{-/-}, scale bar = 50 μm). **B.** Antibodies against Sox9 recognized the Sertoli cells, confirming the expression of neuroplastin by Sertoli cells in *Nptn*^{+/+} mice but not in *Nptn*^{-/-} mice (scale bar left = 50 μm ; middle = 20 μm ; right = 10 μm ; for *Nptn*^{-/-}, scale bar = 50 μm). It's important to note that, whether it's Stra8 or Sox9, their expression in *Nptn*^{-/-} is consistent with that in *Nptn*^{+/+} mice.

To investigate whether reproduction relies on the expression of neuroplastin during spermatogenesis or in Sertoli cells, gene inactivation through Cre recombinase was employed.

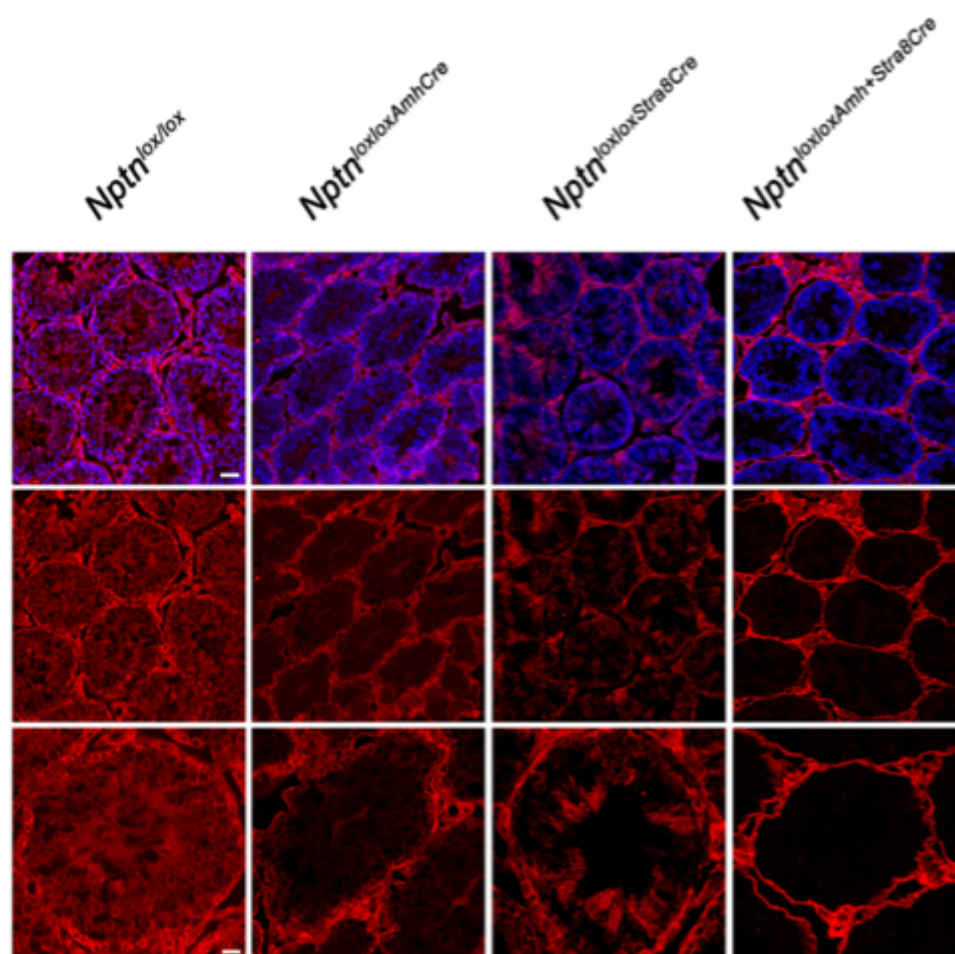


Figure 16: Ablation of neuroplastin expression in spermatocytes, spermatogonia, and Sertoli cells

When Cre recombinase expression was guided by the Stra8 promoter in *Nptn*^{lox/loxStra8Cre} mice, neuroplastin expression was no longer detected in spermatogonia and spermatocytes. In *Nptn*^{lox/loxAmhCre} mice, neuroplastin expression in Sertoli cells was eliminated. In *Nptn*^{lox/loxAmhCre+Stra8Cre} mice, neuroplastin

expression in interstitial cells and myoid cells remained unaffected, but it was completely absent in spermatocytes, spermatogonia, and Sertoli cells (first and second row images: lower magnification, scale bar = 50 μm , third row: higher magnification, scale bar = 20 μm).

However, *Nptn*^{loxloxStra8Cre}, *Nptn*^{loxloxAmhCre}, and *Nptn*^{loxloxAmhCre+Stra8Cre} males successfully produced offspring, indicating that neuroplastin expression in spermatocytes, spermatogonia, and Sertoli cells in the testes is not essential for fertility or reproduction.

To address the potential neuronal function of neuroplastin that might interfere with reproduction, the fertility of male *Nptn*^{loxloxEmx1Cre} mice was analyzed, which specifically lack neuroplastin expression in glutamatergic neurons (Herrera-Molina et al., 2017), and male *Nptn*^{loxloxPrCreERT} mice, where the *Nptn* gene can be inactivated by tamoxifen injection selectively in neurons (Bhattacharya et al., 2017). *Nptn*^{loxloxEmx1Cre} males reproduced offspring similar to wild-type males. Likewise, male *Nptn*^{loxloxPrCreERT} mice continued to reproduce offspring for over 2 months after *Nptn* gene inactivation.

3.3 The testosterone level in the testis of adult neuroplastin-deficient (*Nptn*^{-/-}) male mice is not different from that in wild-type (*Nptn*^{+/+}) male mice

In males, testosterone helps to develop and maintain the male reproductive system, including the penis, testes, prostate gland, and seminal vesicles. It also promotes the development of male secondary sexual characteristics, such as increased muscle mass and bone density (Nassar and Leslie, 2023). To determine whether there were differences in intratesticular testosterone levels between *Nptn*^{+/+} and *Nptn*^{-/-} mice, we conducted ELISA tests. The results indicated that there was no statistically significant difference in intratesticular testosterone levels between the two genotypes of mice.

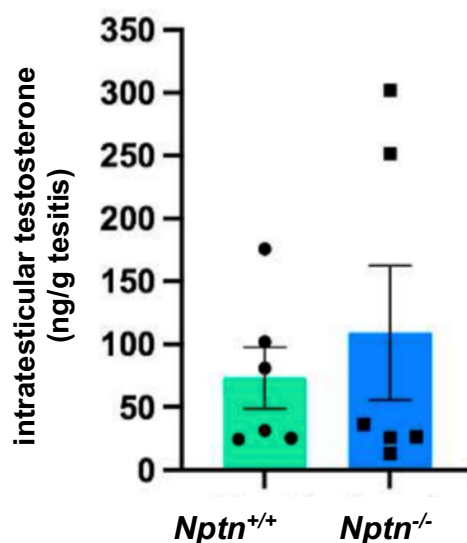


Figure 17: Intratesticular testosterone in *Nptn*^{+/+} and *Nptn*^{-/-} mice

Intratesticular testosterone levels, as determined by ELISA in adult *Nptn*^{+/+} (n=6) and *Nptn*^{-/-} (n=6) male mice, were found to be similar (one-way ANOVA).

Costa et al. (2010) clearly demonstrated how testosterone is released into the testes and bloodstream. Upon binding of LH to its receptor on the interstitial cell membrane, LH receptor-G protein coupling leads to an increase in cAMP formation. cAMP stimulates the mobilization and transport of cholesterol to the mitochondria via activation of PKA signaling. Cholesterol is transferred to the mitochondria, where it is converted to pregnenolone by binding with CYP11A1 and then transported from the mitochondria to the smooth endoplasmic reticulum. Within the smooth endoplasmic reticulum, pregnenolone is converted to testosterone by enzymes (HSD3b, CYP17A1, and HSD17b) and subsequently released. Therefore, I examined the expression of LHR, HSD3B, CYP17A1, and PKA in the testis by Western blotting and observed no changes between mice *Nptn*^{+/+} and *Nptn*^{-/-} as depicted in Figure 18A and Figure 18B. But the fluorescence staining intensity of PKA[R11a] was significantly reduced by immunohistochemistry (Figure 18C and Figure 18D).

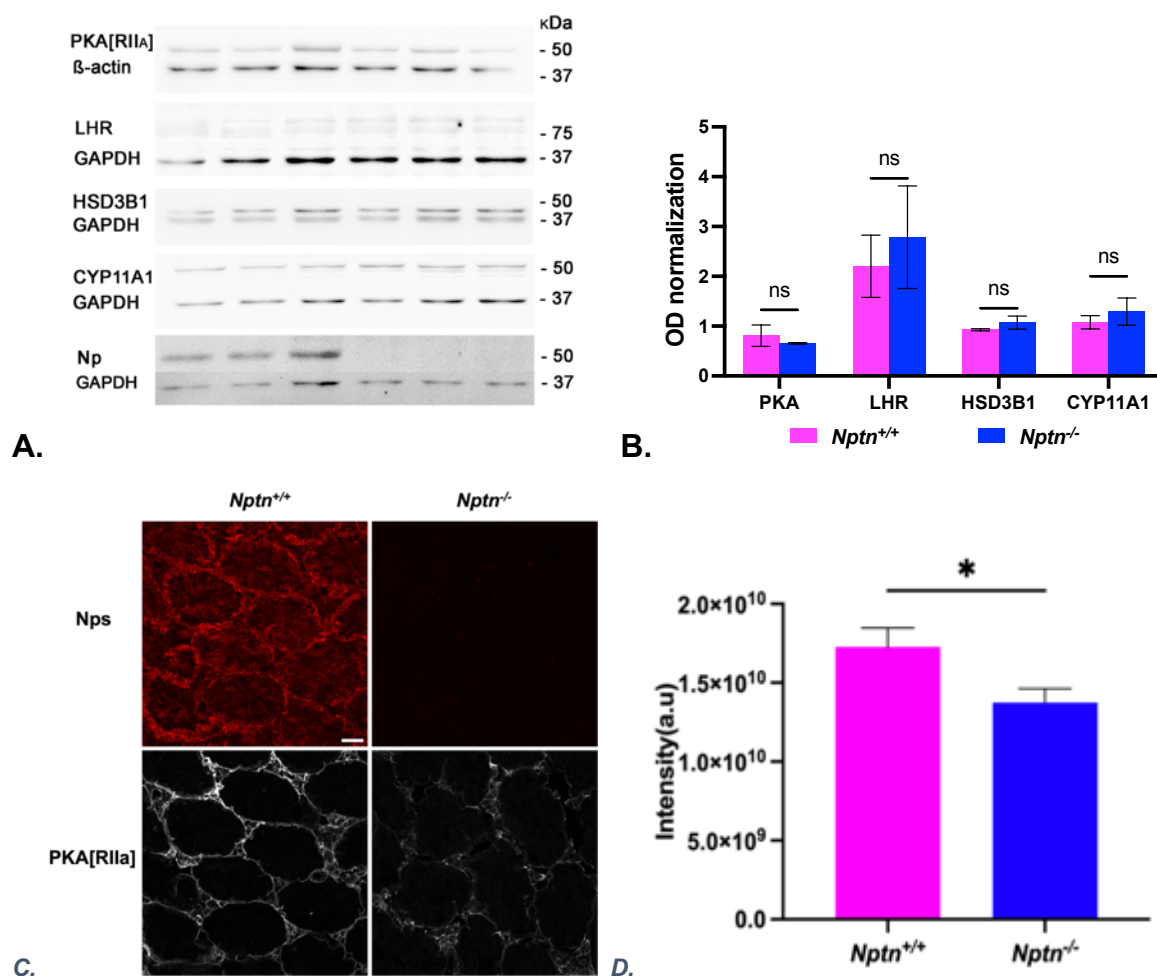


Figure 18: Analysis of adult testis

A. The Western blot analysis of adult mice testis (left three bands: *Nptn*^{+/+}; right three bands: *Nptn*^{-/-}) utilizing antibodies against PKARII α , β -actin, LH-receptor, HSD3B1, CYP11A1, neuroplastin55/65, and GAPDH. **B.** No statistically significant differences of the staining intensity of PKA[RII α], β -actin, LH-receptor, HSD3B1, CYP11A1 were observed between *Nptn*^{+/+} and *Nptn*^{-/-} mice by Western blot. **C.** Immunohistochemical staining of PKA[RII α] in testis sections from *Nptn*^{+/+} and *Nptn*^{-/-} mice. **D.** A notable reduction in PKA[RII α] staining intensity was observed in the testis of *Nptn*^{-/-} male mice compared to *Nptn*^{+/+} counterparts (one-way ANOVA), *Nptn*^{-/-} n=14 sections (132 tubules), *Nptn*^{+/+} n=9 sections (100 tubules), F (1,21) =5.795, p=0.0254).

3.4 PMCA1 is reduced in Leydig cells of neuroplastin- deficient (*Nptn*^{-/-}) mice

Our analysis did not reveal abnormal testicular morphology or altered spermatogenesis in *Nptn*^{-/-} males arguing against the possibility of LH or FSH deficits. Additionally, we noted normal blood concentrations of LH and FSH in *Nptn*^{-/-} males,

providing evidence for a functional HPA axis. Report from Costa et al. (2010) provided a potential explanation for the low testosterone level in the blood of *Nptn*^{-/-} male mice could be a partially abnormal response to LH signal processing which is associated with elevation of intracellular Ca²⁺. Therefore, I used immunohistochemistry to investigate whether the loss of neuroplastin might potentially interfere with the expression of PMCA, as previously observed in other cell types (Herrera-Molina et al., 2017; Korthals et al., 2017; Schmidt et al., 2017). Reduced expression levels of PMCA1 were observed in the testes of *Nptn*^{-/-} males, particularly in Leydig cells when compared to *Nptn*^{+/+} littermates (Figure 19).

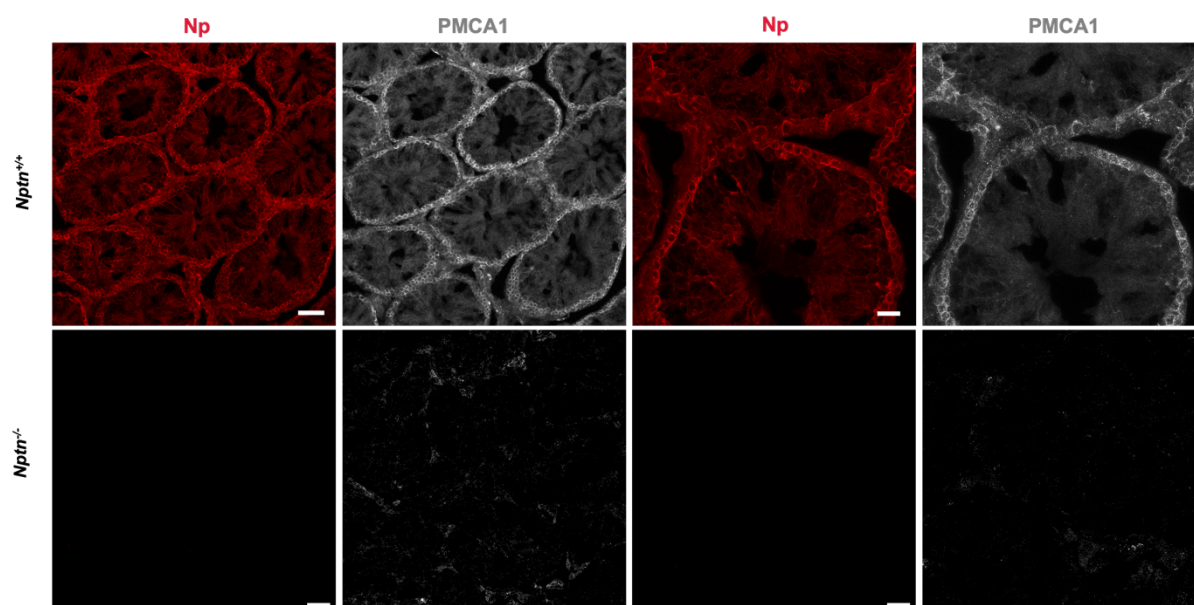


Figure 19: PMCA1 expression in the testis and particularly in the Leydig cells

Immunohistochemistry reveals decreased expression of PMCA1 in the testes of *Nptn*^{-/-} males compared to *Nptn*^{+/+} males (top row: *Nptn*^{+/+}, scale bar left = 50 μ m, scale bar right = 20 μ m; bottom row: *Nptn*^{-/-}, scale bar left = 50 μ m, scale bar right = 20 μ m).

The expression of PMCA1 is reduced in mice lacking neuroplastin (Bhattacharya et al., 2017). To investigate this further, I also investigated the expression of PMCA1 in the brain and testis of *Nptn*^{+/+} and *Nptn*^{-/-} male mice (Figure 20).

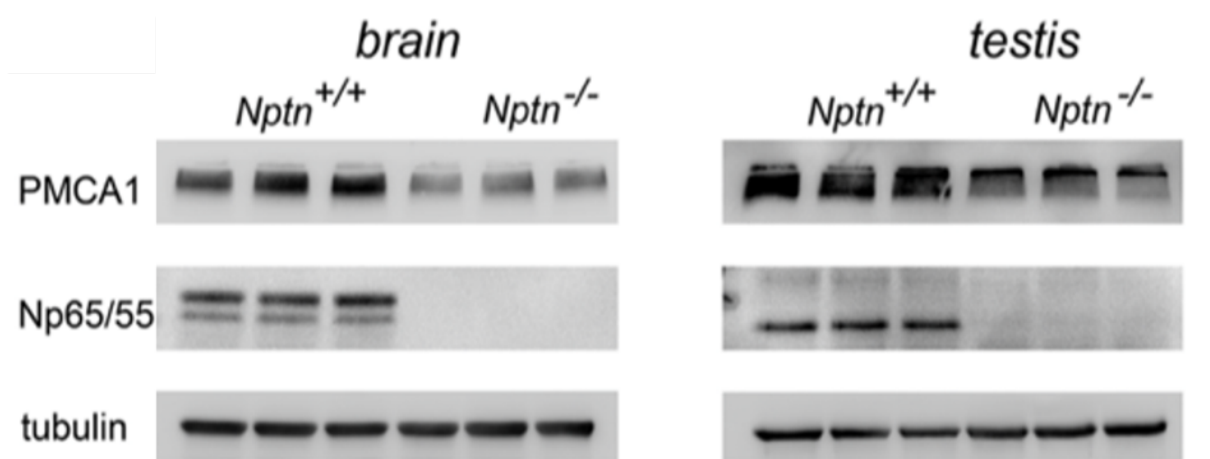


Figure 20: PMCA1 expression in the brain and testis

Reduced expression of PMCA1 in brain (46% decrease) and testis (39% decrease) of adult *Nptn*^{-/-} (n = 3) compared to *Nptn*^{+/+} (n = 3) male mice was revealed by Western blot analysis (one-way ANOVA). Equal loading was revealed by Western blot analysis using tubulin as reference protein.

3.5 Inducible Cre recombinase with promoter GAD2 mediated inactivation of the neuroplastin gene results in retrograde amnesia with significantly reduced memory

As mentioned at the beginning, *Nptn*^{-/-} mice and induced *Nptn*^{lox/loxPrCreERT} mice both exhibit impaired learning in the two-way active avoidance test (Bhattacharya et al., 2017). The concept of disinhibition, defined as 'a momentary interruption in the balance of excitation and inhibition' within glutamatergic projection neurons regulated by GABAergic interneurons, emerges as crucial for the acquisition and expression of associative fear conditioning (Augustine et al., 2003). The findings by Herrera-Molina et al. (2017) suggest that the expression of neuroplastins in glutamatergic neurons is not essential for acquisition. Instead, they propose that GABAergic interneurons expressing neuroplastins may play a modulatory role in inhibiting glutamatergic neurons in the *Nptn*^{lox/loxEmx1Cre} mutant.

To support the above hypothesis, *Nptn*^{lox/loxGAD2CreERT} mice allowing inactivation of the neuroplastin gene in GABAergic interneurons by tamoxifen activation of the GAD2 promoter driven Cre recombinase were generated. The rate-limiting enzyme glutamic acid decarboxylase produces gamma-aminobutyric acid (GABA) (GAD). GAD 65 is encoded by the GAD2 gene, which is important for GABAergic transmission (Wu et al., 2007). *Gad2-CreERT2* drivers provide robust and flexible genetic tools to manipulate GABAergic neurons throughout the mouse CNS (Taniguchi et al., 2011). In *GAD2*^{tm1(Cre/ERT2)} mouse (The Jackson Laboratory, Stock No:010702), the insertion both abolishes *Gad2* gene function and expresses a Cre-ERT2 fusion protein from the *Gad2* promoter. These mice were crossed with *Nptn*-floxed mice and further intercrossing resulting in homozygously floxed *Nptn* mice with and without GAD2-Cre-ERT2 allele allowing tamoxifen inducible conditional neuroplastin-deficiency. The homozygous floxed *Nptn* mice carrying the GAD2-Cre-ERT2 allele were designated *Nptn*^{lox/loxGAD2CreERT} mice (Figure 21).

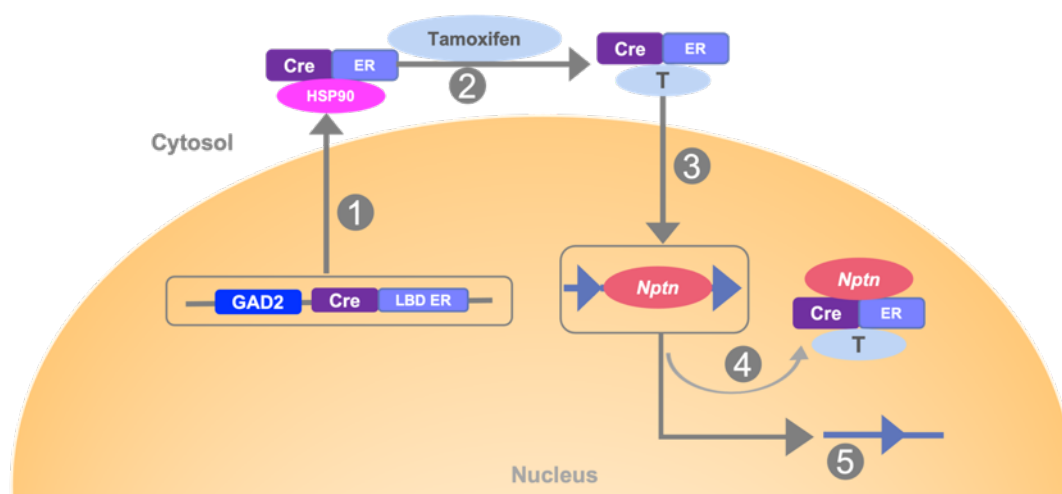


Figure 21: GABAergic neuron-specific inducible neuroplastin-deficient mice

Tamoxifen (Tam)-inducible System of estrogen receptor fused to Cre (CreER) (Kim et al. 2018). **1.** The GAD2 promoter leads to specific expression of the transgene in GABAergic neurons. In the absence of tamoxifen, the expressed fusion protein, CreERT, interacts with heat shock protein 90 (HSP90) and in the cytoplasm. **2.** Administration of Tam disrupts the interaction between HSP90 and CreER. **3.** Interaction of ER with Tam makes the nuclear localization signal accessible allowing nuclear translocation of Cre. **4.** In the nucleus, the CreER recognizes the loxP sites introduced into the *Nptn*

gene. 5. Exision of the region between the lox sites inactivates the gene *Nptn* in GABAergic interneurons.

Neuroplastins expression were analyzed by immunofluorescence staining in brains of *Nptn*^{+/+} mice, neuroplastin-deficient (*Nptn*^{-/-}) mice, *Nptn*^{lox/loxEmx1Cre} mice (mice ablated neuroplastin in cortical and hippocampal glutamatergic neurons), *Nptn*^{lox/loxGAD2ERT} (mice allowed inactivation of the neuroplastin gene in GABAergic interneurons by tamoxifen activation of the GAD2 promoter driven Cre recombinase) and *Nptn*^{lox/loxEmx1CreGAD2ERT} mice (inactivation of the neuroplastin both of glutamatergic and GABAergic neurons). Figures 22-24 show staining of the brains of *Nptn*^{+/+}, *Nptn*^{-/-}, *Nptn*^{lox/loxEmx1CreGAD2ERT}, *Nptn*^{lox/loxEmx1Cre}, *Nptn*^{lox/loxGAD2ERT} mice using anti-Neuroplastin 55/65, anti-Calbindin, and anti-Parvalbumin antibodies (Figure 22, scale bar = 1mm; Figure 23, scale bar=100 μm and scale bar = 5 μm; Figure 24, scale bar=100 μm and scale bar = 5 μm).

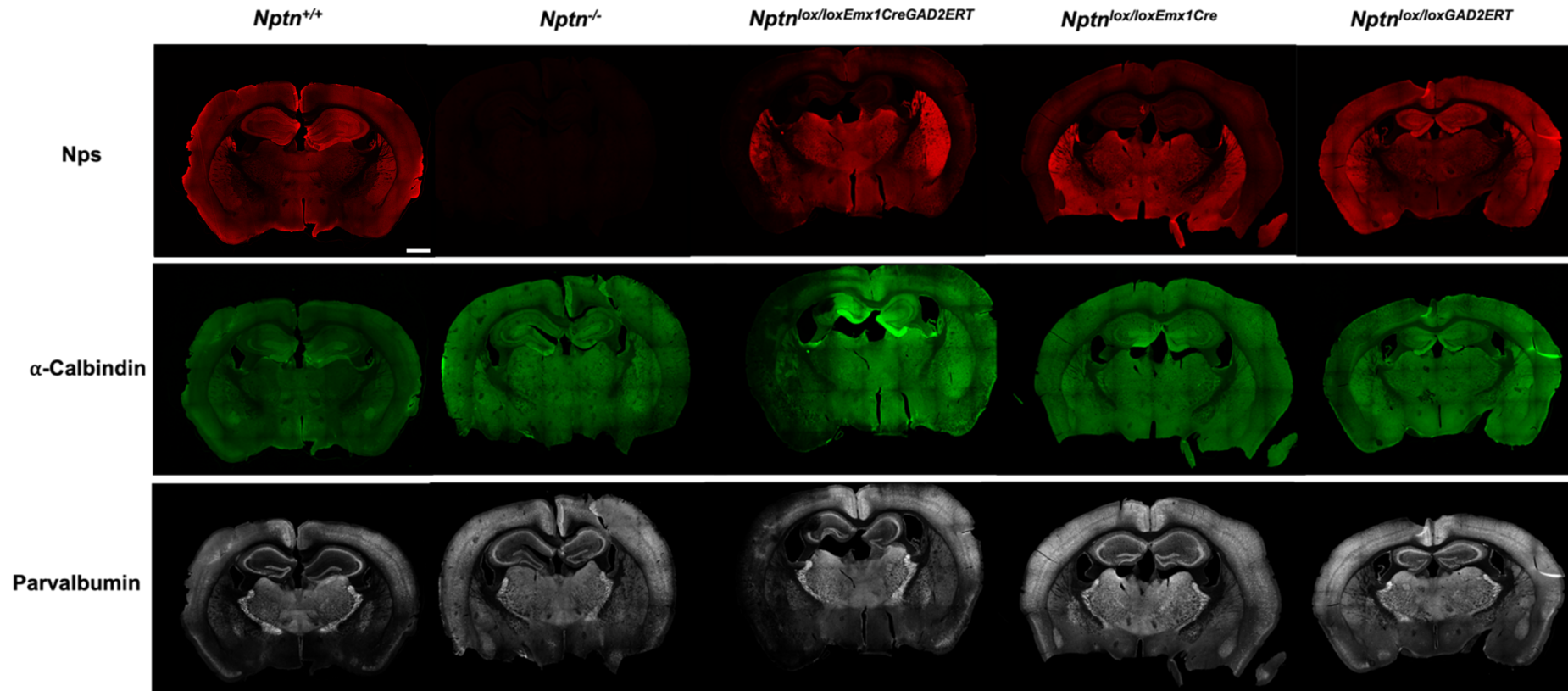


Figure 22: Expression of neuroplastins, α -calbindin and parvalbumin in various mutant mice brain

The staining of the mice brains of five different genotypes using primary antibodies (scale bar = 1mm): anti-Neuroplastin 55/65 (sheep, 1:300), anti-Calbindin (mouse, 1:500), anti-Parvalbumin (rabbit, 1:500), and secondary antibodies Cy3-anti-Sheep IgG(H+L) (1:1000), Cy5-Anti-Rabbit IgG(H+L) (1:1000), and Alexa Fluor 488-Anti-Mouse IgG(H+L) (1:1000).

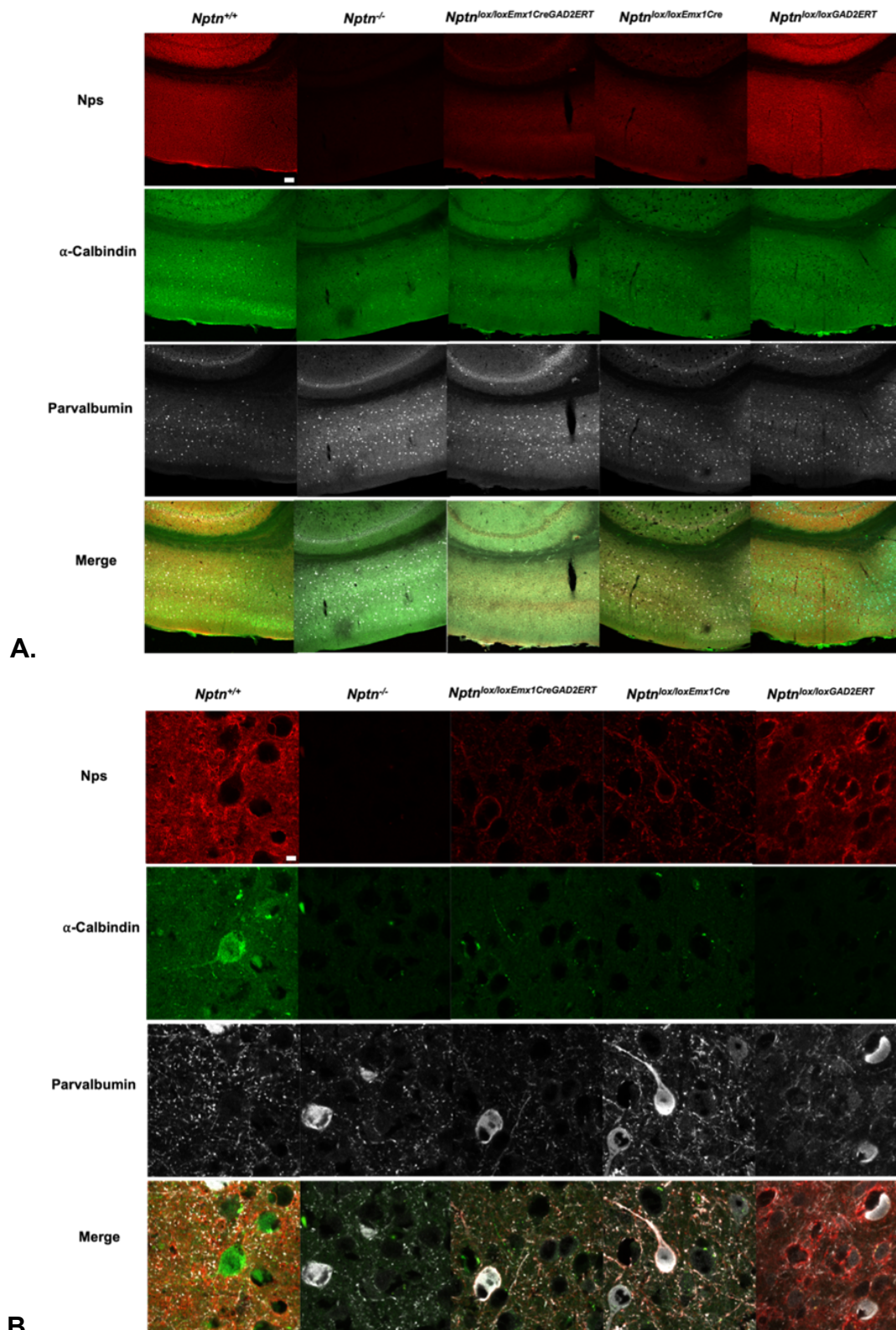


Figure 23: Expression of neuroplastins, α -calbindin and parvalbumin in various mutant mice motor cortex

A. Expression of neuroplastins, α -calbindin and parvalbumin in various mutant mice motor cortex (scale bar =100 μ m). **B.** Expression of neuroplastins, α -calbindin and parvalbumin in various mutant mice motor cortex (higher magnification, scale bar = 5 μ m).

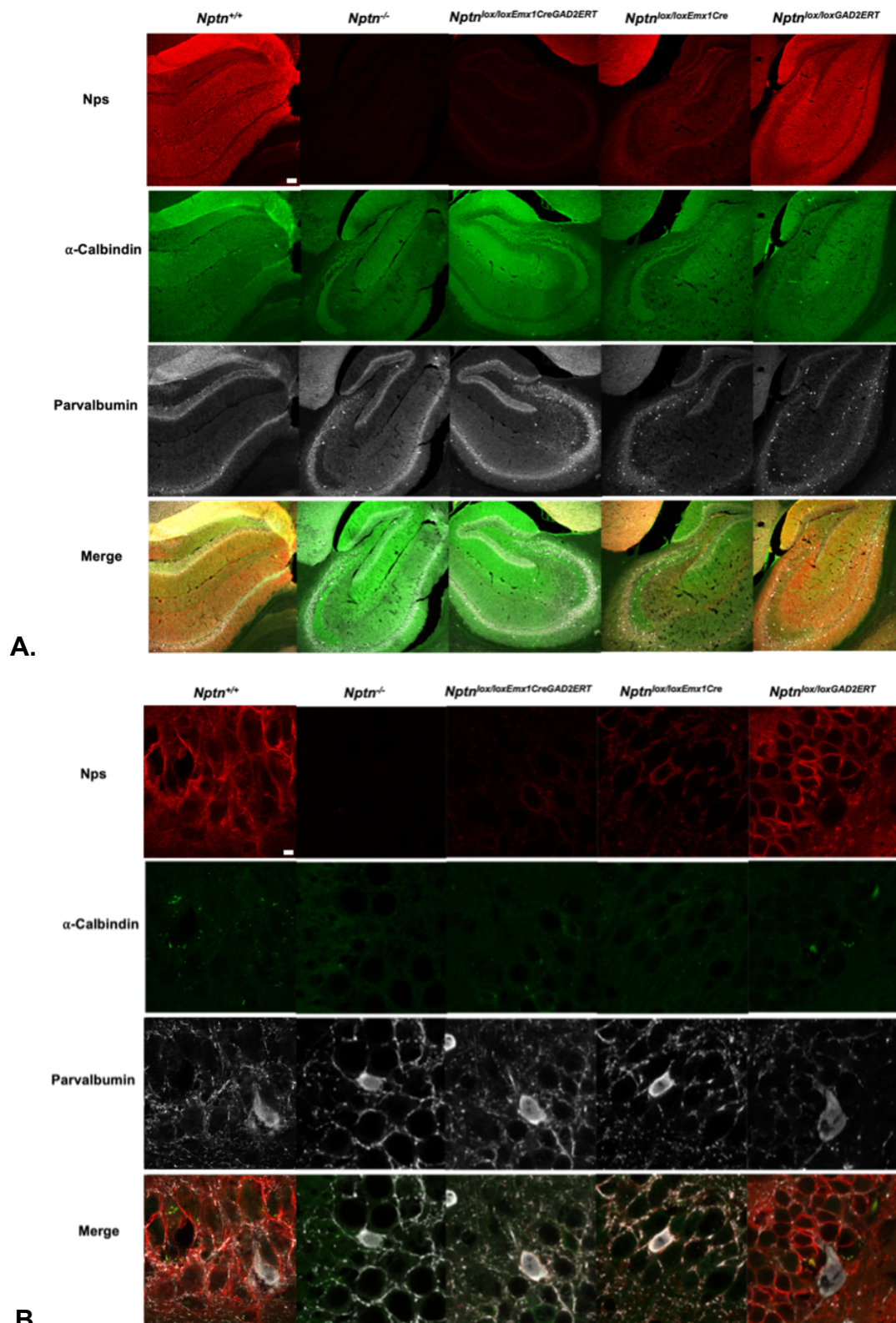


Figure 24: Expression of neuroplastins, α -calbindin and parvalbumin in various mutant mice hippocampus

A. Expression of neuroplastins, α -calbindin and parvalbumin in various mutant mice hippocampus (scale bar = 100 μ m). **B.** Expression of neuroplastins, α -calbindin and parvalbumin in various mutant mice hippocampus (higher magnification, scale bar = 5 μ m).

From the neuroplastins staining results presented in Figure 22, it is apparent that the brains of *Nptn*^{-/-} mice exhibit a lack of neuroplastins expression. In the cortex and hippocampus of *Nptn*^{lox/loxEmx1CreGAD2CreERT} mice, there are very limited neuroplastins expression. In the brains of *Nptn*^{lox/loxEmx1Cre} mice, where neuroplastin in glutamatergic neurons is knocked out, the staining remarkably resembles that of *Nptn*^{lox/loxEmx1CreGAD2CreERT} mice. *Nptn*^{lox/loxGAD2CreERT}, characterized by the specific elimination of neuroplastin expression in GABAergic interneurons, exhibits staining nearly identical to the wild type. This is attributed to the fact that GABAergic neurons represent a very small proportion in the cortex and hippocampus. Figures 23 and 24 were examined at higher resolutions, focusing on the motor cortex and the hippocampal region. Antibodies anti-Calbindin and anti-Parvalbumin were employed to stain two different types of GABAergic neurons, providing a more detailed illustration of the findings presented in Figures 23 and 24.

The induced ablation of neuronal neuroplastins mice *Nptn*^{lox/loxPrCreERT} yielded no significant impact on Water Maze performance or in the light/dark avoidance experiment. However, after training in active avoidance and fear conditioning paradigms, ablation of *Nptn* in neurons did reveal impairments indicating selective retrograde amnesia for associative memories, as demonstrated by Bhattacharya et al. in 2017. In our study, the same two-way active avoidance test (Figure 25) was used to explore the potential reduction in memory and learning abilities in *Nptn*^{lox/loxGAD2CreERT} mice following tamoxifen administration. The experimental design was specifically tailored to assess associative learning and associative memory capabilities as described by Bhattacharya et al. 2017.

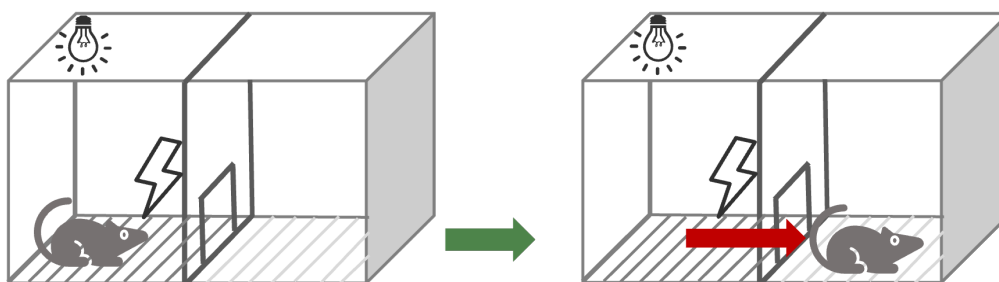


Figure 25: Shuttle box for two-way active avoidance test

A standard two-chambered shuttlebox (TSE) was used. During the conditioning stimulus (CS, 10 seconds light), the animal had to move to the dark side of the shuttlebox to avoid an electrical footshock (US, 5 seconds, 0.3mA pulsed) delivered after the light. Inter-trial duration ranged from 5 to 15 seconds when the animals could move between the compartments. The mice were trained for 5 days with 80 trials each day. Compartment transitions during presentation of the CS were counted as correct or conditioned avoidance reactions while transition during the US were counted as unconditioned avoidance reaction.

The learning experiment involved the administration of tamoxifen at a dosage of 2 mg/day for a duration of 10 days initially. Subsequently, an 8-week waiting period was implemented to facilitate neuroplastins degradation. Following this waiting period, the mice underwent a training phase, encompassing 80 trials per day over a period of five days, to assess their learning ability (Figure 26). The results show that ablation of neuroplastins in GABAergic interneurons does not affect associative learning (Figure 27).



Figure 26: Two-way active avoidance test for associative learning

Nptn^{lox/lox} and *Nptn^{lox/loxGAD2CreERT}* were injected with tamoxifen for 10 days and then trained 2 months later in the two-way active avoidance test.

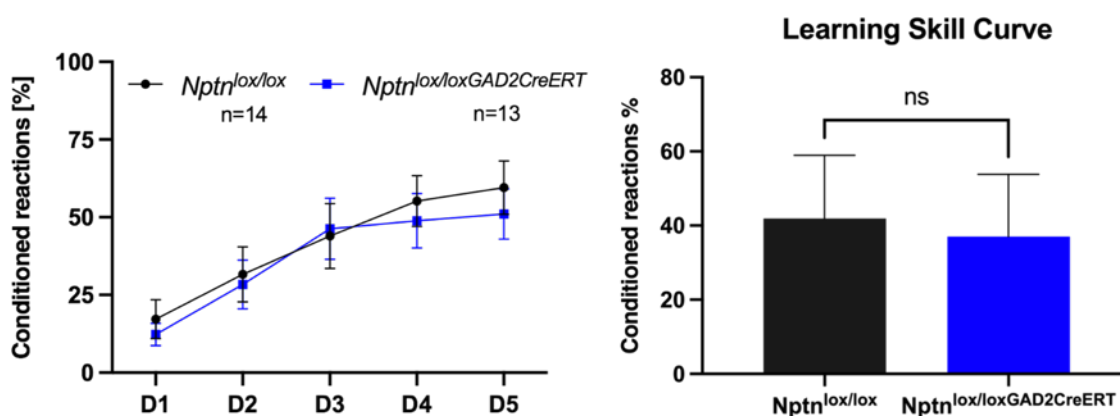


Figure 27: Learning skill from two-way active avoidance test

Two-way active avoidance test shows similar learning ability with no significant difference between *Nptn*^{lox/loxGAD2CreERT} and *Nptn*^{lox/lox} mice. Tamoxifen induced mice performed normal in acquiring associative learning skills in the two-way active avoidance.

In the memory test, mice *Nptn*^{lox/lox} and *Nptn*^{lox/loxGAD2CreERT} underwent training with 80 trials per day for 5 days. Mice that attained a performance level of more than 75% correct responses were selected and subjected to tamoxifen treatment, constituting the memory experiment group. This group received tamoxifen treatment for a duration of 10 days, followed by an 8-week waiting period to facilitate neuroplastins degradation. Subsequently, associative memory was assessed in two-way active avoidance test (Figure 28).



Figure 28: Two-way active avoidance test for associative memory

Nptn^{lox/lox} and *Nptn*^{lox/loxGAD2CreERT} mice were trained for two-way active avoidance to more than 75% correct responses for 5 days, then induced with tamoxifen for 10 days and 2 months later tested for associative memory.

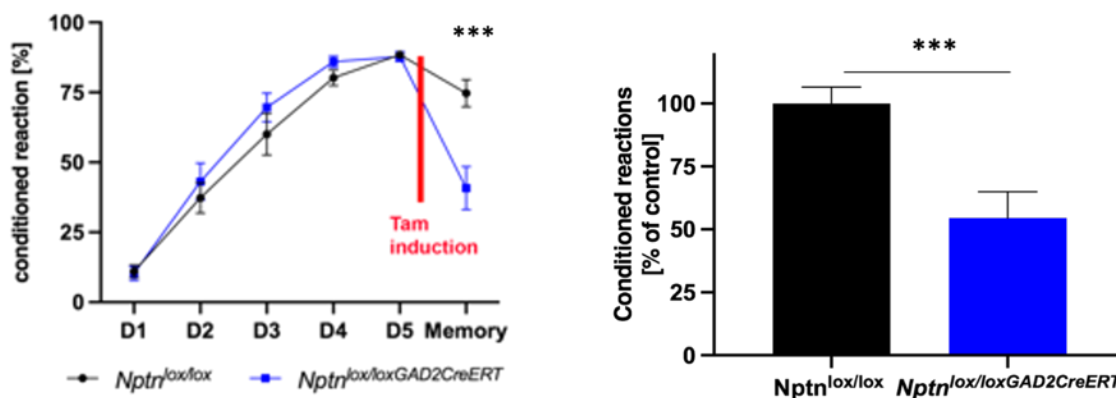


Figure 29: Associative memory from two-way active avoidance test

Adult *Nptr^{lox/lox}* (n = 14, black) and *Nptr^{lox/loxGAD2-CreERT}* (n = 14, blue) exhibited differences in memory for the two-way active avoidance test after ablation of neuroplastin in GABAergic neurons.

Nptr^{lox/loxGAD2CreERT} mice exhibited low performance in associative memory during the two-way active avoidance task. This outcome (Figure 29) indicates that the loss of neuroplastins in GABAergic interneurons resulted in retrograde amnesia.

3.6 Ablation of neuroplastins expression in Parvalbumin positive interneurons

Inhibitory GABAergic interneurons are a specific type of neurons that are distinguished by the co-expression of several small proteins that primarily function as neuromodulators or Ca^{2+} -binding proteins (Hu et al., 2014). One such type of inhibitory GABAergic interneuron, the PV+ interneurons, is defined by the expression of the Ca^{2+} -binding protein parvalbumin (PV), which has a molecular weight of approximately 12 kD in mice. PV plays a critical role in accelerating Ca^{2+} sequestration, decreasing presynaptic Ca^{2+} levels, influencing short-term synaptic plasticity, and inhibiting cumulative facilitation (Caillard et al., 2000). Because PV rapidly sequesters Ca^{2+} , it significantly reduces the Ca^{2+} -activated potassium conductance that is responsible for post-spike hyperpolarization, thereby enabling PV+ interneurons to repolarize and fire faster than other neurons. As a result, PV+ interneurons are characterized by fast-spiking action potentials at high energy costs (Hu et al., 2014).

I conducted studies on mice with different neuroplastin mutations (*Nptn*^{lox/loxEmx1Cre}, *Nptn*^{lox/loxGAD2CreERT}, *Nptn*^{lox/loxEmx1CreGAD2ERT}) using fluorescent immunostaining and confocal microscopy (Figure 30). Analyzing over 1204 images and 1571 neurons in the mouse motor cortex and hippocampal regions (CA1-3 and DG), we found that the distribution of PV+ interneurons in the motor cortex regions and hippocampal areas showed no statistically significant differences among the three genotypes of mice. The distribution of PV+ interneurons in *Nptn*^{lox/loxGAD2CreERT} mice was $4.66 \times 10^3 \text{ mm}^2$ in the motor cortex and $5.73 \times 10^3 \text{ mm}^2$ in the hippocampus. For *Nptn*^{lox/loxEmx1CreGAD2ERT} mice, the distribution was $4.93 \times 10^3 \text{ mm}^2$ in the motor cortex and $5.76 \times 10^3 \text{ mm}^2$ in the hippocampus, while for *Nptn*^{lox/loxEmx1Cre} mice, it was $4.82 \times 10^3 \text{ mm}^2$ in the motor cortex and $5.24 \times 10^3 \text{ mm}^2$ in the hippocampus.

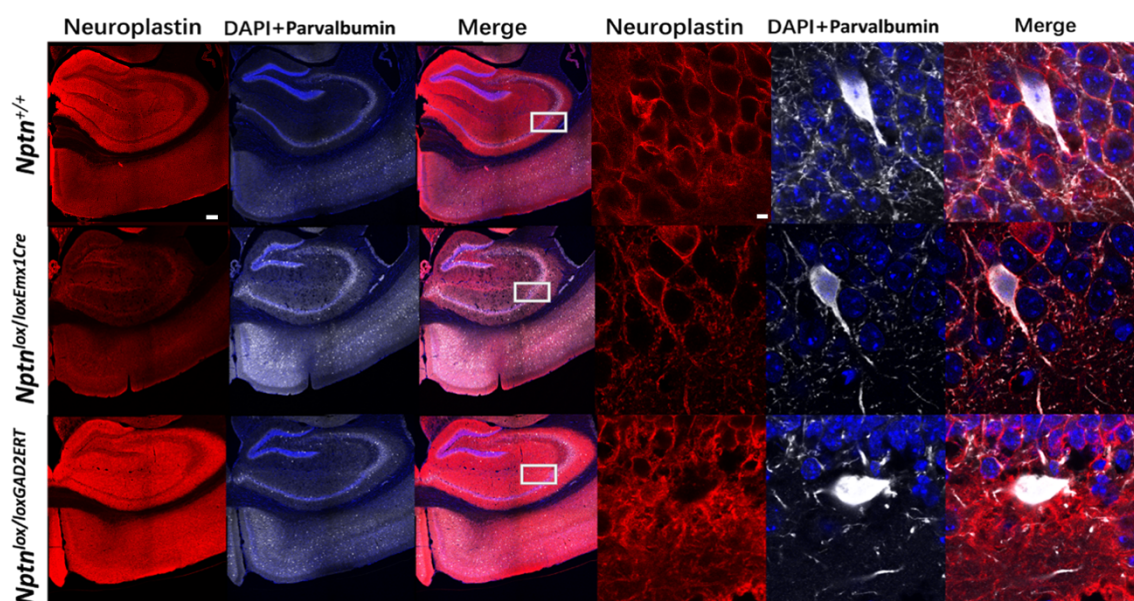
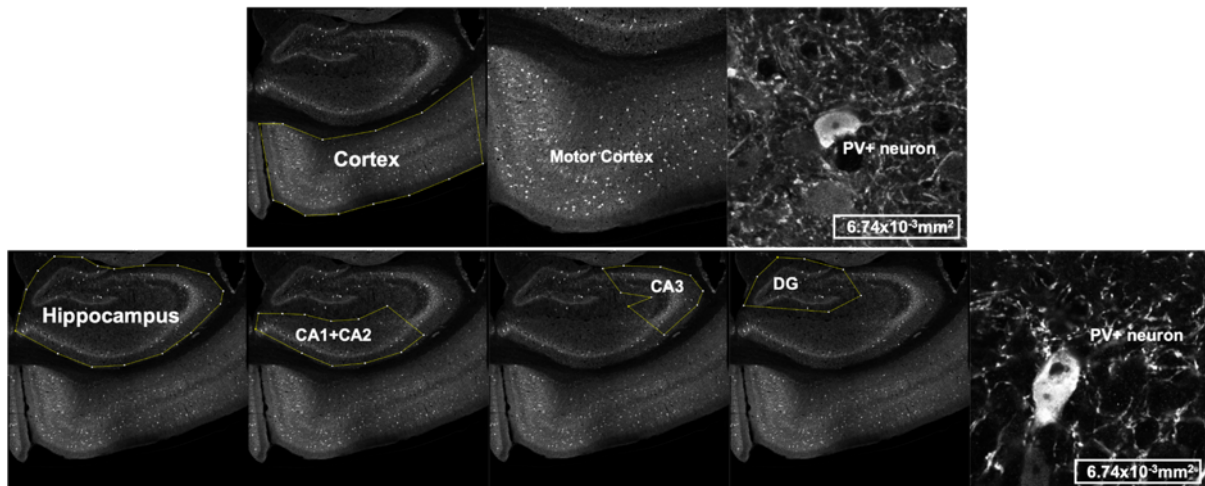


Figure 30: Ablation of neuroplastins in GABAergic Interneurons

Immunolabelling of brain cryosections using anti-neuroplastin (red) and anti-parvalbumin antibodies (white) counterstained with DAPI (blue). *Nptn*^{lox/lox} and *Nptn*^{lox/loxEmx1Cre} mice express neuroplastins in parvalbumin positive interneurons delineating the cell membrane whereas in *Nptn*^{lox/loxGAD2CreERT} after induction parvalbumin positive interneurons are not surrounded by neuroplastin (scale bar left = 200 μm ; scale bar right = 5 μm).

A.



B.

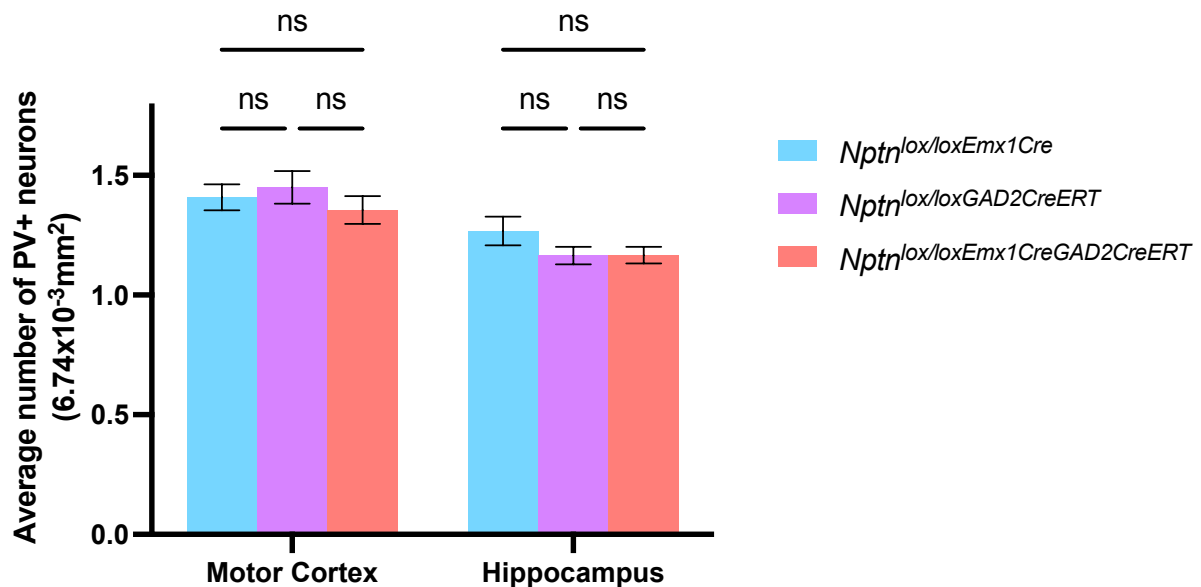


Figure 31: The expression of PV+ interneurons in mice motor cortex and hippocampus

A. Quantified region in cortex and hippocampus **B.** Average number of PV+ interneurons

I also quantified the expression of neuroplastins in PV+ interneurons among *Nptn*^{lox/loxEmx1Cre} and *Nptn*^{lox/loxGAD2CreERT} mice. In *Nptn*^{lox/loxEmx1Cre} mice, 98.92% of PV+ interneurons expressed neuroplastins in the cortex, 99.47% in the hippocampus. In

contrast, in *Nptn^{lox/loxGAD2CreERT}* mice, only 4.8% of PV+ interneurons expressed neuroplastins in the cortex, and 3.32% in the hippocampus.

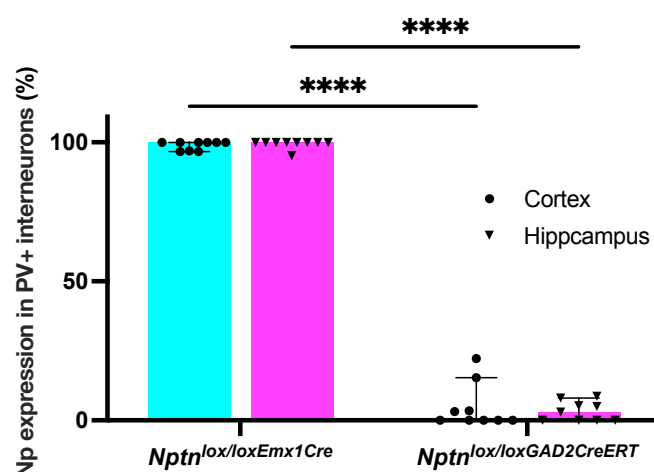


Figure 32: Neuroplastins expression in PV+ interneurons

Neurons were collected from 3 *Nptn^{lox/loxEmx1Cre}* mice (7-8 months old) and 3 induced *Nptn^{lox/loxGAD2CreERT}* mice (7-8 months old), with 3 sections per mouse (*Nptn^{lox/loxEmx1Cre}*, n=9, neuron number from cortex 285, from hippocampus 292; *Nptn^{lox/loxGAD2CreERT}*, n=9, neuron number from cortex 262, from hippocampus 241) taken from the same dissection region to assess the percentage of Np expression in PV+ interneurons. In *Nptn^{lox/loxEmx1Cre}*, nearly 100% of PV+ interneurons showed Np expression, whereas the *Nptn^{lox/loxGAD2CreERT}* mice after induction exhibited significantly lower Np expression compared to *Nptn^{lox/loxEmx1Cre}* mice (*p < 0.05, **p < 0.01, ***p < 0.001; two-way ANOVA).

The result is that over 98,92% of the PV+ interneurons express neuroplastins in *Nptn^{lox/loxEmx1Cre}* mice whereas in the induced *Nptn^{lox/loxGAD2CreERT}* mice only less than 4.8% of the PV+ neurons express neuroplastins, thus neuroplastin expression can be specifically ablated in GABAergic interneurons in *Nptn^{lox/loxGAD2CreERT}*.

3.7 PMCA2 is reduced in GABAergic neuron-specific inducible Neuroplastin - deficient mice

PMCA2 expression levels are significantly reduced in *Nptn^{-/-}* and induced *Nptn^{lox/loxPrCreERT}* mice (Bhattacharya et al., 2017). To determine the alterations in the levels of PMCA2, we performed Western blot analysis using individual cortex,

hippocampus and striatum obtained from $Nptn^{+/+}$, $Nptn^{-/-}$, $Nptn^{lox/loxEmx1Cre}$, induced $Nptn^{lox/loxGAD2CreERT}$, and induced $Nptn^{lox/loxEmx1CreGAD2ERT}$ (Figure 33).

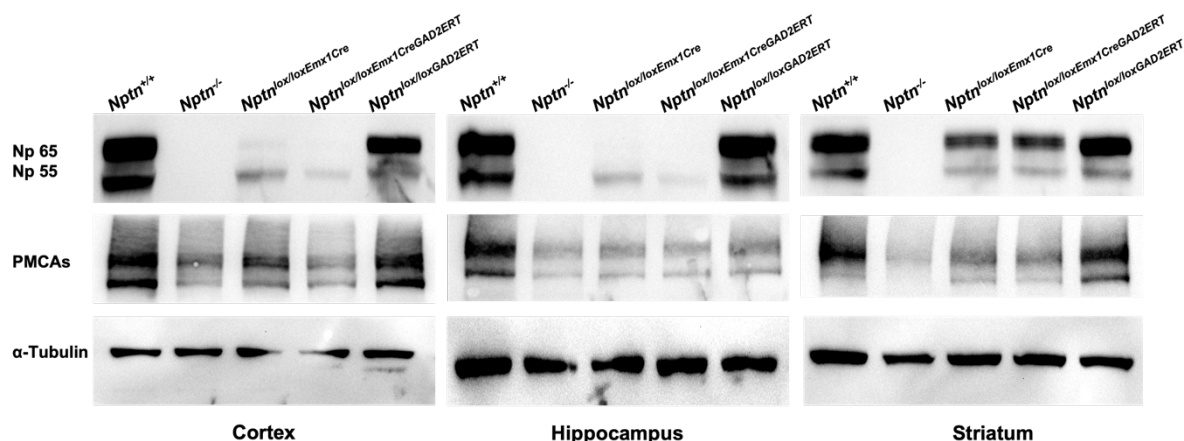
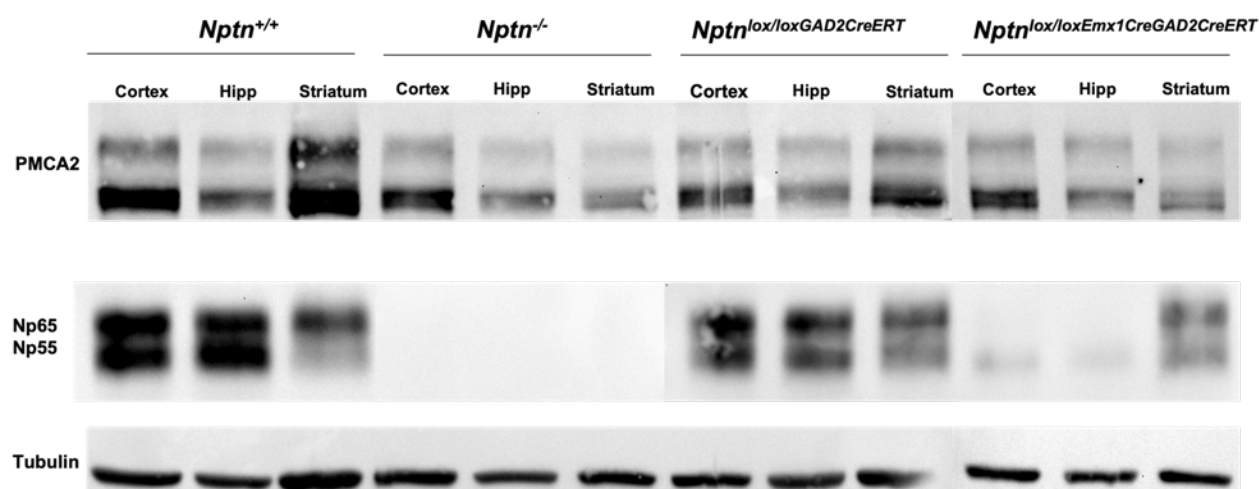


Figure 33: PMCA expressed in different genotype mice

By Western blot analysis of PMCA, the expression levels of PMCA in different neuroplastin mutant mice were examined, indicating a positive correlation between PMCA expression and neuroplastin expression.

Additionally, ablation of $Nptn$ in glutamatergic neurons affected the expression of PMCA1, 3, and 4, whereas PMCA2 expression was not affected (Herrera-Molina et al., 2017), suggesting expression of PMCA2 predominantly by GABAergic interneurons. Therefore, I investigated the expression of PMCA2 in GABAergic neuron-specific induced-neuroplastin-deficient mouse brains using a paralog-specific PMCA2 antibody and Western blot analysis (Figure 34).



A.

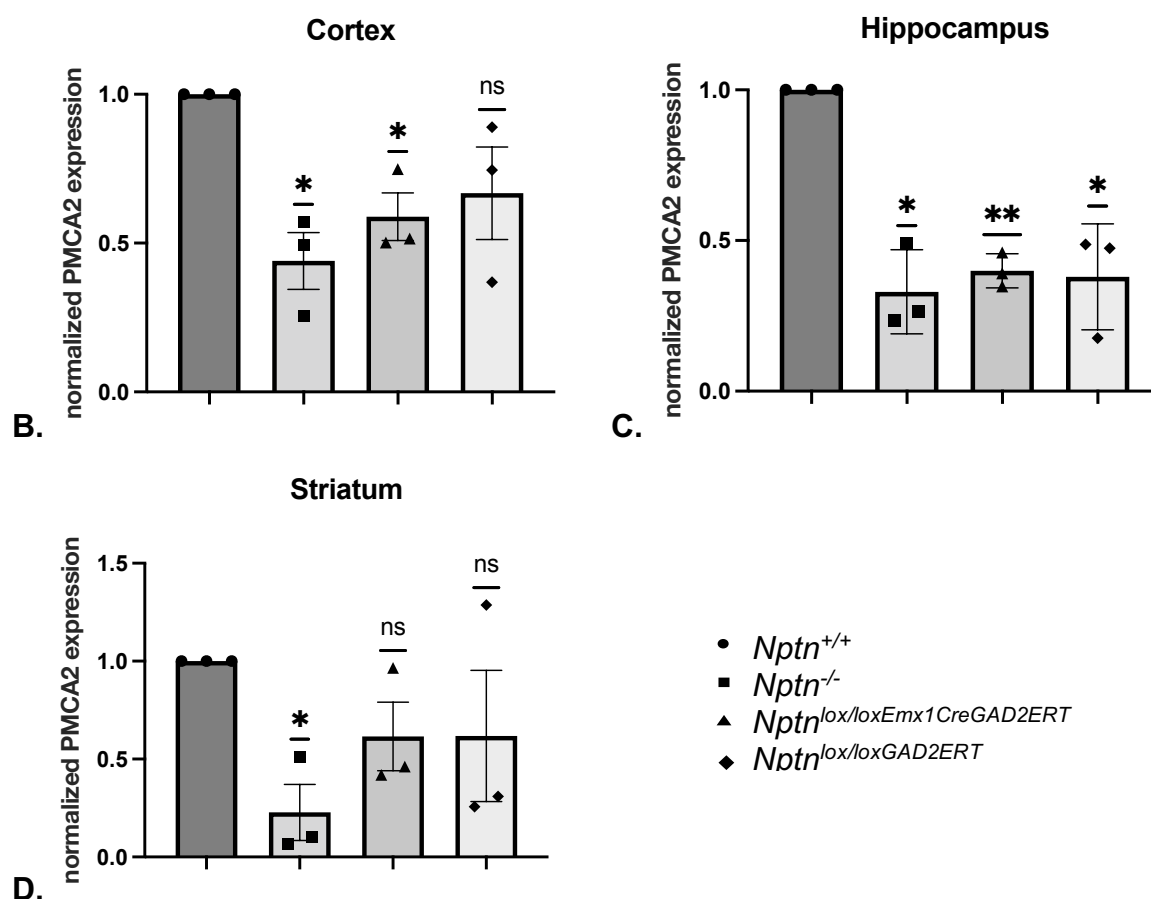


Figure 34: PMCA2 expressed in different genotype mice

A. The decrease in PMCA2 expression in the cortex, hippocampus and striatum were confirmed by Western blot analysis. **B.** Quantification of PMCA2 levels in cortex, **C.** hippocampus and **D.** striatum of *Nptn*^{+/+}, *Nptn*^{-/-}, induced *Nptn*^{lox/loxEmx1CreGAD2ERT} and induced *Nptn*^{lox/loxGAD2ERT} mice (* p<0.05, ** p<0.01, *** p<0.001), each genotype n≥3.

This finding is consistent with the assumption that in the mouse cortex and hippocampus, PMCA2 is predominantly expressed by GABAergic interneurons, displaying minimal expression in glutamatergic neurons. This is substantiated by the similar reduced PMCA2 expression observed in induced *Nptn*^{lox/loxGAD2ERT} and *Nptn*^{lox/loxEmx1CreGAD2ERT} mice, in which *Nptn* ablation in glutamatergic neurons does not further affect PMCA2 expression compared to induced *Nptn*^{lox/loxGAD2ERT}. Immunohistochemistry (IHC) double-staining of PMCA2 and PV+ interneurons (refer to chapter 3.8 Figure 35) also lends support to this proposition. Furthermore, these results reinforce the observations made by Herrera-Molina et al. (2017), suggesting that unchanged PMCA2 expression in *Nptn*^{lox/loxEmx1Cre} mice is associated with the expression of neuroplastins in GABAergic neurons.

3.8 PMCA2 is reduced in PV+ GABAergic interneurons

PMCA2 is expressed in the hippocampus, with particular isoforms restricted to GABAergic presynapses (Burette et al., 2009) or glutamatergic spines (Burette et al., 2010). To further explore the expression of PMCA2 in *Nptn*^{-/-}, *Nptn*^{lox/loxEmx1CreGAD2ERT} and *Nptn*^{lox/loxGAD2ERT} mice, we performed staining in the hippocampal region using anti-PMCA2 and anti-Parvalbumin antibodies. The results showed that the expression of PMCA2 on PV interneurons was significantly reduced in *Nptn*^{-/-}, and induced *Nptn*^{lox/loxEmx1CreGAD2ERT} and *Nptn*^{lox/loxGAD2ERT} mice consistent with the Western blot experiments in chapter 3.7, Figure 34.

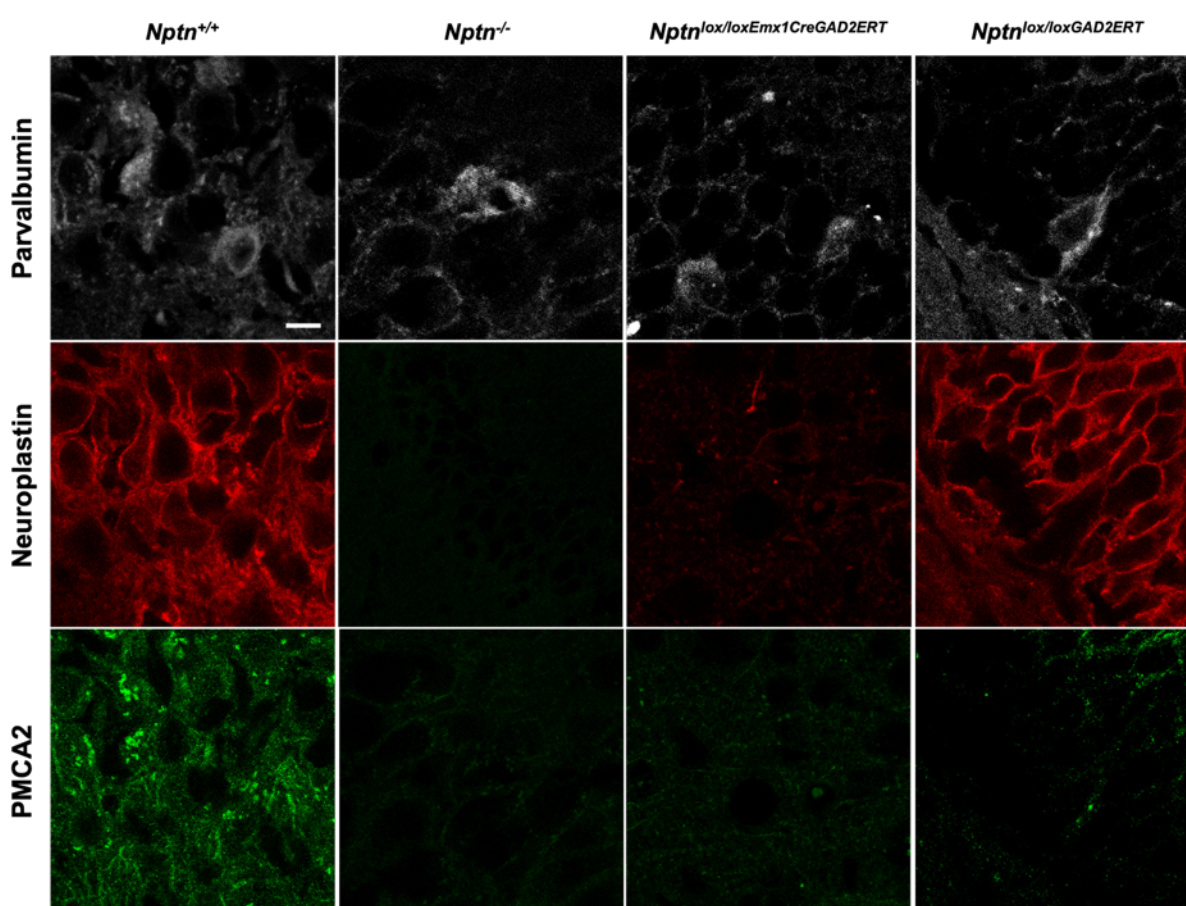


Figure 35: PMCA2 expressed in parvalbulmin interneurons

Immunolabelling of brain cryosections using anti-Neuroplastins, anti-PMCA2, and anti-parvalbumin antibodies. Compared to the *Nptn*^{+/+} hippocampus region, PMCA2 was substantially reduced in *Nptn*^{-/-}, and induced *Nptn*^{lox/loxEmx1CreGAD2ERT} and *Nptn*^{lox/loxGAD2ERT} mice, consistent with the results of the Western blot analysis (scale bar = 10 μ m).

4 Discussion

4.1 Neuroplastin-deficient (*Nptn*^{-/-}) male mice do not reproduce nor display normal mating behavior

In a preceding unpublished study conducted by Soumee Bhattacharya in our group, it was found that homozygous *Nptn*^{-/-} male mice did not sire offspring. Additionally, the *Nptn*^{-/-} male mice displayed abnormal investigatory behavior by spending significantly less time engaged in anogenital sniffing (1.4 ± 0.4 min) compared to the wild-type *Nptn*^{+/+} counterparts (2.8 ± 0.2 min). However, the total interaction time, which includes body sniffing, anogenital sniffing, and direct contact, did not show any difference between the genotypes. These mating abnormalities and the observed infertility of homozygous *Nptn*^{-/-} male mice were the basis to investigate the role of neuroplastin for fertility in this current study.

4.2 The ability of male mice to produce offspring was not affected by the ablation of Neuroplastins expression in spermatogonia, Sertoli cells or central nervous system

According to Langnaese et al. (1997), Np55 is expressed in the testis of rats. The polyclonal antibody against neuroplastins detects two bands at 55 kDa and 65 kDa in the brain of *Nptn*^{+/+} male mice. Immunofluorescence staining using the same antibody, as shown e.g. in image 22, confirms the expression of neuroplastin in the central nervous system. RT-PCR experiments show that *Nptn* mRNA is also expressed in other organs, including the testis of *Nptn*^{+/+} male mice (Chen, et al., 2023). This aligns with the data from Green et al. in 2018, who reported the expression of neuroplastin mRNA by several cell types (e.g., in myoid, Leydig, Sertoli cells, spermatogonia, spermatocytes, and spermatids) in the testis of adult male mice using single-cell RNA sequencing. We further confirmed this by immunofluorescence staining. Expression patterns of markers for Leydig cells (CPY11A), Sertoli cells (Sox9), spermatogonia, spermatocytes (Stra8), and myoid cells (alpha smooth muscle actin) appear normal in

the adult *Nptn*^{-/-} testis. As shown in Figure 14 and Figure 15, the expression of neuroplastin in the testis, specifically in Leydig cells, peritubular myoid cells, spermatogonia, spermatocytes, and Sertoli cells was revealed at the protein level confirming the mRNA expression data. In Figure 16, we utilized Cre recombinase-mediated gene inactivation to investigate whether reproduction depends on neuroplastin expression during spermatogenesis or in Sertoli cells. Specific ablation of neuroplastin in spermatogonia and spermatocytes (*Nptn*^{loxloxStra8Cre}), or in Sertoli cells (*Nptn*^{loxloxAmhCre}), or all (*Nptn*^{loxloxAmhCre+Stra8Cre}), as confirmed by our immunohistochemistry results, did not affect the ability of male mice to produce offspring. This suggests that the expression of neuroplastin in spermatocytes, spermatogonia, and Sertoli cells in the testis is not essential for reproduction or fertility. These findings indicate that neuroplastin expression is not necessary for spermatogenesis. Additionally, the expression of neuroplastin in Sertoli cells, spermatogonia, and spermatocytes is dispensable for reproduction. This is in stark contrast to basigin expression, which is essential on Sertoli cells for the maturation of spermatogonia into spermatocytes (Toyama et al.,1999). Notably, the pattern of neuroplastin staining on mature sperm is punctate, whereas basigin exhibits a more uniform expression along sperm heads and tails. However, the selective lack of neuroplastins from glutamatergic neurons or inactivation of the neuroplastin gene in the adult central nervous system (CNS) also did not interfere with the reproductive abilities of males.

Expression of neuroplastin can clearly be observed in sperm (Figure 13A), by Western blot analysis the neuroplastin band detected in sperm is slightly lower at approximately 45 kDa than in the testis. Differences in glycosylation may account for this. In further experiments conducted by our cooperation partners Wennemuth & Wiesehofer (Univ. Hospital Duisburg-Essen), the quantity and concentration of sperm isolated from the cauda of the epididymis in adult *Nptn*^{-/-} mice (140 days old, n=6, $18.25 \pm 0.78 \times 10^6$ /cauda) were found to be similar to those of wildtype littermate males (n=6, $15.08 \pm 1.30 \times 10^6$ /cauda) (Chen, et al., 2023). The isolated sperm from both *Nptn*^{+/+} and *Nptn*^{-/-} male mice exhibited comparable beat frequencies, which were similarly increased after activation with 15mM bicarbonate. To investigate whether neuroplastin is essential for sperm development or if there might be a delay in sperm maturation in *Nptn*^{-/-} male mice, we examined spermatogenic activity in the testes of male mice at

different ages during maturation. The assessment of the ploidy status of testicular cell nuclei by K. Müller (Cooperation IZW Berlin) at 20, 28, 34, and 45 days of age revealed that the proportion of haploid, diploid, and tetraploid cells did not differ between *Nptn*^{+/+} and *Nptn*^{-/-} male mice.

Anatomical differences of the testis or sperm from *Nptn*^{-/-} compared to *Nptn*^{+/+} male mice were not detected (Figure 12), clearly ruling out the possibility that issues with testicular development are affecting the generation of offspring by *Nptn*^{-/-} mice. Statistically significant differences in testicular perimeter or the number of seminiferous tubules were not observed in *Nptn*^{+/+} and *Nptn*^{-/-} male mice testicular sections. Additionally, testosterone levels in the testes of both *Nptn*^{+/+} and *Nptn*^{-/-} male mice also showed no significant difference (see Figure 17).

Unfortunately, due to the absence of suitable Cre-deleter mouse strains, it was not possible to conditionally eliminate neuroplastin specifically in Leydig or smooth muscle cells. This leaves open the possibility that neuroplastin expression by these cells may be crucial.

4.3 Testosterone plays a crucial role in the development and maintenance of the male reproductive system

In males, testosterone helps to develop and maintain the male reproductive system, including the penis, testes, prostate gland, and seminal vesicles. It also promotes the development of male secondary sexual characteristics (Nassar and Leslie, 2023). The anterior pituitary gland releases the gonadotropins LH and FSH which synergistically stimulate the production of testosterone in the Leydig cells of the testis (O'Shaughnessy et al., 2006). Chronic stress and elevated circulating corticosterone levels inhibit the secretion of LH (Li et al., 2004). Leydig cells in the interstitial tissue of the seminiferous tubules in the testes are the primary site of testosterone production in mammals (Quigley et al., 1995). Testosterone synthesis is triggered by LH and FSH, which are two essential gonadotropic hormones secreted by the anterior pituitary gland (O'Shaughnessy et al., 2006; Lejeune et al., 1998). FSH influences testis size and is necessary for supporting normal Sertoli and germ cell numbers; the absence of

FSH reduces sperm motility (Kumar et al., 1997; Wreford et al., 2001). Mice with FSH receptor gene knockout exhibit decreased testosterone levels, reduced testis size, impaired sperm production and motility, abnormal sperm morphology, and diminished fertility (Krishnamurthy et al., 2000). LH receptor knockout mice completely lack LH signaling, preventing postnatal (rather than prenatal) Leydig cell maturation and testosterone production, resulting in developmental and morphological defects leading to infertility, which can be partially overcome by testosterone replacement (Pakarainen et al., 2017). Notably, as observed in *Nptn*^{-/-} mice (Bhattacharya et al., 2017), cortisol levels above physiological levels may inhibit testosterone production in Leydig cells (Rengarajan and Balasubramanian, 2007).

Figure 17 illustrates the intratesticular testosterone levels between *Nptn*^{+/+} and *Nptn*^{-/-} mice, revealing no statistically significant difference. Therefore, Soumee Bhattacharya investigated serum levels of testosterone in *Nptn*^{-/-} and littermate *Nptn*^{+/+} male mice at various developmental stages. Indicated by her experimental results, testosterone levels as determined by ELISA in the blood of juvenile males were low. At 3 months of age, testosterone levels in *Nptn*^{+/+} male mice were approximately 19-fold higher compared to juvenile 1-month-old *Nptn*^{+/+} males. At an age of 11 months, *Nptn*^{+/+} males displayed approximately 3-fold lower levels of testosterone compared to the 3-month-old male mice. In contrast, testosterone levels of *Nptn*^{-/-} males examined at 1, 3, or 11 months age were not significantly different from each other. These results reveal the absence of the anticipated increase of testosterone levels in blood from puberty to adulthood in *Nptn*^{-/-} males. This observation is remarkable, as the interstitial cells evidently produce sufficient testosterone to enable the normal development of testes and sperm. However, the amount of testosterone released into the bloodstream during adulthood is insufficient to meet the continuous demand.

Furthermore, our analysis did not provide any clues to abnormal testicular morphology or changes in sperm capacity in *Nptn*^{-/-} males, arguing against LH or FSH deficiencies. Additionally, we observed that blood concentrations of LH and FSH in *Nptn*^{-/-} males were normal, supporting the functionality of the HPA axis, and the testosterone levels in the testes themselves were not affected by the absence of neuroplastin.

4.4 The reduced PMCA1 level in Leydig cells of *Nptn*^{-/-} male mice may result in an elevated intracellular Ca²⁺ level preventing a correct response to LH signals triggering testosterone production

Leydig cells are responsible for secretion of testosterone into the blood stream. LH mediated stimulation of testosterone production by Leydig cells is accompanied by elevation of the intracellular Ca²⁺ level (Gorczyńska et al., 1995).

Costa et al. (2010) have demonstrated that the release of calcium from internal stores is a significant mechanism triggering testosterone secretion. Following signal transduction, PMCA extrudes Ca²⁺ into the extracellular space, thereby restoring normal intracellular Ca²⁺ levels (Lopreiato et al., 2014). The formation of a complex between neuroplastin and PMCA is crucial for maintaining normal PMCA expression levels (Bhattacharya et al., 2017; Korthals et al., 2017; Schmidt et al., 2017; Herrera-Molina et al., 2017; Lin et al., 2021b). However, a reduction in PMCA1 levels may elevate intracellular calcium, disrupting the balance of calcium ions both inside the cell, and may lead to a partially abnormal response in LH signal processing due to decreased PMCA1.

I observed that PMCA1 levels, particularly in Leydig cells within the testes of *Nptn*^{-/-} males, were lower compared to wild-type males. Similar to the alterations in Ca²⁺ extrusion dynamics due to decreased PMCA observed in various cell types (e.g., neurons, T cells; Herrera-Molina et al., 2017; Korthals et al., 2017), the reduction in PMCA1 levels in Leydig cells may result in changes in intracellular Ca²⁺ dynamics, ultimately leading to an inadequate response to LH signaling. Potentially, the increase in intracellular Ca²⁺ to trigger testosterone production by Leydig cells via LH receptor signal transduction is silenced due to neuroplastin loss decreasing PMCA1 and, consequently, raising intracellular Ca²⁺ levels and altering Ca²⁺ dynamics, resulting in less testosterone being released. Thus, neuroplastin is required to achieve testosterone levels in the adult bloodstream, ensuring successful mounting and male mating behavior (Figure 36).

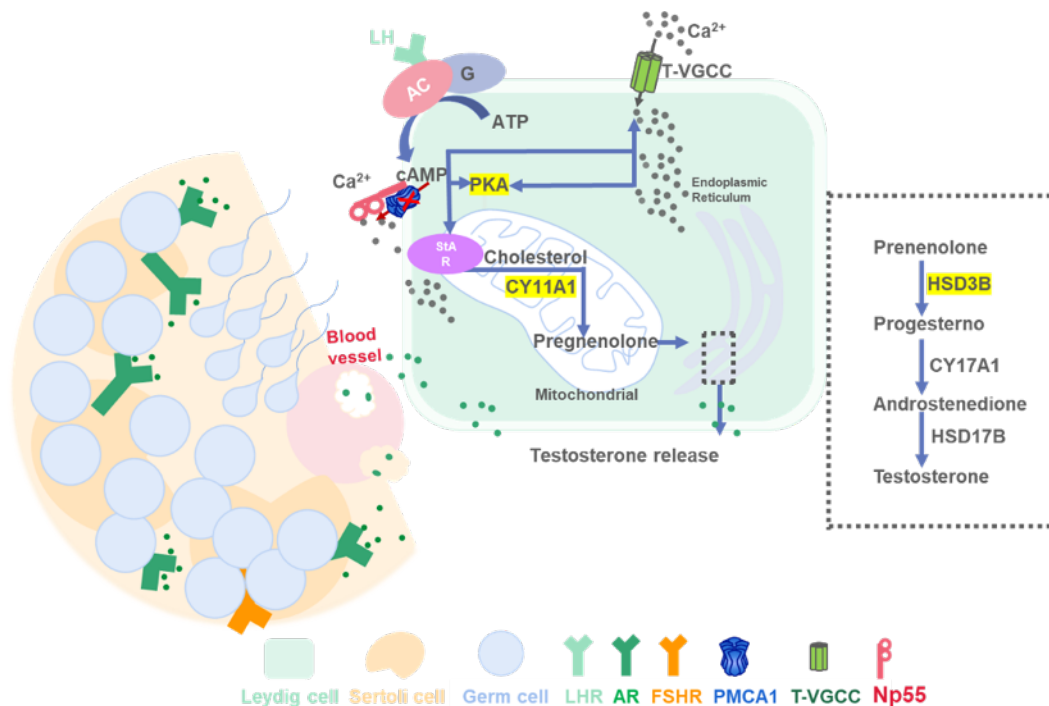


Figure 36: Regulation of testosterone release in Leydig cells of *Nptn*^{-/-} males by PMCA1 levels

Upon LH binding to LHCGR, the activation of LHCGR stimulates adenylate cyclase (AC), leading to an increase in the conversion of ATP to cyclic AMP (cAMP). This, in turn, causes the influx of Ca^{2+} into the cells and induces the activation of various kinases, including protein kinase A (PKA). This results in the upregulated expression of genes involved in steroidogenesis, ultimately leading to increased testosterone production. PMCA1, in conjunction with neuroplastin, regulates intracellular Ca^{2+} concentration.

This represents a novel discovery of neuroplastin function in other organ and could potentially serve as an entry point for studying male reproduction. Nevertheless, some questions could not be explored due to limitations in experimental conditions. For example, if testosterone is injected into these mice, could it alter their behavior? Could artificial insemination or in vitro fertilization be successful? These questions would help further to investigate the role of neuroplastin in male fertility.

4.5 Ablation of neuroplastin in GABAergic interneurons after associative learning is sufficient to induce retrograde amnesia of associative memories

Neuroplastins are essential for associative learning and memories (Bhattacharya et al., 2017). Various mutant mouse models with altered expression of neuroplastin have been utilized to investigate its impact on learning and memory function (Bhattacharya et al., 2017). Research on *Nptn*^{-/-} mice, which lack neuroplastins in all cells, has revealed that despite no gross anatomical differences in the nervous system compared to wild-type mice, they exhibit reduced locomotor capacity and abnormal swimming behavior (Bhattacharya et al., 2017). In addition, they display reduced anxiety behaviors in the open field and light/dark avoidance tests, altered social interactions, depression-like behaviors, and are unable to achieve associative learning even with extensive training in the shuttle box (Bhattacharya et al., 2017). Bhattacharya et al. (2017) used *Nptn*^{lox/loxPrCreERT} mice, in which selective ablation of neuroplastins in all CNS neurons can be induced by tamoxifen treatment. To further investigate the role of neuroplastins in memory acquisition and retention, *Nptn*^{lox/loxPrCreERT} mice and control mice (*Nptn*^{lox/lox} without Cre recombinase) were first trained in a shuttle box to achieve high performance (greater than 75% correct responses) before inducing neuroplastin gene ablation. Two months after tamoxifen treatment, control mice retained more than 50% of their previous performance, while *Nptn*^{lox/loxPrCreERT} mice performed poorly, displaying retrograde amnesia. Hence, the expression of neuroplastins is critical for both associative learning and associative memory (Bhattacharya et al., 2017).

In 2017, Herrera-Molina et al. utilized *Nptn*^{loxloxEmx1Cre} mice, which have selective ablation of neuroplastins in glutamatergic interneurons, to investigate the role of neuroplastins in different neurons and revealed the indispensable role of neuroplastins in specific neural circuits related to neural circuits cognition. The experiments indicate that ablating neuroplastins in glutamatergic neurons of the cortex and hippocampus results in pronounced and specific behavioral deficits, closely associated with reduced neural activity and decreased levels of PMCAs in the mutant brain regions and demonstrated that neuronal neuroplastin is critical for PMCA expression and regulation of cytosolic Ca²⁺ levels (Herrera-Molina et al. 2017).

However, in the associative learning experiment, *Nptn*^{loxloxEmx1Cre} mice exhibited better learning compared to normal mice, suggesting that the expression of neuroplastins in glutamatergic neurons is not necessary for associative learning. This contrasts

strongly with the performance of both *Nptn*^{-/-} mice and induced *Nptn*^{lox/loxPrpCreERT}mice, as neither group demonstrated associative learning in the two-way active avoidance task. The disparity between *Nptn*^{-/-} and *Nptn*^{lox/loxEmx1Cre} suggests that the key to associative learning and memory lies in the expression of neuroplastins in GABAergic neurons (Herrera-Molina et al., 2017).

To test the above hypothesis, *Nptn*^{lox/loxGAD2CreERT} mice were utilized, resulting in the selective ablation of neuroplastins in GABAergic interneurons upon tamoxifen treatment. Both *Nptn*^{lox/loxGAD2CreERT} mice and control mice (*Nptn*^{lox/lox} without Cre recombinase) initially underwent training in a shuttle box, achieving over 75% correct responses before inducing neuroplastin gene ablation. Two months after tamoxifen treatment, control mice retained over 50% of their previous performance, whereas *Nptn*^{lox/loxGAD2CreERT} mice exhibited behavior similar to *Nptn*^{lox/loxPrCreERT} mice, displaying retrograde amnesia. However, unlike *Nptn*^{-/-} mice and *Nptn*^{lox/loxPrCreERT} mice, *Nptn*^{lox/loxGAD2CreERT} mice retained the capacity for associative learning (refer to Figure 27). When induced by tamoxifen injection to ablate the expression of neuroplastins in GABAergic interneurons after acquisition, *Nptn*^{lox/loxGAD2CreERT} mice demonstrated an impact on their associative memory. This underscores the crucial role of neuroplastins expressed by GABAergic neurons for associative memory, contributing to retrograde amnesia.

To better prove this hypothesis, another mutant mouse model, *Nptn*^{lox/loxEmx1CreGAD2ERT} has been utilized, which was generated by crossing *Nptn*^{lox/loxEmx1Cre} mice and *Nptn*^{lox/loxGAD2CreERT} mice. This resulted in genetic ablation of neuroplastins expression in glutamatergic and GABAergic interneurons when treated with tamoxifen (see Figures 22-24). Similar to *Nptn*^{-/-} mice or tamoxifen-treated *Nptn*^{lox/loxPrCreERT} mice, *Nptn*^{lox/loxEmx1CreGAD2ERT} mice showed problems in the associative memory task (as seen in table 15, below) as *Nptn*^{lox/loxGAD2CreERT} mice (also see Figures 28 and 29). These results further support the notion that the expression of neuroplastins in glutamatergic neurons is not essential for acquisition but suggest that the loss of neuroplastins in GABAergic interneurons is responsible for inducing retrograde amnesia. Therefore, the expression of neuroplastins in GABAergic interneurons is critical for associative memory.

Mice Behavior Experiment	<i>NPTN</i> ^{lox/lox}	<i>NPTN</i> ^{-/-}	<i>Nptn</i> ^{lox/loxEmx1Cre}	<i>Nptn</i> ^{lox/loxPrCreERT}		<i>Nptn</i> ^{lox/loxGAD2CreERT}		<i>Nptn</i> ^{lox/loxEmx1CreGAD2ERT}	
				Ablation before Training	Ablation after Training	Ablation before Training	Ablation after Training	Ablation before Training	Ablation after Training
Fear conditioning	+	-			-				
Grip strength	+	-	-	+					
Light-dark Avoidance	+	-	+	+					
Light/Dark Avoidance Memory	+	+	+	+	+				
Morris Water maze	+	-	-		+				
O-Maze	+	+		+					
Open field	+	-	-	+					
Social Interaction test	+	-		+					
Startle response and repulse inhibition (PPI)	+	-	+	-					
Rotarod	+	-	++	++					
Tail Suspension	+	-							
Two-way active avoidance test (Shuttle Box)	+	-	+		-	+	-	-	-

Table 15: Behavior of neuroplastin mutants Mice

The results are based on the studies by Bhattacharya et al. and Herrera- Molina et al. that were previously discussed. The '+', positive; '++', better than control; '-' negative; 'X', no acquisition of the task. 'Associative learning test', ablation before test, 'Associative memory test', ablation after test.

4.6 Parvalbumin positive interneurons play an important role in associative learning and memories

In 1997, Gonchar et al. demonstrated the predominant expression of PV (parvalbumin), CR (calretinin), and SOM (somatostatin) in three distinct groups of GABAergic interneurons in the rat prefrontal and visual cortices using double-label immunocytochemistry. In 2008, Gonchar et al. further confirmed through triple immunostaining with PV, CR, and SOM antibodies that during postnatal development, PV never colocalized with CR and SOM in mice. PV+ interneurons, comprising approximately 40% of interneurons, emerged as the largest interneuron group. As early as 1982, Celio and Heizmann reported the importance of Parvalbumin as a calcium-binding protein involved in many cellular processes, such as cell movement, muscle excitation-contraction, nerve impulse transmission, neurotransmitter release, membrane permeability, and cellular secretion. Recent research indicates that PV+ interneurons have a role in plasticity and learning control and not only control learning but also induce plastic changes in themselves (Donato et al., 2013). Activation of PV+ interneurons in the prefrontal cortex accelerates the extinction of reward-seeking behavior (Sparta et al., 2014). During monocular deprivation, PV+ interneurons in the visual cortex are temporarily suppressed; this down-regulation appears to be necessary to allow ocular dominance plasticity during the critical period (Yazaki-Sugiyama et al., 2009; Kuhlman et al., 2013). In an auditory fear-conditioning paradigm, unpleasant foot shocks block PV+ interneurons in the auditory cortex, and this inhibition is required for associative fear learning (Letzkus et al., 2015).

Through fluorescent immunostaining and confocal microscopy observations (Figure 28), we found that neuroplastin is expressed in PV+ interneurons in both *Nptn*^{lox/lox} and *Nptn*^{lox/loxEmx1Cre} mice. The experiments conducted by Herrera-Molina et al. in 2017 demonstrated that in associative learning experiments, *Nptn*^{lox/loxEmx1Cre} mice exhibited better learning abilities compared to the wild-type. Hence the expression of neuroplastins in glutamatergic neurons is not essential for the acquisition/learning skill. Here, the key factor driving associative learning and memory may be the expression of neuroplastins in PV+ interneurons. Further experiments supported this point, in *Nptn*^{lox/loxGAD2CreERT} mice, the expression of neuroplastins in PV+ interneurons is notably absent. In the conducted two-way active avoidance experiment, the

Nptn^{lox/loxGAD2CreERT} mice exhibited retrograde amnesia, as shown in results chapter 3.5, Figures 29 and results chapter 3.6, Figure 30. Therefore, we infer that the observed retrograde amnesia in *Nptn*^{lox/loxGAD2CreERT} mice, related to associative memory, is associated with the expression of neuroplastins in PV+ interneurons, and is linked to the regulation of GABA release from these PV+ interneurons.

Furthermore, Hashemi et al. (2017) suggested that the quantification of the number of PV+ interneurons in three cortical areas (BA46, BA47, and BA9) revealed a significant reduction in the number of these neurons in autistic patients compared to the control group. This reduction in the number of parvalbumin-positive interneurons is believed to disrupt the balance of excitation/inhibition and alter gamma oscillations in the cortical regions of autistic subjects. In my study, I quantified PV+ interneurons in mice with different neuroplastin genotypes and found no significant differences in the distribution of PV+ interneurons in the motor cortex and hippocampal regions (see in results chapter 3.6, Figure 31). Therefore, this rules out a decrease in the number of PV+ interneurons as a factor in the retrograde amnesia observed in *Nptn*^{lox/loxGAD2CreERT} mice and further supports the idea that it is related to the absence of neuroplastins expression on PV+ interneurons.

4.7 Reduced PMCA2 levels may affect GABA release from PV+ interneurons, leading to retrograde amnesia of associative memories

The results from Figure 34 indicate that in the mouse cortex and hippocampus, only a small amount of PMCA2 is expressed by glutamatergic neurons, as there is almost no difference in the expression of PMCA2 in the cortex and hippocampus between induced *Nptn*^{lox/loxGAD2CreERT} and *Nptn*^{lox/loxEmx1CreGAD2ERT} mice. This further confirms that PMCA2 is primarily expressed by GABAergic interneurons.

PV+ interneurons are characterized by their fast-spiking profiles and can be found almost everywhere in the brain. It is linked to short-action potentials and the capacity to maintain a high firing frequency (Bartholome et al., 2020). The unique calcium buffer composition of FS basket cells serves to limit Ca²⁺ transients at their terminals, preventing asynchronous release and adaptation (Aponte et al., 2008). It is important to note that non-FS basket cells may have longer calcium transients at their synapses,

and their GABA release is mediated by different VDCCs than FS basket cells. (Tao et al. 2006; Kawamoto et al., 2012; Stafford et al., 2017).

In addition to their distinct calcium buffer composition, recent research has revealed that GABA release from FS basket cells is exclusively mediated by P/Q-type VDCCs, while N-type VDCCs solely mediate GABA release from CCK-positive basket cells (Hefft and Jonas, 2005). However, the downregulation of PMCA2 in these cells may decrease calcium excretion efficiency, resulting in increased intracellular Ca^{2+} concentration (see Figure 37).

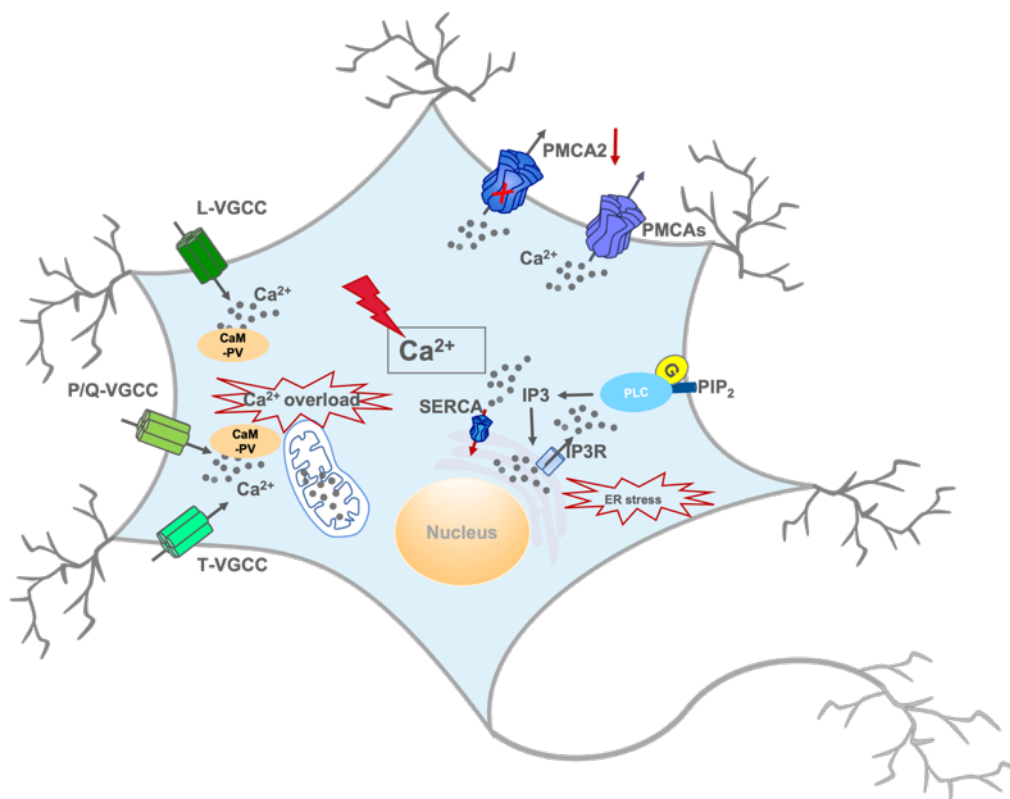


Figure 37: Functional changes in PV⁺ interneurons with reduced PMCA2 expression

Activation of the P/Q-VGCC Ca^{2+} channel leads to excessive Ca^{2+} influx and overload due to decreased PMCA2 expression in mice. GABA release also interacts with other GPCRs, leading to the production of IP₃, which potentiates Ca^{2+} release via IP₃R from the ER to the cytosol. Intracellular Ca^{2+} concentration increases, causing Ca^{2+} to enter the ER via SERCA and resulting in ER stress. Modified from Boczek et al. 2019.

Through Western blot experiments and immunofluorescence staining on different neuroplastin mutant mice, we have shown that PMCA2 expression is correspondingly reduced in different neuroplastin-deficient mice *Nptn*^{-/-}, *Nptn*^{lox/loxEmx1CreGAD2ERT} and *Nptn*^{lox/loxGAD2ERT} (Figure 34 and Figure 35). Consequently, we hypothesize that in PV+ neurons, the decrease in PMCA2 leads to an elevated intracellular Ca²⁺ concentration, causing Ca²⁺ overload and disrupting the intracellular calcium ion balance, ultimately resulting in retrograde amnesia.

Research from Thanawala and Regehr in 2013 showed that the presynaptic Ca²⁺ influx controls neurotransmitter release and the calcium dependence of neurotransmitter release is determined jointly by the calcium dependence of the probability of vesicular exocytosis and the effective size of the readily releasable pool (RRP), which depends on calcium influx through the VGCC. Splice variants of PMCA2 have a much lower Ca²⁺ Kd value compared to other PMCAs, which allows it to extrude Ca²⁺ to significantly lower levels than other PMCA isoforms (Elwess et al., 1997). PMCA2 has a high affinity for CaM, which results in a sluggish inactivation rate, meaning that PMCA2 remains pre-activated during ongoing activity, ready to respond to the next Ca²⁺ spike. The noteworthy is, unlike other PMCA2 variations, PMCA2a activates extremely quickly in response to an increase in Ca²⁺ (Caride et al., 2001). All of these properties make PMCA2a an excellent fit for the Ca²⁺ handling needs of parvalbumin terminals, allowing for consistent transmitter release even during continuous high-frequency firing (Burette et al., 2009).

The current status of GABA release from my study remains unclear and awaits further validation. Neurotransmitter release is closely related to calcium ion concentration, and it is well-established that neurotransmitter release is triggered by exceptionally high concentrations within microdomains (Neher et al., 2008). However, the findings of Lisek et al. (2022) suggest that PMCA2b regulation is involved in the gene expression related to both glutamate and GABA signaling. Thus, could a reduction in PMCA2 expression correspondingly lead to decreased GABA release? Moreover, calcium overload or dysregulation may activate negative feedback mechanisms or cellular damage pathways, ultimately reducing GABA release to prevent cellular damage or death. In the following experiments, it is necessary to compare and measure the level of GABA release.

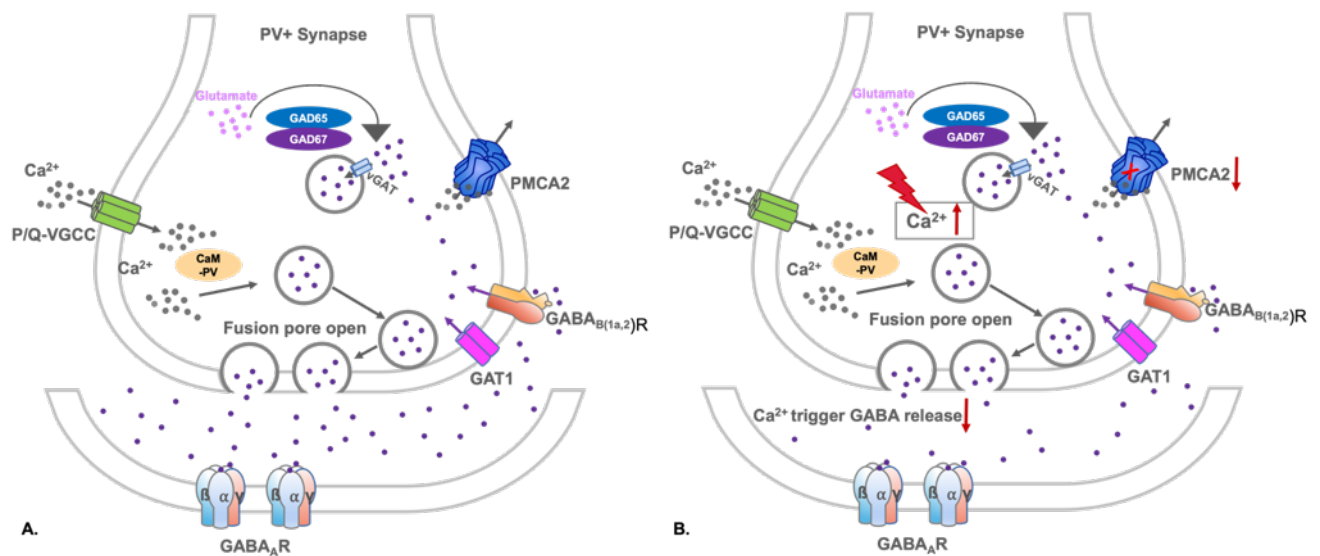


Figure 38: GABA release changes in reduced PMCA2 PV+ interneuron

A. Scheme showing a nerve terminal from a PV+ GABA interneuron shortly after an action potential triggered Ca²⁺-dependent GABA release, highlighting components currently hypothesized to be altered by PMCA2 reduction. In PV+ terminals, GABA release is tightly synchronized with Ca²⁺ influx by P/Q-VGCC. GAD65 and GAD67 drive GABA synthesis in the cytosol near synaptic vesicles. Vesicles uptake newly synthesized GABA via the vesicular GABA transporter vGAT. Ca²⁺ triggers the fusion pore opening to release the GABA. B. Reduced PMCA2 increase Ca²⁺ concentration due to lowered Ca²⁺ extrusion. Ca²⁺ buffering by PV mainly accelerates the decay of the interterminal Ca²⁺ transient and resulting permanent increase in intercellular Ca²⁺.

Carlen et al. (2012) reported that disruptions in the excitability of PV+ interneurons could result in selective impairments in working memory and associative learning. Basar-Eroglu et al. (2007) showed, task-evoked gamma oscillations, a frequency band believed to be reliant on the firing of PV+ interneurons, exhibit reductions in individuals with schizophrenia and are closely associated with the extent of functional impairment in working memory. My studies surmise that neuroplastins change GABAergic signaling by modulating the expression of PMCA2 in PV+ interneurons. Reduced expression of PMCA2 in PV+ interneurons of induced *Nptn*^{lox/loxGAD2CreERT} mice may affect the GABA release resulting in an imbalance of glutamate/GABA metabolism and further affecting disinhibition. This may ultimately affect learning and memory abilities

and result in retrograde amnesia. Further investigation of the molecular pathways of neuroplastins may potentially identify new targets for neurodegenerative diseases.

4.8 Conclusion

Neuroplastins play an essential role in male mouse fertility and in learning and memory, especially associative memory. Its close association with PMCA expression means that a decrease in neuroplastin levels leads to a reduction in PMCA expression. PMCA acts as a regulator of calcium ions, pumping out excess calcium ions to maintain suitable calcium levels. A decrease in PMCA expression leads to an increase in intracellular calcium concentration, disrupting calcium homeostasis and impairing hormone and neurotransmitter release, which may even result in premature cell aging.

The reduced expression of PMCA1 in Leydig cells of *NPTN*^{-/-} male mice may lead to an elevated intracellular Ca²⁺ level, disrupting the normal response to LH signals responsible for triggering testosterone release. This disruption can ultimately result in impaired fertility in these male mice.

PMCA2 is primarily expressed by GABAergic interneurons but not by glutamatergic neurons. PMCA2 expression in PV⁺ interneurons could be critical for associative learning and memory. As a calcium pump that removes Ca²⁺ ions from the cytosol, PMCA2 works in concert with PV to accelerate the sequestration of Ca²⁺. The interaction between PMCA2 and PV is therefore essential in regulating Ca²⁺ levels in PV⁺ interneurons. Our study suggests that the reduced expression of PMCA2 in PV⁺ interneurons may be associated with impaired learning and memory.

Reduced PMCA2 expression in PV⁺ interneurons caused by reduction of neuroplastins expression may dysregulate the excitation/inhibition balance by altering GABA release, which can impact disinhibition and result in impaired learning and memory in neuroplastin-ablated mice, including *Nptn*^{-/-} mice, *Nptn*^{lox/loxPrCreERT} mice, *Nptn*^{lox/loxGAD2CreERT} mice or *Nptn*^{lox/loxEmx1CreGAD2ERT} mice. Therefore, the expression of PMCA2 in PV⁺ interneurons appears to be a critical factor in the formation and retention of associative memories, hence, the expression of neuroplastins in GABAergic interneurons is critical for associative memory.

5 References

- Abraham WC. How long will long-term potentiation last? *Philos Trans R Soc Lond B Biol Sci.* 2003 Apr 29;358(1432):735-44. doi: 10.1098/rstb.2002.1222. PMID: 12740120; PMCID: PMC1693170.
- Akhtar MK, Kelly SL, Kaderbhai MA. Cytochrome b(5) modulation of 17 α hydroxylase and 17-20 lyase (CYP17) activities in steroidogenesis. *J Endocrinol.* 2005 Nov;187(2):267-74. doi: 10.1677/joe.1.06375. PMID: 16293774.
- Amaral S, Amaral A, Ramalho-Santos J. Aging and male reproductive function: a mitochondrial perspective. *Front Biosci (Schol Ed).* 2013 Jan 1;5(1):181-97. doi: 10.2741/s365. PMID: 23277044.
- Aponte Y, Bischofberger J, Jonas P. Efficient Ca²⁺ buffering in fast-spiking basket cells of rat hippocampus. *J Physiol.* 2008 Apr 15;586(8):2061-75. doi: 10.1113/jphysiol.2007.147298. Epub 2008 Feb 14. PMID: 18276734; PMCID: PMC2465201.
- Augustine GJ, Santamaria F, Tanaka K. Local calcium signaling in neurons. *Neuron.* 2003 Oct 9;40(2):331-46. doi: 10.1016/s0896-6273(03)00639-1. PMID: 14556712.
- Bagur R, Hajnóczky G. Intracellular Ca²⁺ Sensing: Its Role in Calcium Homeostasis and Signaling. *Mol Cell.* 2017 Jun 15;66(6):780-788. doi: 10.1016/j.molcel.2017.05.028. PMID: 28622523; PMCID: PMC5657234.
- Bartholome O, de la Brassinne Bonardeaux O, Neirinckx V, Rogister B. A Composite Sketch of Fast-Spiking Parvalbumin-Positive Neurons. *Cereb Cortex Commun.* 2020 Jun 19;1(1):tgaa026. doi: 10.1093/texcom/tgaa026. PMID: 34296100; PMCID: PMC8153048.

- Beesley P, Kraus M, Parolaro N. The neuroplastins: multifunctional neuronal adhesion molecules--involvement in behaviour and disease. *Adv Neurobiol.* (2014a);8:61-89. doi: 10.1007/978-1-4614-8090-7_4. PMID: 25300133.
- Beesley PW, Herrera-Molina R, Smalla KH, Seidenbecher C. The Neuroplastin adhesion molecules: key regulators of neuronal plasticity and synaptic function. *J Neurochem.* 2014 Nov;131(3):268-83. doi: 10.1111/jnc.12816. Epub (2014b) Aug 14. PMID: 25040546.
- Berlucchi G, Buchtel HA. Neuronal plasticity: historical roots and evolution of meaning. *Exp Brain Res.* 2009 Jan;192(3):307-19. doi: 10.1007/s00221-008-1611-6. Epub 2008 Nov 12. PMID: 19002678.
- Bernhardi RV, Nicholls JG. Transformation of leech microglial cell morphology and properties following co-culture with injured central nervous system tissue. *J Exp Biol.* 1999 Mar;202 (Pt 6):723-8. doi: 10.1242/jeb.202.6.723. PMID: 10021325.
- Bhattacharya S, Herrera-Molina R, Sabanov V, Ahmed T, Iscru E, Stöber F, Richter K, Fischer KD, Angenstein F, Goldschmidt J, Beesley PW, Balschun D, Smalla KH, Gundelfinger ED, Montag D. Genetically Induced Retrograde Amnesia of Associative Memories After Neuroplastin Ablation. *Biol Psychiatry.* 2017 Jan 15;81(2):124-135. doi: 10.1016/j.biopsych.2016.03.2107. Epub 2016 Apr 11. PMID: 27215477.
- Blottner S, Hingst O, Meyer HH. Seasonal spermatogenesis and testosterone production in roe deer (*Capreolus capreolus*). *J Reprod Fertil.* 1996 Nov;108(2):299-305. doi: 10.1530/jrf.0.1080299. PMID: 9038789.
- Brackenbury R, Rutishauser U, Edelman GM. Distinct calcium-independent and calcium-dependent adhesion systems of chicken embryo cells. *Proc Natl Acad Sci U S A.* 1981 Jan;78(1):387-91. doi: 10.1073/pnas.78.1.387. PMID: 6165990; PMCID: PMC319058.

- Brini M, Carafoli E. Calcium pumps in health and disease. *Physiol Rev.* 2009 Oct;89(4):1341-78. doi: 10.1152/physrev.00032.2008. PMID: 19789383.
- Brini M, Carafoli E. The plasma membrane Ca²⁺ ATPase and the plasma membrane sodium calcium exchanger cooperate in the regulation of cell calcium. *Cold Spring Harb Perspect Biol.* 2011 Feb 1;3(2):a004168. doi: 10.1101/cshperspect.a004168. PMID: 21421919; PMCID: PMC3039526.
- Burette A, Rockwood JM, Strehler EE, Weinberg RJ. Isoform-specific distribution of the plasma membrane Ca²⁺ ATPase in the rat brain. *J Comp Neurol.* 2003 Dec 22;467(4):464-76. doi: 10.1002/cne.10933. PMID: 14624481.
- Burette AC, Strehler EE, Weinberg RJ. "Fast" plasma membrane calcium pump PMCA2a concentrates in GABAergic terminals in the adult rat brain. *J Comp Neurol.* 2009 Feb 1;512(4):500-13. doi: 10.1002/cne.21909. PMID: 19025983; PMCID: PMC2635118.
- Burette AC, Strehler EE, Weinberg RJ. A plasma membrane Ca²⁺ ATPase isoform at the postsynaptic density. *Neuroscience.* 2010 Sep 1;169(3):987-93. doi: 10.1016/j.neuroscience.2010.05.062. Epub 2010 Jun 3. PMID: 20678993; PMCID: PMC2915942.
- Caillard O, Moreno H, Schwaller B, Llano I, Celio MR, Marty A. Role of the calcium-binding protein parvalbumin in short-term synaptic plasticity. *Proc Natl Acad Sci U S A.* 2000 Nov 21;97(24):13372-7. doi: 10.1073/pnas.230362997. PMID: 11069288; PMCID: PMC27231.
- Carlén M, Meletis K, Siegle JH, Cardin JA, Futai K, Vierling-Claassen D, Rühlmann C, Jones SR, Deisseroth K, Sheng M, Moore CI, Tsai LH. A critical role for NMDA receptors in parvalbumin interneurons for gamma rhythm induction and behavior. *Mol Psychiatry.* 2012 May;17(5):537-48. doi: 10.1038/mp.2011.31. Epub 2011 Apr 5. PMID: 21468034; PMCID: PMC3335079.

- Carafoli E. Calcium pump of the plasma membrane. *Physiol Rev.* 1991 Jan;71(1):129-53. doi: 10.1152/physrev.1991.71.1.129. PMID: 1986387.
- Carafoli E. Biogenesis: plasma membrane calcium ATPase: 15 years of work on the purified enzyme. *FASEB J.* 1994 Oct;8(13):993-1002. PMID: 7926378.
- Carafoli, E., Lim, D. Plasma Membrane Calcium ATPase. In: Lajtha, A., Mikoshiba, K. (eds) *Handbook of Neurochemistry and Molecular Neurobiology.* 2009 Springer, Boston, MA. https://doi.org/10.1007/978-0-387-30370-3_32
- Caride AJ, Filoteo AG, Penheiter AR, Pászty K, Enyedi A, Penniston JT. Delayed activation of the plasma membrane calcium pump by a sudden increase in Ca²⁺: fast pumps reside in fast cells. *Cell Calcium.* 2001 Jul;30(1):49-57. doi: 10.1054/ceca.2001.0212. PMID: 11396987.
- Celio MR, Heizmann CW. Calcium-binding protein parvalbumin is associated with fast contracting muscle fibres. *Nature.* 1982 Jun 10;297(5866):504-6. doi: 10.1038/297504a0. PMID: 6211622.
- Chen J, Lin X, Bhattacharya S, Wiesehöfer C, Wennemuth G, Müller K, Montag D. Neuroplastin Expression in Male Mice Is Essential for Fertility, Mating, and Adult Testosterone Levels. *Int J Mol Sci.* 2023 Dec 22;25(1):177. doi: 10.3390/ijms25010177. PMID: 38203350; PMCID: PMC10779036.
- Chothia C, Jones EY. The molecular structure of cell adhesion molecules. *Annu Rev Biochem.* 1997;66:823-62. doi: 10.1146/annurev.biochem.66.1.823. PMID: 9242926.
- Collin T, Chat M, Lucas MG, Moreno H, Racay P, Schwaller B, Marty A, Llano I. Developmental changes in parvalbumin regulate presynaptic Ca²⁺ signaling. *J Neurosci.* 2005 Jan 5;25(1):96-107. doi: 10.1523/JNEUROSCI.3748-04.2005. PMID: 15634771; PMCID: PMC6725212.

- Costa RR, Varanda WA, Franci CR. A calcium-induced calcium release mechanism supports luteinizing hormone-induced testosterone secretion in mouse Leydig cells. *Am J Physiol Cell Physiol*. 2010 Aug;299(2):C316-23. doi: 10.1152/ajpcell.00521.2009. Epub 2010 Jun 2. PMID: 20519450.
- de Kretser DM, Loveland KL, Meinhardt A, Simorangkir D, Wreford N. Spermatogenesis. *Hum Reprod*. 1998 Apr;13 Suppl 1:1-8. doi: 10.1093/humrep/13.suppl_1.1. PMID: 9663765.
- Desrivères S, Lourdasamy A, Tao C, Toro R, Jia T, Loth E, Medina LM, Kepa A, Fernandes A, Ruggeri B, Carvalho FM, Cocks G, Banaschewski T, Barker GJ, Bokde AL, Büchel C, Conrod PJ, Flor H, Heinz A, Gallinat J, Garavan H, Gowland P, Brühl R, Lawrence C, Mann K, Martinot ML, Nees F, Lathrop M, Poline JB, Rietschel M, Thompson P, Fauth-Bühler M, Smolka MN, Pausova Z, Paus T, Feng J & Schumann G; IMAGEN Consortium (2014): Single nucleotide polymorphism in the neuroplastin locus associates with cortical thickness and intellectual ability in adolescents. *Molecular Psychiatry* 20 263–274. doi: 10.1038/mp.2013.197.
- Di Leva F, Domi T, Fedrizzi L, Lim D, Carafoli E. The plasma membrane Ca²⁺ ATPase of animal cells: structure, function and regulation. *Arch Biochem Biophys*. 2008 Aug 1;476(1):65-74. doi: 10.1016/j.abb.2008.02.026. Epub 2008 Mar 4. PMID: 18328800.
- Dityatev A, Bukalo O, Schachner M. Modulation of synaptic transmission and plasticity by cell adhesion and repulsion molecules. *Neuron Glia Biol*. 2008 Aug;4(3):197-209. doi: 10.1017/S1740925X09990111. Epub 2009 Aug 13. PMID: 19674506.
- Donato F, Rompani SB, Caroni P. Parvalbumin-expressing basket-cell network plasticity induced by experience regulates adult learning. *Nature*. 2013 Dec 12;504(7479):272-6. doi: 10.1038/nature12866. PMID: 24336286.

- Duffau H. A two-level model of interindividual anatomo-functional variability of the brain and its implications for neurosurgery. *Cortex*. 2017 Jan;86:303-313. doi: 10.1016/j.cortex.2015.12.009. Epub 2016 Jan 29. PMID: 26920729.
- Elwess NL, Filoteo AG, Enyedi A, Penniston JT. Plasma membrane Ca²⁺ pump isoforms 2a and 2b are unusually responsive to calmodulin and Ca²⁺. *J Biol Chem*. 1997 Jul 18;272(29):17981-6. doi: 10.1074/jbc.272.29.17981. PMID: 9218424.
- Flavell SW, Greenberg ME. Signaling mechanisms linking neuronal activity to gene expression and plasticity of the nervous system. *Annu Rev Neurosci*. 2008;31:563-90. doi: 10.1146/annurev.neuro.31.060407.125631. PMID: 18558867; PMCID: PMC2728073.
- Gonchar Y, Burkhalter A. Three distinct families of GABAergic neurons in rat visual cortex. *Cereb Cortex*. 1997 Jun;7(4):347-58. doi: 10.1093/cercor/7.4.347. PMID: 9177765.
- Gonchar Y, Wang Q, Burkhalter A. Multiple distinct subtypes of GABAergic neurons in mouse visual cortex identified by triple immunostaining. *Front Neuroanat*. 2008 Mar 28; 1:3. doi: 10.3389/neuro.05.003.2007. PMID: 18958197; PMCID: PMC2525923.
- Gong D, Chi X, Ren K, Huang G, Zhou G, Yan N, Lei J, Zhou Q. Structure of the human plasma membrane Ca²⁺-ATPase 1 in complex with its obligatory subunit neuroplastin. *Nat Commun*. 2018 Sep 6;9(1):3623. doi: 10.1038/s41467-018-06075-7. PMID: 30190470; PMCID: PMC6127144.
- Gorczyńska E, Handelsman DJ. Androgens rapidly increase the cytosolic calcium concentration in Sertoli cells. *Endocrinology*. 1995 May;136(5):2052-9. doi: 10.1210/endo.136.5.7720654. PMID: 7720654.
- Green CD, Ma Q, Manske GL, Shami AN, Zheng X, Marini S, Moritz L, Sultan C, Gurczynski SJ, Moore BB, Tallquist MD, Li JZ, Hammoud SS. A Comprehensive

- Roadmap of Murine Spermatogenesis Defined by Single-Cell RNA-Seq. *Dev Cell*. 2018 Sep 10;46(5):651-667.e10. doi: 10.1016/j.devcel.2018.07.025. Epub 2018 Aug 23. PMID: 30146481; PMCID: PMC6713459.
- Griswold MD. The central role of Sertoli cells in spermatogenesis. *Semin Cell Dev Biol*. 1998 Aug;9(4):411-6. doi: 10.1006/scdb.1998.0203. PMID: 9813187.
- Gruart A, Leal-Campanario R, López-Ramos JC, Delgado-García JM. Functional basis of associative learning and its relationships with long-term potentiation evoked in the involved neural circuits: Lessons from studies in behaving mammals. *Neurobiol Learn Mem*. 2015 Oct;124:3-18. doi: 10.1016/j.nlm.2015.04.006. Epub 2015 Apr 25. PMID: 25916668.
- Gumbiner BM. Cell adhesion: the molecular basis of tissue architecture and morphogenesis. *Cell*. 1996 Feb 9;84(3):345-57. doi: 10.1016/s0092-8674(00)81279-9. PMID: 8608588.
- Hansen SM, Berezin V, Bock E. Signaling mechanisms of neurite outgrowth induced by the cell adhesion molecules NCAM and N-cadherin. *Cell Mol Life Sci*. 2008 Nov;65(23):3809-21. doi: 10.1007/s00018-008-8290-0. PMID: 18791849.
- Hayes R.A, Nahrung H.F, Wilson J.C. The response of native Australian rodents to predator odours varies seasonally: A by-product of life-history variations? *Anim Behav*. 2006; 71:1307–14.
- Hefft S, Jonas P. Asynchronous GABA release generates long-lasting inhibition at a hippocampal interneuron-principal neuron synapse. *Nat Neurosci*. 2005 Oct;8(10):1319-28. doi: 10.1038/nn1542. Epub 2005 Sep 11. PMID: 16158066.
- Herrera-Molina R, Sarto-Jackson I, Montenegro-Venegas C, Heine M, Smalla KH, Seidenbecher CI, Beesley PW, Gundelfinger ED, Montag D. Structure of excitatory synapses and GABAA receptor localization at inhibitory synapses are regulated by neuroplastin-65. *J Biol Chem*. 2014 Mar 28;289(13):8973-88. doi:

- 10.1074/jbc.M113.514992. Epub 2014 Feb 19. PMID: 24554721; PMCID: PMC3979398.
- Herrera-Molina R, Mlinac-Jerkovic K, Ilic K, Stöber F, Vemula SK, Sandoval M, Milosevic NJ, Simic G, Smalla KH, Goldschmidt J, Bognar SK, Montag D. Neuroplastin deletion in glutamatergic neurons impairs selective brain functions and calcium regulation: implication for cognitive deterioration. *Sci Rep*. 2017 Aug 4;7(1):7273. doi: 10.1038/s41598-017-07839-9. PMID: 28779130; PMCID: PMC5544750.
- Hill IE, Selkirk CP, Hawkes RB, Beesley PW. Characterization of novel glycoprotein components of synaptic membranes and postsynaptic densities, gp65 and gp55, with a monoclonal antibody. *Brain Res*. 1988 Sep 27;461(1):27-43. doi: 10.1016/0006-8993(88)90722-6. PMID: 3224275.
- Hu H, Gan J, Jonas P. Interneurons. Fast-spiking, parvalbumin⁺ GABAergic interneurons: from cellular design to microcircuit function. *Science*. 2014 Aug 1;345(6196):1255263. doi: 10.1126/science.1255263. Epub 2014 Jul 31. PMID: 25082707.
- Hunkin NM, Parkin AJ, Bradley VA, Burrows EH, Aldrich FK, Jansari A, Burdon-Cooper C. Focal retrograde amnesia following closed head injury: a case study and theoretical account. *Neuropsychologia*. 1995 Apr;33(4):509-23. doi: 10.1016/0028-3932(94)00136-d. PMID: 7617158.
- Ilic K, Mlinac-Jerkovic K, Sedmak G, Rosenzweig I, Kalanj-Bognar S. Neuroplastin in human cognition: review of literature and future perspectives. *Transl Psychiatry*. 2021 Jul 16;11(1):394. doi: 10.1038/s41398-021-01509-1. PMID: 34282131; PMCID: PMC8289873.
- Jensen TP, Buckby LE, Empson RM. Expression of plasma membrane Ca²⁺ ATPase family members and associated synaptic proteins in acute and cultured organotypic hippocampal slices from rat. *Brain Res Dev Brain Res*. 2004 Sep 17;152(2):129-36. doi: 10.1016/j.devbrainres.2004.06.004. PMID: 15351500.

- Jensen TP, Filoteo AG, Knopfel T, Empson RM. Presynaptic plasma membrane Ca²⁺ ATPase isoform 2a regulates excitatory synaptic transmission in rat hippocampal CA3. *J Physiol.* 2007 Feb 15;579(Pt 1):85-99. doi: 10.1113/jphysiol.2006.123901. Epub 2006 Dec 14. PMID: 17170045; PMCID: PMC2075377.
- Kawamoto EM, Vivar C, Camandola S. Physiology and pathology of calcium signaling in the brain. *Front Pharmacol.* 2012 Apr 13;3:61. doi: 10.3389/fphar.2012.00061. PMID: 22518105; PMCID: PMC3325487.
- Kim H, Kim M, Im SK, Fang S. Mouse Cre-LoxP system: general principles to determine tissue-specific roles of target genes. *Lab Anim Res.* 2018 Dec;34(4):147-159. doi: 10.5625/lar.2018.34.4.147. Epub 2018 Dec 31. PMID: 30671100; PMCID: PMC6333611.
- Kiselyov VV, Skladchikova G, Hinsby AM, Jensen PH, Kulahin N, Soroka V, Pedersen N, Tsetlin V, Poulsen FM, Berezin V, Bock E. Structural basis for a direct interaction between FGFR1 and NCAM and evidence for a regulatory role of ATP. *Structure.* 2003 Jun;11(6):691-701. doi: 10.1016/s0969-2126(03)00096-0. PMID: 12791257.
- Korthals M, Langnaese K, Smalla KH, Kähne T, Herrera-Molina R, Handschuh J, Lehmann AC, Mamula D, Naumann M, Seidenbecher C, Zuschratter W, Tedford K, Gundelfinger ED, Montag D, Fischer KD, Thomas U. A complex of Neuroplastin and Plasma Membrane Ca²⁺ ATPase controls T cell activation. *Sci Rep.* 2017 Aug 21;7(1):8358. doi: 10.1038/s41598-017-08519-4. PMID: 28827723; PMCID: PMC5566957.
- Kreutz MR, Langnaese K, Dieterich DC, Seidenbecher CI, Zuschratter W, Beesley PW, Gundelfinger ED. Distribution of transcript and protein isoforms of the synaptic glycoprotein neuroplastin in rat retina. *Invest Ophthalmol Vis Sci.* 2001 Jul;42(8):1907-14. PMID: 11431460.

- Kuhlman SJ, Olivas ND, Tring E, Ikrar T, Xu X, Trachtenberg JT. A disinhibitory microcircuit initiates critical-period plasticity in the visual cortex. *Nature*. 2013 Sep 26;501(7468):543-6. doi: 10.1038/nature12485. Epub 2013 Aug 25. PMID: 23975100; PMCID: PMC3962838.
- Krishnamurthy H, Danilovich N, Morales CR, Sairam MR. Qualitative and quantitative decline in spermatogenesis of the follicle-stimulating hormone receptor knockout (FORKO) mouse. *Biol Reprod*. 2000 May;62(5):1146-59. doi: 10.1095/biolreprod62.5.1146. PMID: 10775161.
- Kumar TR, Wang Y, Lu N, Matzuk MM. Follicle stimulating hormone is required for ovarian follicle maturation but not male fertility. *Nat Genet*. 1997 Feb;15(2):201-4. doi: 10.1038/ng0297-201. PMID: 9020850.
- Langnaese K, Beesley PW, Gundelfinger ED. Synaptic membrane glycoproteins gp65 and gp55 are new members of the immunoglobulin superfamily. *J Biol Chem*. 1997 Jan 10;272(2):821-7. doi: 10.1074/jbc.272.2.821. PMID: 8995369.
- Latash LP, Latash ML, Meijer OG. 30 years later: On the problem of the relation between structure and function in the brain from a contemporary viewpoint (1996), part II. *Motor Control*. 2000 Apr;4(2):125-49. doi: 10.1123/mcj.4.2.125. PMID: 11500572.
- Lejeune H, Habert R, Saez JM. Origin, proliferation and differentiation of Leydig cells. *J Mol Endocrinol*. 1998 Feb;20(1):1-25. doi: 10.1677/jme.0.0200001. PMID: 9513078.
- Letzkus JJ, Wolff SB, Lüthi A. Disinhibition, a Circuit Mechanism for Associative Learning and Memory. *Neuron*. 2015 Oct 21;88(2):264-76. doi: 10.1016/j.neuron.2015.09.024. PMID: 26494276.
- Li XF, Bowe JE, Mitchell JC, Brain SD, Lightman SL, O'Byrne KT. Stress-induced suppression of the gonadotropin-releasing hormone pulse generator in the

- female rat: a novel neural action for calcitonin gene-related peptide. *Endocrinology*. 2004 Apr;145(4):1556-63. doi: 10.1210/en.2003-1609. Epub 2004 Jan 21. PMID: 14736738.
- Lin YN, Matzuk MM. Genetics of male fertility. *Methods Mol Biol*. 2014;1154:25-37. doi: 10.1007/978-1-4939-0659-8_2. PMID: 24782004.
- Lin X, Liang Y, Herrera-Molina R, Montag D. Neuroplastin in Neuropsychiatric Diseases. *Genes (Basel)*. (2021a) Sep 26;12(10):1507. doi: 10.3390/genes12101507. PMID: 34680901; PMCID: PMC8535836.
- Lin X, Brunk MGK, Yuanxiang P, Curran AW, Zhang E, Stöber F, Goldschmidt J, Gundelfinger ED, Vollmer M, Happel MFK, Herrera-Molina R, Montag D. Neuroplastin expression is essential for hearing and hair cell PMCA expression. *Brain Struct Funct*. (2021b) Jun;226(5):1533-1551. doi: 10.1007/s00429-021-02269-w. Epub 2021 Apr 12. PMID: 33844052; PMCID: PMC8096745.
- Lisek M, Mackiewicz J, Sobolczyk M, Ferenc B, Guo F, Zylinska L, Boczek T. Early Developmental PMCA2b Expression Protects From Ketamine-Induced Apoptosis and GABA Impairments in Differentiating Hippocampal Progenitor Cells. *Front Cell Neurosci*. 2022 May 23;16:890827. doi: 10.3389/fncel.2022.890827. PMID: 35677757; PMCID: PMC9167922.
- Louvet JP, Harman SM, Ross GT. Effects of human chorionic gonadotropin, human interstitial cell stimulating hormone and human follicle-stimulating hormone on ovarian weights in estrogen-primed hypophysectomized immature female rats. *Endocrinology*. 1975 May;96(5):1179-86. doi: 10.1210/endo-96-5-1179. PMID: 1122882.
- Lopreiato R, Giacomello M, Carafoli E. The plasma membrane calcium pump: new ways to look at an old enzyme. *J Biol Chem*. 2014 Apr 11;289(15):10261-10268. doi: 10.1074/jbc.O114.555565. Epub 2014 Feb 25. PMID: 24570005; PMCID: PMC4036151.

- Luu-The V, Labrie F. The intracrine sex steroid biosynthesis pathways. *Prog Brain Res.* 2010;181:177-92. doi: 10.1016/S0079-6123(08)81010-2. PMID: 20478438.
- Lyng FM, Jones GR, Rommerts FF. Rapid androgen actions on calcium signaling in rat sertoli cells and two human prostatic cell lines: similar biphasic responses between 1 picomolar and 100 nanomolar concentrations. *Biol Reprod.* 2000 Sep;63(3):736-47. doi: 10.1095/biolreprod63.3.736. PMID: 10952915.
- Maness PF, Schachner M. Neural recognition molecules of the immunoglobulin superfamily: signaling transducers of axon guidance and neuronal migration. *Nat Neurosci.* 2007 Jan;10(1):19-26. doi: 10.1038/nn1827. Erratum in: *Nat Neurosci.* 2007 Feb;10(2):263. PMID: 17189949.
- Markowitsch HJ, Chapter 7 Anterograde amnesia, *Handbook of Clinical Neurology*, Elsevier, Volume 88, 2008, Pages 155-183, ISSN 0072-9752, ISBN 9780444518972, [https://doi.org/10.1016/S0072-9752\(07\)88007-9](https://doi.org/10.1016/S0072-9752(07)88007-9).
- Mohammadi M, Olsen SK, Ibrahim OA. Structural basis for fibroblast growth factor receptor activation. *Cytokine Growth Factor Rev.* 2005 Apr;16(2):107-37. doi: 10.1016/j.cytogfr.2005.01.008. PMID: 15863029.
- Montag D. Retrograde Amnesia - A Question of Disturbed Calcium Levels? *Front Cell Neurosci.* 2021 Dec 17;15:746198. doi: 10.3389/fncel.2021.746198. PMID: 34975406; PMCID: PMC8718400.
- Montag-Sallaz M, Montag D. Severe cognitive and motor coordination deficits in tenascin-R-deficient mice. *Genes Brain Behav.* 2003 Feb;2(1):20-31. doi: 10.1034/j.1601-183x.2003.00003.x. PMID: 12882316.
- Morris RG. Long-term potentiation and memory. *Philos Trans R Soc Lond B Biol Sci.* 2003 Apr 29;358(1432):643-7. doi: 10.1098/rstb.2002.1230. PMID: 12740109; PMCID: PMC1693171.

- Mooradian AD, Morley JE, Korenman SG. Biological actions of androgens. *Endocr Rev.* 1987 Feb;8(1):1-28. doi: 10.1210/edrv-8-1-1. PMID: 3549275.
- Nassar GN, Leslie SW. Physiology, Testosterone. 2023 Jan 2. In: StatPearls [Internet]. Treasure Island (FL): StatPearls Publishing; 2023 Jan–. PMID: 30252384.
- Neher E, Sakaba T. Multiple roles of calcium ions in the regulation of neurotransmitter release. *Neuron.* 2008 Sep 25;59(6):861-72. doi: 10.1016/j.neuron.2008.08.019. PMID: 18817727.
- O'Shaughnessy PJ, Baker PJ, Johnston H. The foetal Leydig cell-- differentiation, function and regulation. *Int J Androl.* 2006 Feb;29(1):90-5; discussion 105-8. doi: 10.1111/j.1365-2605.2005.00555.x. PMID: 16466528.
- OAKBERG EF. A description of spermiogenesis in the mouse and its use in analysis of the cycle of the seminiferous epithelium and germ cell renewal. *Am J Anat.* 1956 Nov;99(3):391-413. doi: 10.1002/aja.1000990303. PMID: 13402725.
- Owczarek S, Kiryushko D, Larsen MH, Kastrup JS, Gajhede M, Sandi C, Berezin V, Bock E, Soroka V. Neuroplastin-55 binds to and signals through the fibroblast growth factor receptor. *FASEB J.* 2010 Apr;24(4):1139-50. doi: 10.1096/fj.09-140509. Epub 2009 Dec 1. PMID: 19952283.
- Owczarek S, Berezin V. Neuroplastin: cell adhesion molecule and signaling receptor. *Int J Biochem Cell Biol.* 2012 Jan;44(1):1-5. doi: 10.1016/j.biocel.2011.10.006. Epub 2011 Oct 20. PMID: 22036663.
- Pakarainen T, Zhang FP, Mäkelä S, Poutanen M, Huhtaniemi I. Testosterone replacement therapy induces spermatogenesis and partially restores fertility in luteinizing hormone receptor knockout mice. *Endocrinology.* 2005 Feb;146(2):596-606. doi: 10.1210/en.2004-0913. Epub 2004 Oct 28. PMID: 15514086.

- Quigley CA, De Bellis A, Marschke KB, el-Awady MK, Wilson EM, French FS. Androgen receptor defects: historical, clinical, and molecular perspectives. *Endocr Rev.* 1995 Jun;16(3):271-321. doi: 10.1210/edrv-16-3-271. Erratum in: *Endocr Rev* 1995 Aug;16(4):546. PMID: 7671849.
- Rato L, Alves MG, Socorro S, Duarte AI, Cavaco JE, Oliveira PF. Metabolic regulation is important for spermatogenesis. *Nat Rev Urol.* 2012 May 1;9(6):330-8. doi: 10.1038/nrurol.2012.77. PMID: 22549313.
- Rengarajan S, Balasubramanian K. Corticosterone has direct inhibitory effect on the expression of peptide hormone receptors, 11 beta-HSD and glucose oxidation in cultured adult rat Leydig cells. *Mol Cell Endocrinol.* 2007 Dec 15;279(1-2):52-62. doi: 10.1016/j.mce.2007.09.001. Epub 2007 Sep 6. PMID: 17950991.
- Saito A, Fujikura-Ouchi Y, Kuramasu A, Shimoda K, Akiyama K, Matsuoka H, Ito C. Association study of putative promoter polymorphisms in the neuroplastin gene and schizophrenia. *Neurosci Lett.* 2007 Jan 16;411(3):168-73. doi: 10.1016/j.neulet.2006.08.042. Epub 2006 Nov 22. PMID: 17123723.
- Sar M, Lubahn DB, French FS, Wilson EM. Immunohistochemical localization of the androgen receptor in rat and human tissues. *Endocrinology.* 1990 Dec;127(6):3180-6. doi: 10.1210/endo-127-6-3180. PMID: 1701137.
- Schmidt N, Kollwe A, Constantin C.E, Henrich, S, Ritzau-Jost, A, Bildl W, Saalbach A, Hallermann S, Kulik A, Fakler B & Schulte U (2017) Neuroplastin and Basigin Are Essential Auxiliary Subunits of Plasma Membrane Ca (2+)-ATPases and Key Regulators of Ca(2+) Clearance. *Neuron* 96 827-838 e829.
- Schulze W. Evidence of a wave of spermatogenesis in human testis. *Andrologia.* 1982 Mar-Apr;14(2):200-7. doi: 10.1111/j.1439-0272.1982.tb03124.x. PMID: 7103139.

- Schwaller B. Cytosolic Ca²⁺ buffers. *Cold Spring Harb Perspect Biol.* 2010 Nov;2(11):a004051. doi: 10.1101/cshperspect.a004051. Epub 2010 Oct 13. PMID: 20943758; PMCID: PMC2964180.
- Shima Y, Miyabayashi K, Haraguchi S, Arakawa T, Otake H, Baba T, Matsuzaki S, Shishido Y, Akiyama H, Tachibana T, Tsutsui K, Morohashi K. Contribution of Leydig and Sertoli cells to testosterone production in mouse fetal testes. *Mol Endocrinol.* 2013 Jan;27(1):63-73. doi: 10.1210/me.2012-1256. Epub 2012 Nov 2. PMID: 23125070; PMCID: PMC5416943.
- Smalla KH, Matthies H, Langnäse K, Shabir S, Böckers TM, Wyneken U, Staak S, Krug M, Beesley PW, Gundelfinger ED. The synaptic glycoprotein neuroplastin is involved in long-term potentiation at hippocampal CA1 synapses. *Proc Natl Acad Sci U S A.* 2000 Apr 11;97(8):4327-32. doi: 10.1073/pnas.080389297. PMID: 10759566; PMCID: PMC18241.
- Sparta DR, Hovelsø N, Mason AO, Katak PA, Ung RL, Decot HK, Stuber GD. Activation of prefrontal cortical parvalbumin interneurons facilitates extinction of reward-seeking behavior. *J Neurosci.* 2014 Mar 5;34(10):3699-705. doi: 10.1523/JNEUROSCI.0235-13.2014. PMID: 24599468; PMCID: PMC3942585.
- Stafford N, Wilson C, Oceandy D, Neyses L, Cartwright EJ. The Plasma Membrane Calcium ATPases and Their Role as Major New Players in Human Disease. *Physiol Rev.* 2017 Jul 1;97(3):1089-1125. doi: 10.1152/physrev.00028.2016. PMID: 28566538.
- Stamatiades GA, Kaiser UB. Gonadotropin regulation by pulsatile GnRH: Signaling and gene expression. *Mol Cell Endocrinol.* 2018 Mar 5;463:131-141. doi: 10.1016/j.mce.2017.10.015. Epub 2017 Nov 2. PMID: 29102564; PMCID: PMC5812824.
- Sternbach H. Age-associated testosterone decline in men: clinical issues for psychiatry. *Am J Psychiatry.* 1998 Oct;155(10):1310-8. doi: 10.1176/ajp.155.10.1310. PMID: 9766760.

- Strehler EE. Plasma membrane calcium ATPases as novel candidates for therapeutic agent development. *J Pharm Pharm Sci.* 2013;16(2):190-206. doi: 10.18433/j3z011. PMID: 23958189; PMCID: PMC3869240.
- Strehler EE. Plasma membrane calcium ATPases: From generic Ca(2+) sump pumps to versatile systems for fine-tuning cellular Ca(2.). *Biochem Biophys Res Commun.* 2015 Apr 24;460(1):26-33. doi: 10.1016/j.bbrc.2015.01.121. PMID: 25998731.
- Strehler EE, Zacharias DA. Role of alternative splicing in generating isoform diversity among plasma membrane calcium pumps. *Physiol Rev.* 2001 Jan;81(1):21-50. doi: 10.1152/physrev.2001.81.1.21. PMID: 11152753.
- Strehler EE, Thayer SA. Evidence for a role of plasma membrane calcium pumps in neurodegenerative disease: Recent developments. *Neurosci Lett.* 2018 Jan 10;663:39-47. doi: 10.1016/j.neulet.2017.08.035. Epub 2017 Aug 19. PMID: 28827127; PMCID: PMC5816698.
- Suzuki WA, Brown EN. Behavioral and neurophysiological analyses of dynamic learning processes. *Behav Cogn Neurosci Rev.* 2005 Jun;4(2):67-95. doi: 10.1177/1534582305280030. PMID: 16251726.
- Taniguchi H, He M, Wu P, Kim S, Paik R, Sugino K, Kvitsiani D, Fu Y, Lu J, Lin Y, Miyoshi G, Shima Y, Fishell G, Nelson SB, Huang ZJ. A resource of Cre driver lines for genetic targeting of GABAergic neurons in cerebral cortex. *Neuron.* 2011 Sep 22;71(6):995-1013. doi: 10.1016/j.neuron.2011.07.026. Epub 2011 Sep 21. Erratum in: *Neuron.* 2011 Dec 22;72(6):1091. Kvitsani, Duda [corrected to Kvitsiani, Duda]. PMID: 21943598; PMCID: PMC3779648.
- Tao YH, Yuan Z, Tang XQ, Xu HB, Yang XL. Inhibition of GABA shunt enzymes' activity by 4-hydroxybenzaldehyde derivatives. *Bioorg Med Chem Lett.* 2006 Feb;16(3):592-5. doi: 10.1016/j.bmcl.2005.10.040. Epub 2005 Nov 14. PMID: 16290145.

- Toyama Y, Maekawa M, Kadomatsu K, Miyauchi T, Muramatsu T, Yuasa S. Histological characterization of defective spermatogenesis in mice lacking the basigin gene. *Anat Histol Embryol.* 1999 Jul;28(3):205-13. doi: 10.1046/j.1439-0264.1999.00194.x. PMID: 10458027.
- Vemula SK, Malci A, Junge L, Lehmann AC, Rama R, Hradsky J, Matute RA, Weber A, Prigge M, Naumann M, Kreutz MR, Seidenbecher CI, Gundelfinger ED, Herrera-Molina R. The Interaction of TRAF6 With Neuroplastin Promotes Spinogenesis During Early Neuronal Development. *Front Cell Dev Biol.* 2020 Dec 9;8:579513. doi: 10.3389/fcell.2020.579513. PMID: 33363141; PMCID: PMC7755605.
- Von Ledeber EI, Almeida JP, Loss ES, Wassermann GF. Rapid effect of testosterone on rat Sertoli cell membrane potential. Relationship with K⁺ATP channels. *Horm Metab Res.* 2002 Oct;34(10):550-5. doi: 10.1055/s-2002-35426. PMID: 12439782.
- Walker WH. Molecular mechanisms of testosterone action in spermatogenesis. *Steroids.* 2009 Jul;74(7):602-7. doi: 10.1016/j.steroids.2008.11.017. Epub 2008 Nov 27. PMID: 19095000.
- Walker WH. Non-classical actions of testosterone and spermatogenesis. *Philos Trans R Soc Lond B Biol Sci.* 2010 May 27;365(1546):1557-69. doi: 10.1098/rstb.2009.0258. PMID: 20403869; PMCID: PMC2871922.
- Walker WH. Testosterone signaling and the regulation of spermatogenesis. *Spermatogenesis.* 2011 Apr;1(2):116-120. doi: 10.4161/spmg.1.2.16956. PMID: 22319659; PMCID: PMC3271653.
- Walsh FS, Doherty P. Neural cell adhesion molecules of the immunoglobulin superfamily: role in axon growth and guidance. *Annu Rev Cell Dev Biol.* 1997;13:425-56. doi: 10.1146/annurev.cellbio.13.1.425. PMID: 9442880.

- Wennemuth G, Westenbroek RE, Xu T, Hille B, Babcock DF. CaV2.2 and CaV2.3 (N- and R-type) Ca²⁺ channels in depolarization-evoked entry of Ca²⁺ into mouse sperm. *J Biol Chem.* 2000 Jul 14;275(28):21210-7. doi: 10.1074/jbc.M002068200. PMID: 10791962.
- Wennemuth G, Carlson AE, Harper AJ, Babcock DF. Bicarbonate actions on flagellar and Ca²⁺ -channel responses: initial events in sperm activation. *Development.* 2003 Apr;130(7):1317-26. doi: 10.1242/dev.00353. PMID: 12588848.
- Wu H, Jin Y, Buddhala C, Osterhaus G, Cohen E, Jin H, Wei J, Davis K, Obata K, Wu JY. Role of glutamate decarboxylase (GAD) isoform, GAD65, in GABA synthesis and transport into synaptic vesicles-Evidence from GAD65-knockout mice studies. *Brain Res.* 2007 Jun 18;1154:80-3. doi: 10.1016/j.brainres.2007.04.008. Epub 2007 Apr 6. PMID: 17482148.
- Wreford NG, Rajendra Kumar T, Matzuk MM, de Kretser DM. Analysis of the testicular phenotype of the follicle-stimulating hormone beta-subunit knockout and the activin type II receptor knockout mice by stereological analysis. *Endocrinology.* 2001 Jul;142(7):2916-20. doi: 10.1210/endo.142.7.8230. PMID: 11416011.
- Yang Y, Calakos N. Presynaptic long-term plasticity. *Front Synaptic Neurosci.* 2013 Oct 17;5:8. doi: 10.3389/fnsyn.2013.00008. PMID: 24146648; PMCID: PMC3797957.

6 Appendix

6.1 Abbreviations

aa	Amino acid
ABP	Androgen binding protein
AC	Adenylyl cyclase
AD	Alzheimer's disease
Asp	Conserved aspartate
AR	Androgen receptor
ATP	Adenosine triphosphate
CAMs	Cell adhesion molecules
cAMP	cyclic adenosine monophosphate
CNS	Central nervous system
DAG	Diacylglycerol
DDEP	4 amino acid acidic 340-Asp-Asp-Glu-Pro-(DDEP)343
DHEA	Dehydroepiandrosterone
DHT	Dihydrotestosterone
ECM	Extracellular matrix
ER	Endoplasmic reticulum
EGFR	Epidermal growth factor receptor
FC	Fragment crystallizable region of immunoglobulin
FGF	Fibroblast growth factor
FGFR	Fibroblast growth factor receptor
FSH	Follicle-stimulating hormone
GABAA	Gamma-aminobutyric acid type A
GnRH	Gonadotropin-releasing hormone
GnIHn	Gonadotropin-Inhibitory Hormone
GPCR	G-protein coupled receptor
3-HSD	3-hydroxysteroid dehydrogenase
17-HSD	17-hydroxysteroid dehydrogenase
ICSH	Interstitial cell-stimulating hormone
Ig	Immunoglobulin
IgSF	Immunoglobulin superfamily
kDA	Kilodalton
Kd	Dissociation constant
LTD	Long-term depression
LTP	Long-term potentiation
LH	Luteinizing hormone

LHR	Luteinizing hormone receptor
L-VGCC	L-type voltage-gated calcium channel
LTSP	Long-term synaptic plasticity
MAO	Monoamine oxidase
NC	Nitrocellulose
NCX	Na ⁺ / Ca ²⁺ exchanger
NMDA	N-Methyl-d-Aspartate
NMDAR	N-Methyl-d-Aspartate ionotropic glutamate receptor
Np	Neuroplastin
Np55	Neuroplastin 55
Np65	Neuroplastin 65
NPTN	Neuroplastin gene
NCAM	Neural cell adhesion molecule
PBR	Peripheral benzodiazepine receptors
PLC	Phospholipase C
PMCA	Plasma membrane calcium ATPase
PV+	Parvalbumin-positive
PSD	Postsynaptic density
RRP	Readily releasable pool
SERCA	Sarco/endoplasmic reticulum Ca ²⁺ ATPase
SPCA	Secretory pathway Ca ²⁺ ATPase
StAR	Steroidogenic acute regulatory protein
STSP	Short-term synaptic plasticity
T	Testosterone
TNF	Tumor necrosis factor
TRAF6	Receptor-associated factor 6
T-VGCC	T-type voltage-gated calcium channel
VGCCs	Voltage-gated Ca ²⁺ channels

6.2 List of figures

Figure 1: Neuroplastin binding interactions	6
Figure 2: Schematic overview of the PMCA structure	8
Figure 3: Exon structure of the regions in alternative splicing from the four mammalian PMCA genes	9
Figure 4: PMCA involved in regulating cellular Ca²⁺ homeostasis	11
Figure 5: Complex formation of neuroplastin and PMCA	12
Figure 6: Progress of spermatogenesis	15
Figure 7: Structure of seminiferous tubule	16
Figure 8: Testosterone release in male mice fertility	19
Figure 9: The regulation of male sexual functions by hormones	20
Figure 10: Steroidogenesis in Leydig Cell and testosterone release	21
Figure 11: Testosterone signaling pathways in Sertoli cell	23
Figure 12: Normal appearance of testis of Nptn^{-/-} male mice	44
Figure 13: Neuroplastin expression in testis and sperm	45
Figure 14: Neuroplastin expression by Leydig and peritubular myoid cells	47
Figure 15: Neuroplastin expression by spermatogonia, spermatocytes, and Sertoli cells	48
Figure 16: Ablation of neuroplastin expression in spermatocytes, spermatogonia, and Sertoli cells	49
Figure 17: Intratesticular testosterone in Nptn^{+/+} and Nptn^{-/-} mice	51
Figure 18: Analysis of adult testis	52
Figure 19: PMCA1 expression in the testis and particularly in the Leydig cells	53
Figure 20: PMCA1 expression in the brain and testis	54
Figure 21: GABAergic neuron-specific inducible neuroplastin-deficient mice 55	
Figure 22: Expression of neuroplastins, α-calbindin and parvalbumin in various mutant mice brain	57
Figure 23: Expression of neuroplastins, α-calbindin and parvalbumin in various mutant mice motor cortex	58
Figure 24: Expression of neuroplastins, α-calbindin and parvalbumin in various mutant mice hippocampus	59

Figure 25: Shuttle box for two-way active avoidance test.....	61
Figure 26: Two-way active avoidance test for associative learning	61
Figure 27: Learning skill from two-way active avoidance test	62
Figure 28: Two-way active avoidance test for associative memory	62
Figure 29: Associative memory from two-way active avoidance test	63
Figure 30: Ablation of neuroplastins in GABAergic Interneurons	64
Figure 31: The expression of PV+ interneurons in mice motor cortex and hippocampus.....	65
Figure 32: Neuroplastins expression in PV+ interneurons.....	66
Figure 33: PMCAs expressed in different genotype mice	67
Figure 34: PMCA2 expressed in different genotype mice	68
Figure 35: PMCA2 expressed in parvalbumin interneurons.....	69
Figure 36: Regulation of testosterone release in Leydig cells of <i>Nptn^{-/-}</i> males by PMCA1 levels	75
Figure 37: Functional changes in PV+ interneurons with reduced PMCA2 expression	81
Figure 38: GABA release changes in reduced PMCA2 PV+ interneuron	83

6.3 List of tables

Table 1: Summary of cell adhesion molecules	4
Table 2: Summary of spermatogenesis	14
Table 3: Primary Antibodies	27
Table 4: Secondary Antibodies	27
Table 5: Chemicals	28
Table 6: Buffers and solution	30
Table 7: Kits	31
Table 8: Equipment	31
Table 9: Gene expression assays	31
Table 10: List of mouse lines	32
Table 11: PCR procedure	34
Table 12: PCR reaction	35
Table 13: Primer	35
Table 14: SDS-PAGE Gels	37
Table 15: Behavior of neuroplastin mutants Mice	78

6.4 Ehrenerklärung

Ich versichere hiermit, dass ich die vorliegende Arbeit ohne unzulässige Hilfe Dritter und ohne Benutzung anderer als der angegebenen Hilfsmittel angefertigt habe; verwendete fremde und eigene Quellen sind als solche kenntlich gemacht.

Ich habe insbesondere nicht wissentlich:

- Ergebnisse erfunden oder widersprüchlich Ergebnisse verschwiegen,
- statistische Verfahren absichtlich missbraucht, um Daten in ungerechtfertigter Weise zu interpretieren,
- fremde Ergebnisse oder Veröffentlichungen plagiiert,
- fremde Forschungsergebnisse verzerrt wiedergegeben.

Mir ist bekannt, dass Verstöße gegen das Urheberrecht Unterlassungs- und Schadensersatzansprüche des Urhebers sowie eine strafrechtliche Ahndung durch die Strafverfolgungsbehörden begründen kann.

Ich erkläre mich damit einverstanden, dass die Arbeit ggf. mit Mitteln der elektronischen Datenverarbeitung auf Plagiate überprüft werden kann.

Die Arbeit wurde bisher weder im Inland noch im Ausland in gleicher oder ähnlicher Form als Dissertation eingereicht und ist als Ganzes auch noch nicht veröffentlicht.

Magdeburg, 11.09.2024

Ella Juanjuan Chen